NASA TN D-1184

TECHNICAL NOTE

D-1184

A MONTE CARLO STUDY OF RESONANCE ESCAPE PROBABILITY IN HETEROGENEOUS SLAB LATTICES CONTAINING RESONANT ABSORBERS AND SCATTERERS

By Harold Schneider, Leo Levitt,
and Kevin J. Sroub

Lewis Research Center
Cleveland, Ohio

NATIONAL AERONAUTICS AND SPACE ADMINISTRATION

WASHINGTON April 1962

NATIONAL AERONAUTICS AND SPACE ADMINISTRATION

TECHNICAL NOTE D-1184

A MONTE CARLO STUDY OF RESONANCE ESCAPE PROBABILITY IN HETEROGENEOUS SLAB LATTICES CONTAINING RESONANT ABSORBERS AND SCATTERERS

E-1434

By Harold Schneider, Leo Levitt,
and Kevin J. Sroub

SUMMARY

Resonance escape probabilities for heterogeneous semi-infinite slab lattice systems were computed by the Monte Carlo method in the energy range 1 kilo-electron-volt to 0.125 electron volt. Absorber-moderator combinations considered were W-H_2O, W-LiH, W-BeO, Au-H_2O, Au-LiH, and Au-BeO. Absorber and moderator thickness and absorber temperature were varied in a parametric study. The Monte Carlo results of neutron absorption for various thicknesses of tungsten and gold slabs at room temperature are in good agreement with experimental results from NASA solution reactor absorption measurements on comparable tungsten and gold samples.

The calculations show the dominating influence of resonance peaks in the absorption of thin samples. With increasing thickness this peak absorption saturates out, and considerably more absorption occurs in the wings of the resonances. Further increase in thickness results in additional absorption due to the valleys between resonances and to the $1/v$ region of the total cross section (where v is neutron velocity).

Strong resonance scattering in several tungsten resonances results in greater self-shielding than would exist if the scattering were absent. This process competes with resonance absorption and back-scatters many incident neutrons into the moderator; neutrons which do penetrate are effectively trapped in the sample, where they scatter about until absorbed or scattered out.

A simple one-collision analytical model to predict $1/v$ and resonance absorption for slabs was devised, and results were compared with corresponding Monte Carlo cases. This model gave excellent agreement with Monte Carlo results for predominantly absorptive resonances but considerably overestimated absorption for predominantly scattering resonances.

INTRODUCTION

High-performance nuclear reactors for space application must employ material with desirable high-temperature physical properties. Many such materials have large neutron resonance absorption and scattering cross sections that can result in significant nonproductive capture during neutron slowing down. One of the important quantities used to calculate reactor criticality, therefore, is the resonance escape probability.

A representative high-temperature fueled material is a mixture of tungsten and uranium oxide. To maximize the high-temperature heat-transfer rates and the resonance escape probability, the moderators and absorptive materials are arranged into heterogeneous arrays.

Several analytical or semianalytical methods exist for calculating resonance escape probabilities in heterogeneous assemblies. These are summarized, described, and discussed by J. Chernick and J. Sampson in reference 1. Of the methods presently available, the Monte Carlo method appears to be the most satisfactory overall approach to the resonance escape problem provided accurate and complete neutron cross sections are available. It may be readily adapted to complicated geometrical configurations, as exemplified by the successful application of the Monte Carlo method by R. D. Richtmeyer in reference 2 to calculation of the resonance escape probability in heterogeneous hexagonal water-uranium lattices.

Resonance scattering causes stronger self-shielding than would exist were the scattering not present. In reference 3 the strong scattering resonance in the cobalt cross section greatly affects resonance capture. Tungsten also exhibits several strongly scattering resonances. Perhaps the greatest advantage of the Monte Carlo method is that significant effects such as resonance scattering or anisotropic scattering can be rigorously treated (within statistical error) without having to resort to excessive idealization of the problem often necessary in order to obtain answers by other methods. A further advantage of the Monte Carlo method is the capacity for studying isolated phenomena with relative ease.

The present investigation considers only the resonance escape probability in repetitive one-dimensional slab lattices consisting of alternate layers of metal and moderator. Various thicknesses of tungsten or gold, and moderators such as lithium-7 hydride, beryllium oxide, or water are considered.

Some 21 resonances of natural tungsten exist between 1 and 250 electron volts for which the level parameters have been accurately measured (ref. 4). The tungsten resonances are interesting and somewhat unique in that they have varying degrees of scattering. The resonances of W^{182} at 4.1 electron volts, W^{186} at 18.8 electron volts, and W^{182} at 21.2 electron volts (fig. 1) are large and account for 28, 40, and 15 percent of the dilute resonance absorption integral. These three resonances are, respectively, predominantly absorptive, predominantly scattering, and "half and half."

Gold differs from tungsten in that gold has one very large absorption resonance near 5 electron volts that constitutes 95 percent of the dilute resonance absorption integral. The remaining 10 resonances are relatively unimportant for thin gold foils, but assume a greater importance for thicker samples. Therefore, the remaining resonances were also considered in the Monte Carlo calculations.

Studies were made to determine the effect of Doppler broadened resonances on the resonance escape probability at temperatures other than room temperature. Other effects such as those produced by the suppression of resonance scattering, the effect of the initial source distribution, the anisotropy of the scattering, and the minimum plate separation necessary to produce negligible cell interaction effects were also briefly studied. Monte Carlo self-shielding results for gold and tungsten were compared with experimental results obtained from reactivity measurements performed at the NASA Lewis Research Center (ref. 5).

SYMBOLS

A	atomic mass of nucleus
A_i	atomic mass of i^{th} type of nucleus
$\mathscr{A}$	number of neutrons
a	moderator half-thickness
$b - a$	fuel half-thickness
C	constant
DRAI	dilute resonance absorption integral, barns
E	neutron energy after collision, ev
E_c	minimum energy cutoff for Monte Carlo calculation, ev

E_M	maximum energy value for Monte Carlo calculation, ev
E_M^+	energy above E_M, ev
E'	neutron energy before collision, ev
$\mathcal{E}_Q$	Q^{th} tabulated energy value, ev
F	transport flux, neutrons/(cm^2)(sec)
K	collision number
k	Boltzmann constant, ergs/^oK
N	number of atoms, cc^{-1}
P	resonance escape probability (to 1.20 ev)
P_M	probability that neutron will be born in moderator
q	integrated slowing-down parameter
R or $R_{i=1,2}$	random number
r	distance to next collision along flight path, cm
S	phase-space source distribution
S_i	total number of neutrons per cc per second slowing down past E_{max} from collisions with i^{th} type of nucleus
T	temperature, ^oK
t	absorber thickness
t_M	moderator thickness between plates, 2a, cm
t_W	total tungsten thickness, 2(b - a), mils
u	lethargy
v	neutron speed, cm/sec
w	neutron weight after a priori fuel absorption has been subtracted from w'

w' or w'_k	neutron weight after k^{th} collision
w_a, w_s	a priori number of neutrons absorbed (scattered) in fuel after colliding at some point in moderator
w_{fe}	a priori number of neutrons that will go from moderator collision point through fuel without colliding
w_M	a priori number of neutrons that will leave moderator collision point and will collide before reaching fuel
x	coordinate along x-axis
x_{sym}	x-coordinate of plane of symmetry in repetitive lattice
y	dummy variable
α	$\frac{(A - 1)^2}{(A + 1)^2}$
β	azimuthal angle of scattering about initial neutron direction
γ	proportionality constant
κ	transformed variable of integration, $\gamma t/v_{min}$
μ	cosine of angle neutron velocity vector makes with x-axis
μ_C	cosine of scattering angle in center of mass system
μ_L	cosine of scattering angle between initial and final directions in laboratory system
$\Sigma, \Sigma_a, \Sigma_s$	macroscopic total, absorption, and scattering cross sections, cm^{-1}
Σ^I	total macroscopic cross section of region I (moderator), cm^{-1}
$\Sigma_i^{II}(E)$	total macroscopic cross section of i^{th} type of nucleus in region II (fuel), cm^{-1}
ξ	average logarithmic energy decrement
ξ_i	average logarithmic energy decrement from i^{th} type of nucleus
σ	microscopic total cross section, barns
φ	total neutron flux, neutrons/(cm^2)(sec)

Subscripts:

a	absorption
F	fission process index
i	element number index
j	resonance band energy index
K	collision number index
M	moderator
max	maximum
min	minimum
Q	lethargy interval index
S	surface
s	scattering
t	total
th	velocity corresponding to thermal energy
0	constant of proportionality
1, 2, 3	source neutron parameter index (used in section Treatment of Source Distribution by Monte Carlo method)
1, 2, 3	material specification index

Superscripts:

F	fuel, or absorber, region
i	energy E_i
L	left
M	moderator region
t	total

W	tungsten
I	moderator region index
II	absorber region index
—	average

ANALYSIS

Neutron histories were originated uniformly in the moderator and uniformly in the absorber but with different probabilities. Neutrons were followed by the Monte Carlo method in an energy range from E_{max} (961 ev) to E_c (0.125 ev) under the assumptions that:

(1) Scattering is isotropic in the center of mass system of the neutron and target nucleus.

(2) A uniform $1/E$ flux exists above 961 electron volts, at which value $P(E)$ is normalized.

(3) Absorption in the moderator is negligible, and the moderator scattering cross sections are taken as constant. These are excellent assumptions for the water, lithium[7] hydride, and beryllium oxide moderators considered.

A neutron history was initiated by picking its direction of travel, position, and energy from the source distribution and was thereafter followed by random sampling from the probability distribution functions of the various events possible during the course of the history.

The rigorous "cell" boundary conditions were considered during the course of neutron diffusion and slowing down. Whenever a collision occurred in the moderator, the a priori fraction of the colliding neutron that would make its next collision in the "fuel" region and be absorbed there was analytically determined and subtracted from the present weight. The given neutron with its weight thus reduced was followed from the moderator collision point by the techniques presented on page 21. If the next collision happened in the absorber, it would necessarily be a scattering collision.

When a neutron collided in the absorber, and the previous collision was also in the absorber, the neutron was weighted by the scattering probability per collision, and the scattered part was followed. This is a well known variance reduction technique.

The energy range from E_{max} to E_c was divided into 108 energy bands to record the output information. This consisted of the resonance escape probabilities $P(E_j)$ past these discrete energies, $j = 1,2,\ldots,108$, and the number of neutrons absorbed in each band and therefore each resonance which must agree with $\Delta P(E)$ over that band. Additional output information was the neutron fission production in each band if the absorber also contained uranium, and the average and maximum number of collisions taken to slow down from E_{max} to E_c.

Since there is no net leakage from the half-cell in any direction, a neutron history could be terminated only when its energy fell below the cutoff value of 0.125 electron volt or when its weight became negligibly small (less than 10^{-6}). By using the two types of statistical estimation just discussed, good accuracy was obtained by running a few thousand histories for each case. The value of resonance escape probability to 0.125 electron volt was obtained by taking the ratio of the number of neutrons that survived to the number of histories started.

Physical Assumptions

Consider sketch (a), which shows a typical two-region semi-infinite slab cell in an infinite repetitive lattice. Because of symmetry, only the half-cell ranging from $x = 0$ to $x = b$ need be considered. The

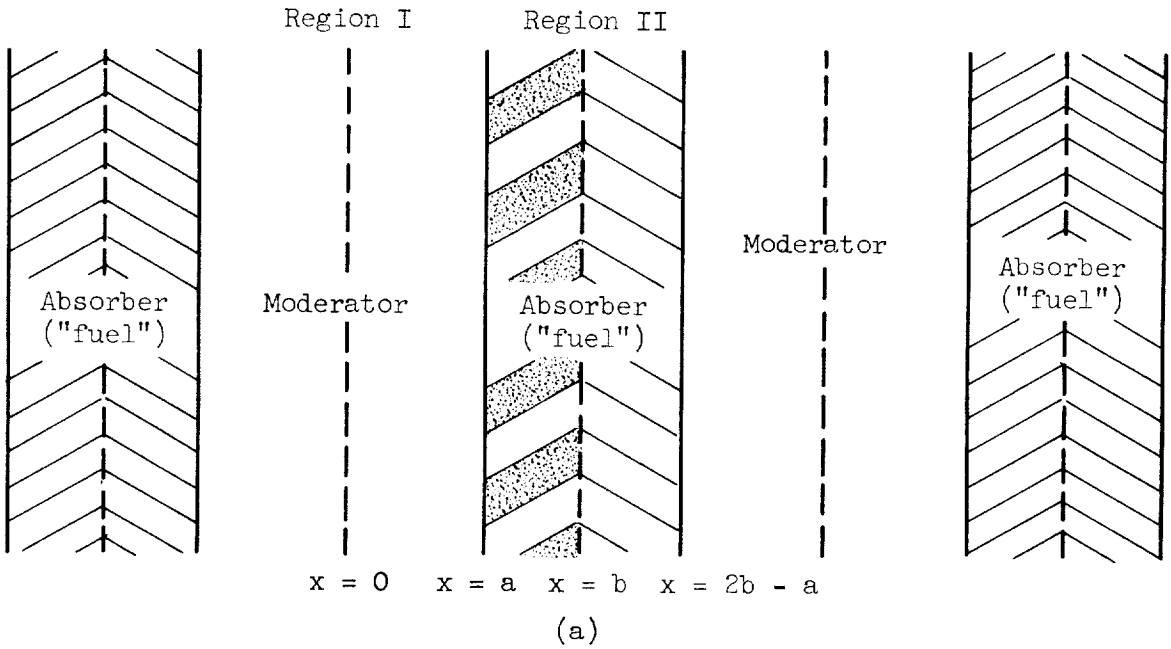

(a)

moderator region and absorber region may consist of several homogenized nuclear species. In particular, the moderator and absorber will be assumed to consist of not more than two and three distinct kinds of nuclei, respectively.

The source input into the resonance region is determined by the neutron flux above E_{max}. This flux will be assumed to have a $1/E$ energy distribution and a uniform spatial distribution. This assumption is based on the fact that, in an infinite homogeneous medium, the flux per unit energy is $1/E$ in the asymptotic slowing-down region and is independent of position. In the problem of interest, the flux will vary with position in the neighborhood of the interface. The deviation from the assumed uniform and $1/E$ dependence in this neighborhood is ignored because the slowing down in the absorber is small relative to the slowing down in the moderator, and the resonance escape probability is not sensitive to small changes in the source distribution input from above E_{max}. To show this, a case was run wherein all neutrons were originated uniformly in the moderator. The resonance escape probability changed from 0.873 to 0.877 in a hydrogeneous moderated case, where the effect should be greatest.

It will be further assumed that the target nuclei are stationary as the neutrons slow down, but that the target motion will be implied in the cross-section data used.

Input Data

All the absorber tabulated cross sections for a given temperature (536 energy values in all) were stored in the IBM 704 core. Thus, the detailed behavior of the various resonances was accurately described. The detailed cross-section data from 0.125 to 257 electron volts for tungsten were taken from reference 4, which assumes a thermal Maxwellian velocity distribution of tungsten atoms. The cross-section values were obtained by applying the Breit-Wigner single-level formula to each resonance and then summing the contributions from the other resonances to the cross section at each of the energies in question. Above 257 electron volts, the cross-section data were taken from reference 6. The slight differences in the resonance parameters from those given in the previous edition were found to produce slight changes in the resonance escape probabilities. Doppler broadened cross sections at temperatures other than thermal (0.0253 ev) were taken from reference 4 for use in the study of the effect of absorber temperature on the resonance escape probability.

Using the resonance parameters for gold from reference 6, the Doppler broadened gold cross sections were calculated by the methods of reference 7.

The cross sections of the beryllium oxide, water, and lithium hydride moderators were taken as constant down to E_c at 0.125 electron volt. Since absorption is negligible in the moderators considered, the macroscopic total cross section equals the macroscopic scattering cross section. These cross sections will be denoted by $\Sigma_i^I(E) = \Sigma_i^I$ and $\Sigma_{s,i}^I(E) = \Sigma_{s,i}^I$, respectively, where the superscript I refers to the moderator region, and the subscript i to the i^{th} element in this region. In the second or absorber region, the total and scattering cross sections at energy E are denoted by $\Sigma_i^{II}(E)$ and $\Sigma_{s,i}^{II}(E)$.

The number of absorber atoms per cubic centimeter and the logarithmic energy decrement are given in the following table:

	N (atoms/cc)	ξ
Tungsten	0.0632×10^{24}	0.010837
Gold	0.0591×10^{24}	0.0101

The number of moderator atoms per cubic centimeter and the total microscopic cross sections of the given moderators are listed in the following table:

	Water	Lithium hydride	Beryllium oxide
Σ_t, cm^{-1}	1.47840	1.296	0.7105
$\overline{\xi}\Sigma_s$, cm^{-1}	1.38077	1.258875	.12280
N_1, atoms/cc	$.0660 \times 10^{24}$	$.06 \times 10^{24}$	$.0725 \times 10^{24}$
N_2, atoms/cc	$.0330 \times 10^{24}$	$.06 \times 10^{24}$	$.0725 \times 10^{24}$
σ_1^t, barns	20.5	1.1	6.0
σ_2^t, barns	3.8	20.5	3.8

Treatment of Source Distribution by Monte Carlo Method

A neutron history is initiated by determining its direction of travel μ_1, position x_1, and energy E_1 immediately upon entering the energy range below E_{max} from its last collision in the $1/E$ region above E_{max}. Stated another way, a neutron is picked from the source distribution

$S(\mu_1, x_1, E_1)$ where $\alpha_1 E_{max} \leq E_1 \leq E_{max}$ and where μ_1 is the cosine of the angle between the velocity vector and the x-axis. For $E_1 < \alpha_1 E_{max}$

$$S(\mu_1, x_1, E_1) = 0$$

where

$$\alpha_1 = \frac{(A_1 - 1)^2}{(A_1 + 1)^2}$$

A_1 being the atomic mass of the lightest element present.

Assuming the source to be isotropic in the laboratory system, μ_1 is picked from an isotropic distribution according to reference 8 (p. E39)

$$\mu_1 = 1 - 2R \qquad (1)$$

where R is a random number. The random numbers were generated by a congruential method (ref. 9) from a standard accepted IBM 704 subroutine.

Equation (1) is precise if the neutron has collided in an absorber which contains only heavy nuclei. If the first collision has occurred in the moderator, the scattering is not isotropic. Equation (1) is still valid, however, because the angular distribution of neutrons in the asymptotic slowing-down region is essentially isotropic except, perhaps, near the moderator-absorber interface. In this neighborhood deviations from source isotropy will not appreciably affect the desired output information.

The initial position x_1 is determined uniformly between $x = 0$ and $x = a$ and between $x = a$ and $x = b$ (sketch (a)) but with different probabilities. Many more neutrons will slow down past E_{max} in the moderator region than in the absorber. To obtain the relative numbers, proceed as follows:

All cross sections at energies above E_{max} are considered constant. It will be understood that a superscript I or II should be affixed

to the expressions in sketch (b) and in the equations that follow according to whether the moderator or absorber region is being considered.

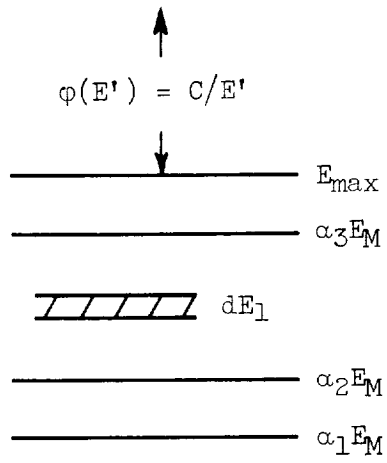

(b)

The number of neutrons per cubic centimeter per second $S_i(E)$ entering dE about E below E_{max} from neutron collisions above E_{max} with the i^{th} element is given by

$$S_i(E) = \begin{cases} \displaystyle\int_{E_M}^{E/\alpha_i} \frac{C}{E'}\, dE' \Sigma_{s,i}(E_M^+)\, \frac{1}{E'(1-\alpha_i)} = \frac{C\Sigma_{s,i}(E_M^+)}{E_M(1-\alpha_i)}\left(1 - \frac{\alpha_i E_M}{E}\right) & \alpha_i E_M < E \le E_M \\ 0 & E \le \alpha_i E_M \end{cases} \quad (2)$$

where $\Sigma_{s,i}(E_M^+)$ is the constant scattering cross section of the i^{th} element for $E > E_{max}$.

The total number of neutrons per cubic centimeter per second slowing down past E_{max} from scattering collisions with the i^{th} element in the given medium is

$$\left.\begin{aligned} \int_{\alpha_i E_M}^{E_M} S_i(E)dE \equiv S_i &= C\Sigma_{s,i}(E_M^+)\xi_i \\ \xi_i &= 1 - \frac{\alpha_i}{1-\alpha_i} \ln \frac{1}{\alpha_i} \end{aligned}\right\} \quad (3)$$

where ξ_i is the average logarithmic energy loss per collision with the i^{th} element.

The total number of neutrons per cubic centimeter per second slowing down past E_{max} in the moderator, which contains two elements, and in the absorber, which contains three elements, is

$$S^I = S_1^I + S_2^I \qquad \text{(moderator)}$$

$$S^{II} = S_1^{II} + S_2^{II} + S_3^{II} \qquad \text{(fuel)}$$

The fraction of neutrons slowing past E_{max} that exist in the moderator is therefore

$$P_M = \frac{(S_1^I + S_2^I)a}{(S_1^I + S_2^I)a + (S_1^{II} + S_2^{II} + S_3^{II})(b - a)} \tag{4}$$

where a and $b - a$ are the half-widths of moderator and absorber in centimeters. Substituting expression (3) into (4) gives

$$P_M = \frac{1}{1 + \frac{C^{II}}{C^I}\frac{(b - a)}{a}\left[\frac{\xi_1^{II}\Sigma_{s,1}^{II}(E_M^+) + \xi_2^{II}\Sigma_{s,2}^{II}(E_M^+) + \xi_3^{II}\Sigma_{s,3}^{II}(E_M^+)}{\xi_1^I\Sigma_{s,1}^I(E_M^+) + \xi_2^I\Sigma_{s,2}^I(E_M^+)}\right]} \tag{5}$$

It is proper to equate the fluxes per unit energy in the absorber and moderator or to write

$$\frac{C^{II}}{C^I} = 1 \tag{6}$$

Substituting (6) into (5) gives P_M. The fraction slowing past E_{max} in the fuel is therefore $1 - P_M$. Thus, the procedure for picking x_1 at random in the fuel or moderator according to the number of neutrons available from slowing down past E_{max} is

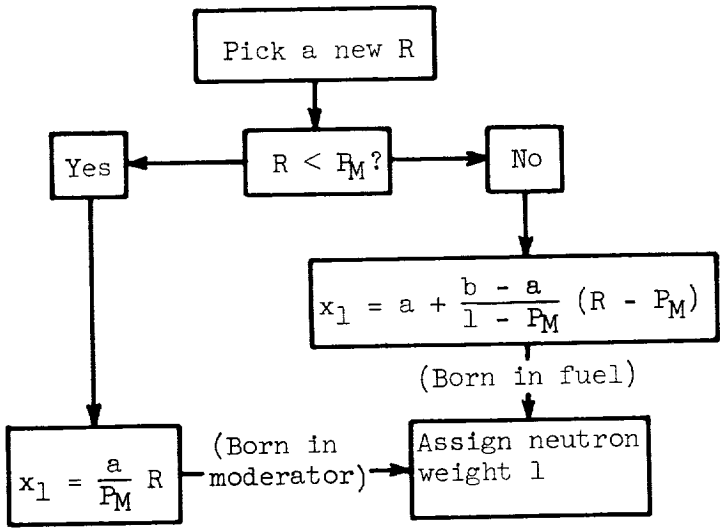

Having determined μ_1 and x_1, it is now necessary to determine the energy E_1. Suppose that the collision has taken place in the absorber. The following procedure determines the type of nucleus hit. The probability that interaction was with i^{th} type nucleus is

$$P_i = \frac{S_i^{II}}{S_1^{II} + S_2^{II} + S_3^{II}} \qquad i = 1,2,3$$

Using equation (3) there follows

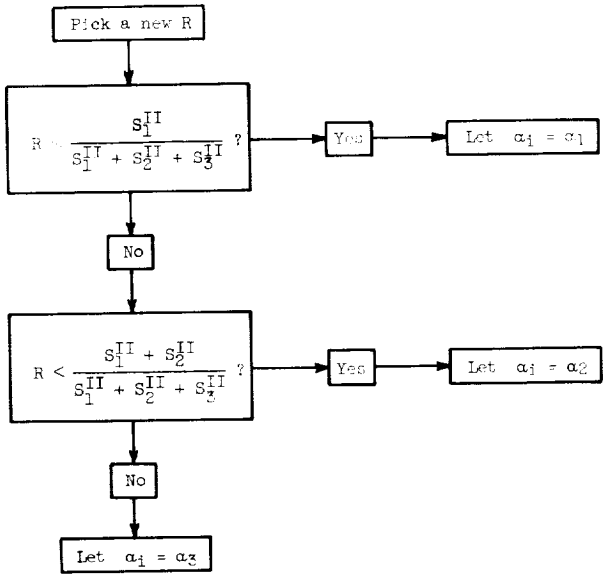

In the moderator the procedure is

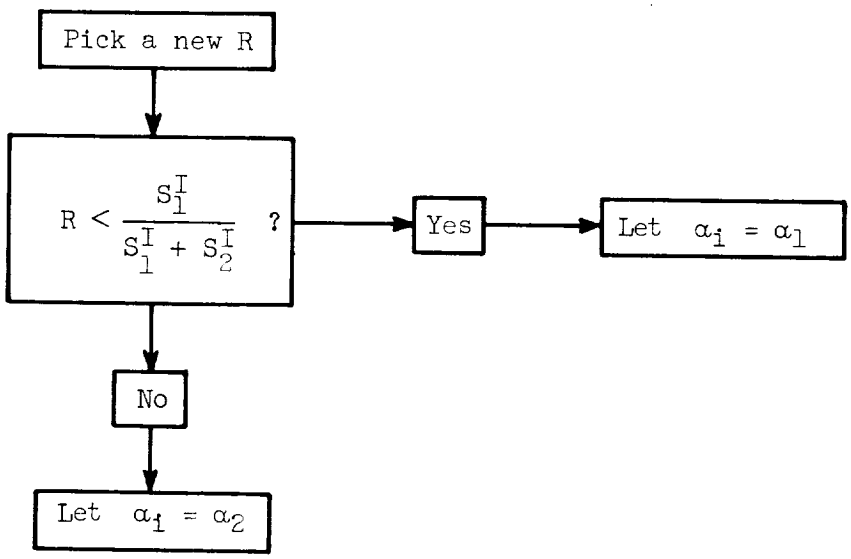

With the nuclear target known, the laws of elastic scattering and isotropic scattering in the center of mass system lead to the following procedure for picking E_1. The probability per cubic centimeter per second that a neutron will enter dE_1 about E_1 if it scattered from the i^{th} element is

$$\frac{S_i(E_1)dE_1}{S_i} = p_i(E_1)dE_1 = \begin{cases} \frac{1}{\xi_i E_M(1-\alpha_i)}\left(1 - \frac{\alpha_i E_M}{E_1}\right)dE_1 & \alpha_i E_M \le E_1 \le E_M \\ 0 & E_1 < \alpha_i E_M \end{cases}$$

where equations (2) and (3) have been utilized. It is readily verified that $\int_{\alpha_i E_M}^{E_M} p_i(E_1)dE_1 = 1$. The maximum value of the probability distribution in this equation is given by

$$p_{i,max} = \frac{1}{\xi_i E_M}$$

A rejection technique (ref. 9) is used to pick E_1 from the distribution $\frac{p_i(E_1)dE_1}{p_{i,max}}$.

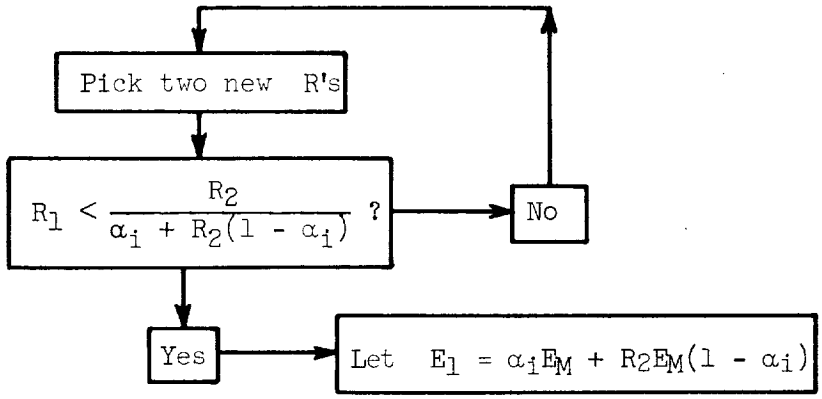

The initial neutron coordinates μ_1, x_1, and E_1 are now completely specified.

Obtaining Cross Sections as Function of Energy

The moderator cross sections have been assumed constant and are consequently no problem. However, the absorber elements with total cross sections $\Sigma_i^{II}(E)$ and $\Sigma_{s,i}^{II}(E)$ have a complicated resonance structure. The total and scattering cross sections for these elements and the fission cross section for U^{235} are stored in the machine for a sufficient number of discrete values of energy $\mathcal{E}_Q$ ($Q = 1, 2, \ldots, 536$) in order to follow the resonances accurately. The neutron energy E will generally fall between the tabulated values of $\mathcal{E}_Q$. The cross section evaluated at energy E was obtained by logarithmic interpolation between the two adjacent tabulated cross sections:

$$\left.\begin{aligned} \ln \Sigma_i^{II}(E) &= \ln \Sigma_i^{II}(\mathcal{E}_{Q-1}) + \frac{E - \mathcal{E}_{Q-1}}{\mathcal{E}_{Q-1} - \mathcal{E}_Q}\left[\ln \Sigma_i^{II}(\mathcal{E}_{Q-1}) - \ln \Sigma_i(\mathcal{E}_Q)\right] \\ \text{or} \\ \Sigma_i^{II}(E) &= \Sigma_i^{II}(\mathcal{E}_{Q-1})\left[\frac{\Sigma_i^{II}(\mathcal{E}_{Q-1})}{\Sigma_i^{II}(\mathcal{E}_Q)}\right]^{\frac{E-\mathcal{E}_{Q-1}}{\mathcal{E}_{Q-1}-\mathcal{E}_Q}} \qquad i = 1, 2 \end{aligned}\right\} \quad (7)$$

This proved more accurate than linear interpolation. The scattering and fission cross sections were evaluated similarly.

Obtaining x-Coordinates of Successive Collisions

The x-coordinate of the $(K + 1)^{th}$ collision point is given in terms of the x-coordinate of the K^{th} collision point by

$$\left.\begin{aligned} x_{K+1} &= x_K + r\mu_K \qquad K = 1, 2, \ldots \\ r &= -\frac{1}{\Sigma(E)} \ln R \end{aligned}\right\} \tag{8}$$

where x_{K+1} does not fall outside the region of x_K; and where r is the distance between the successive collision points x_K, x_{K+1} at the angle $\cos^{-1}\mu_K$; μ_K is the direction cosine of the neutron velocity vector after the K^{th} collision; $\Sigma(E)$ is the total cross section of the region; and R is a random number.

If x_{K+1} falls outside the region of x_K bounded by a surface with coordinate x_S, then the neutron calculation must be altered at x_S with $\Sigma(E)$ replaced by $\Sigma'(E)$ beyond x_S. The direction μ_K and energy E_K remain unchanged. A new random number R' is picked and x_{K+1} in the "primed" region is calculated as

$$\left.\begin{aligned} x_{K+1} &= x_s + r'\mu_K \\ r' &= -\frac{1}{\Sigma'(E)} \ln R' \end{aligned}\right\} \tag{9}$$

Cell Boundary Conditions

Denoting the transport flux by $F(x,\mu,E)$ and the lines of symmetry $x = 0, \pm b, \pm 2b$ (sketch (a)) by x_{sym}, the following conditions on the transport flux apply to a repetitive slab lattice:

$$F(x,\mu,E) = F(-x,-\mu,E) \tag{1}$$

$$F(x,\mu,E) = F(2x_{sym} - x,-\mu,E) \tag{2}$$

$$F^{I}(a,\mu,E) = F^{II}(a,\mu,E)$$

Conditions (1) and (2) were utilized in the Monte Carlo calculation as follows. A neutron inside the fuel at x with direction cosine $\mu < 0$ was replaced by an equivalent neutron at $2b - x$ with direction $|\mu|$. A neutron arriving at $x = 2b - a$ with direction $\mu > 0$ was replaced by an equivalent neutron at $x = -a$ with direction μ. A neutron

inside the moderator at x, with direction $\mu < 0$, was replaced by an equivalent neutron at $-x$ with direction $+|\mu|$. In this manner neutrons were always followed toward the right.

Determining Target Nucleus Hit

When a neutron of energy E_K and weight w_K collides and scatters, the procedure for determining the target nucleus hit for three types of nuclei with atomic masses A_i is as follows:

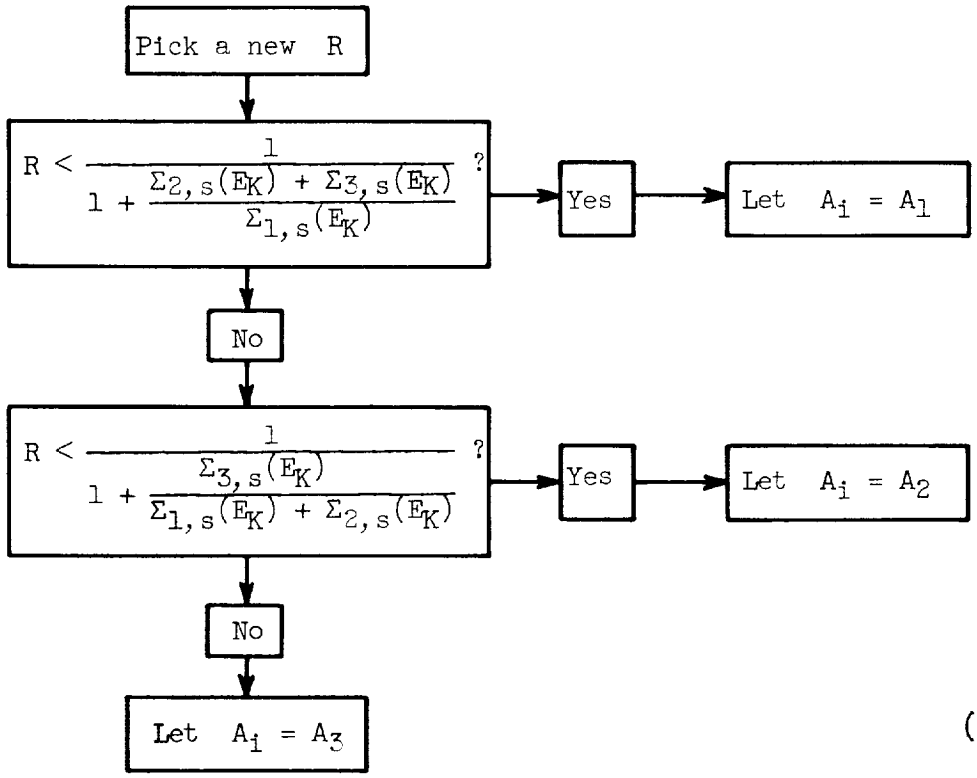

(10)

In the moderator, $\Sigma_{3,s} = 0$ because there are only two elements present, and equation (10) still applies but with the scattering cross sections being given as constants. In the absorber region, the variation of cross section with energy is determined in accordance with the discussion leading up to equation (7).

Statistical Estimation of A Priori Fuel Absorption

For purposes of efficiency and accuracy, whenever a neutron has made its previous or K^{th} collision in the fuel followed by its $(K + 1)^{th}$ collision in the fuel with the i^{th} element, the collision is assumed to be a scattering collision and the emergent neutron is properly weighted as

$$w_{K+1} = w_K \frac{\Sigma^{II}_{s,i}(E_K)}{\Sigma^{II}_{i}(E_K)} \tag{11a}$$

where w_K is its weight immediately after the K^{th} collision. If the i^{th} type of nucleus is U^{235} $(i = 2)$, the fraction of the incident neutron resulting in fissions is

$$w_F = w_K \frac{\Sigma^{II}_{F,2}(E_K)}{\Sigma^{II}_{2}(E_K)} = w_{K+1} \frac{\Sigma^{II}_{F,2}(E_K)}{\Sigma^{II}_{s,2}(E_K)} \tag{11b}$$

where $\Sigma^{II}_{F,2}(E_K)$ is the macroscopic fission cross section of U^{235} at energy E_K.

Suppose, however, that the K^{th} collision has taken place at position x_K in the moderator. Since there is no moderator absorption, $w_K = w_{K-1}$. Suppose that energy E_K and direction μ_K after the collision have been determined. The a priori fraction of w_{K-1} that will make the $(K + 1)^{th}$ collision in the nearest absorber slab at energy E_K and direction $\mu_K > 0$ and be absorbed there is

$$w_a = w_{K-1} e^{-\frac{\Sigma^{I}(a-x_K)}{\mu_K}} \left[1 - e^{-\Sigma^{II}(E_K)\frac{2(b-a)}{\mu_K}} \right] \frac{\Sigma^{II}_{a}(E_K)}{\Sigma^{II}(E_K)} \tag{12a}$$

and the weight of the neutron at x_K is adjusted to

$$w_K = w_{K-1} - w_a \tag{12b}$$

The physical meaning of each term in equation (12a) is apparent.

Dropping the subscript K, these remaining w neutrons at x, μ, E (eq. (12b)) will be divided as follows with regard to the next or $(K + 1)^{th}$ collision:

(1) w_M of the w neutrons at x_K will make their next collision in the region $x_K < x < a$ (μ is positive) without reaching the absorber region (see fig. 1).

(2) w_s of the w neutrons at x_K will go directly to the absorber and scatter there.

(3) w_{fe} of the neutrons at x_K will escape the moderator and the absorber and thus reenter the moderator at $x = 2b - a$ (sketch (a)). Thus

$$\left.\begin{aligned} w &= w_M + w_s + w_{fe} \\ w_s &= w_a \frac{\Sigma_s^{II}(E_K)}{\Sigma_a^{II}(E_K)} \\ w_M &= w_{K-1}\left[1 - e^{-\frac{\Sigma^I(a-x_K)}{\mu_K}}\right] \end{aligned}\right\} \qquad (12c)$$

After subtracting the a priori fuel absorption w_a from the original w_{K-1} neutrons at x_K, the remaining w neutrons see a different probability of making their next collision in the moderator or in the absorber. In particular, the probabilities of directly colliding in the absorber before and after this weight reduction are $(w_a + w_s)/w_{K-1}$ and w_s/w_K respectively.

As discussed in the section Cell Boundary Conditions, neutrons in the Monte Carlo calculation are always followed toward the right with a positive μ. Whenever a neutron escapes from the fuel at $x = 2b - a$, it is placed at $x = -a$ with the same μ, and its weight is reduced according to equation (12b). A neutron escaping from the absorber at $x = a$ is placed at $x = -a$ with the direction reversed and then w_a is subtracted out. A neutron inside the absorber or the moderator having a negative direction is transferred to the mirror image point and the sign of μ is reversed in accordance with the discussion in the section Cell Boundary Conditions. Thus, the weight of the neutron is reduced by w_a after it has collided inside the moderator or after it has reached the moderator boundary from inside the absorber. It is weighted according to equation (11a) only after two consecutive collisions within the absorber.

Given then a neutron of weight w_{K-1}, energy E_K, and direction $\mu_K > 0$ at $x_K = -a$ or at some point inside the moderator, the Monte Carlo procedure is as follows:

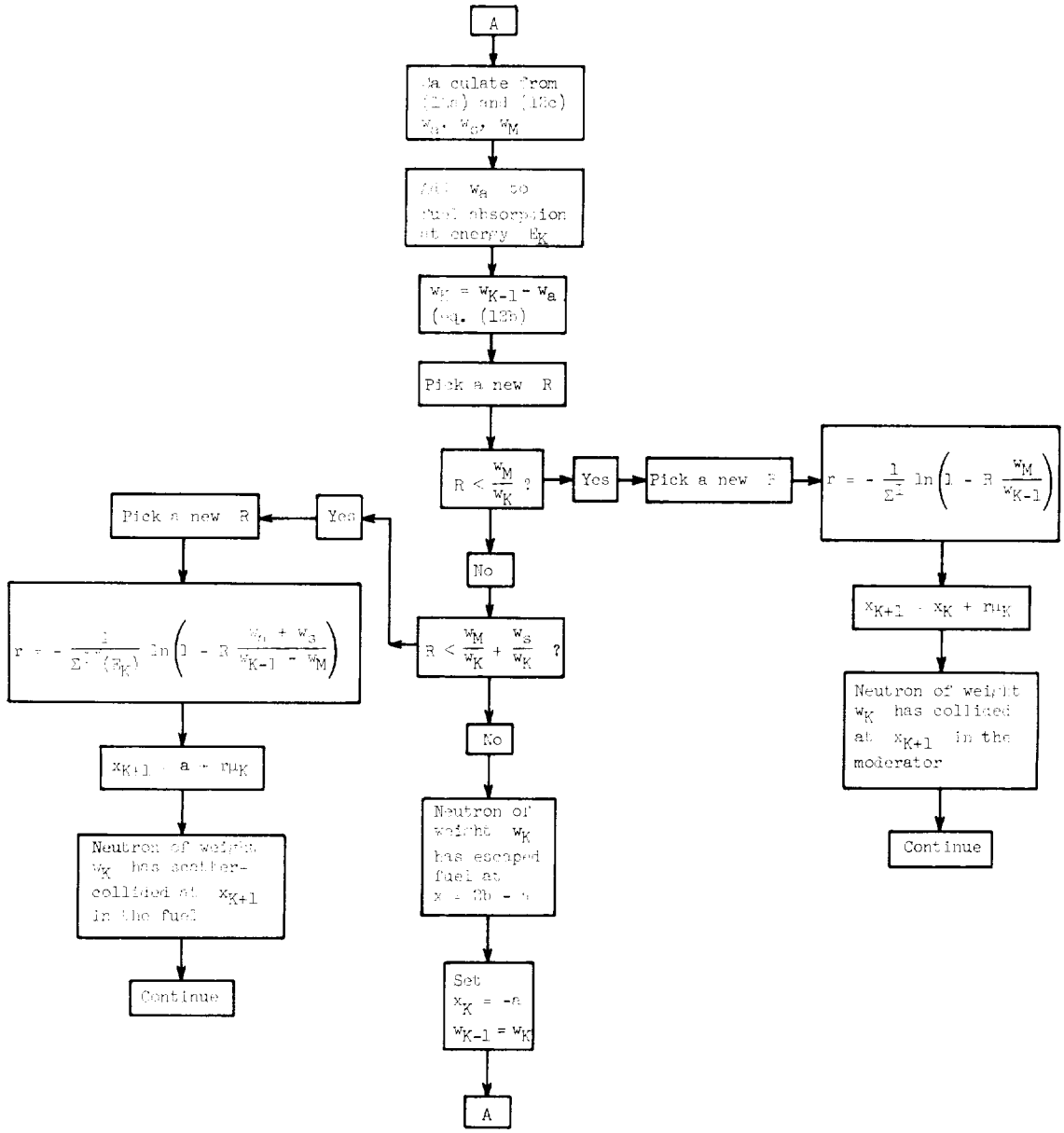
A
Calculate from (12a) and (12c) w_a, w_s, w_M
Add w_a to fuel absorption at energy E_K
$w_K = w_{K-1} - w_a$ (eq. (12b))
Pick a new R
$R < \frac{w_M}{w_K}$?
Yes
Pick a new R
$r = -\frac{1}{\Sigma^-} \ln\left(1 - R \frac{w_M}{w_{K-1}}\right)$
$x_{K+1} = x_K + r\mu_K$
Neutron of weight w_K has collided at x_{K+1} in the moderator
Continue
No
$R < \frac{w_M}{w_K} + \frac{w_s}{w_K}$?
Yes
Pick a new R
$r = -\frac{1}{\Sigma^-(E_K)} \ln\left(1 - R \frac{w_a + w_s}{w_{K-1} - w_M}\right)$
$x_{K+1} = a + r\mu_K$
Neutron of weight w_K has scatter-collided at x_{K+1} in the fuel
Continue
No
Neutron of weight w_K has escaped fuel at $x = 2b - a$
Set $x_K = -a$ $w_{K-1} = w_K$
A

Thus, the neutron of reduced weight w_K scatters in the absorber, for example, with the correct frequency w_S/w_K. The remainder of this branch in the block diagram consists of a technique that forces this neutron to attenuate exponentially and yet remain confined within the absorber. An equivalent method of achieving "restricted exponential attenuation" for this branch would be

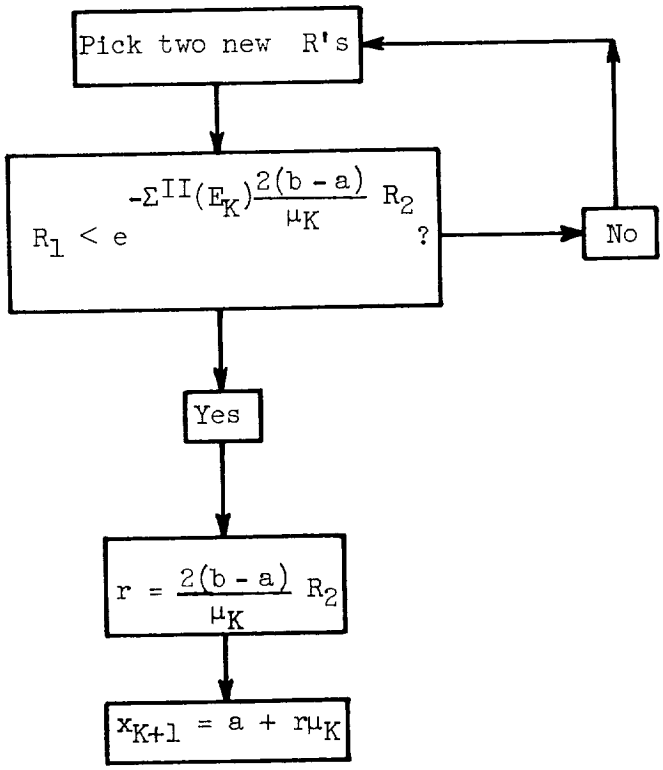

The difficulty here would be that, for $\mu_K \sim 0$, the rejection technique becomes very inefficient and would consequently need modification.

Obtaining Neutron Energy After Elastic Collision

If a neutron of energy E_K has elastically scattered from the i^{th} element of mass A_i and the scattering is isotropic in the center of mass system, the probability that the neutron will emerge with an energy in dE about E is

$$f(E)dE = \begin{cases} \dfrac{dE}{E_K(1-\alpha_i)} & \alpha_i E_K \le E \le E_K \\ 0 & \text{otherwise} \end{cases}$$

where

$$\alpha_i = \frac{(A_i - 1)^2}{(A_i + 1)^2}$$

The expression for $f(E)dE$ implies that E occurs uniformly between $\alpha_i E_K$ and E_K. Hence the procedure is

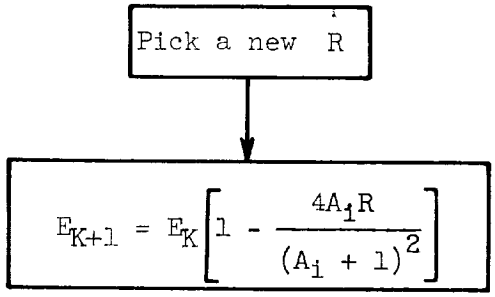

(13)

Obtaining Cosine of Angle Between Neutron Velocity Vector and x-axis After Anisotropic Scattering Collision

In appendix A it is proven that μ_{K+1} is given by

$$\mu_{K+1} = \mu_K \mu_L + \sqrt{(1 - \mu_K^2)(1 - \mu_L^2)}\cos\beta \qquad (14)$$

where μ_L is the cosine of the scattering angle in the laboratory system and β is the azimuthal angle of the scattering (sketch (d)) about the original direction of neutron travel before the scattering. Formulas to determine the azimuthal angle of the neutron velocity vector in the y,z-plane are also derived in appendix A; they are not needed in this Monte Carlo calculation, but in configurations where two angular coordinates are required to specify the neutron velocity vector.

The scattering is isotropic in the center of mass system, and the azimuthal angle β is uniformly distributed between $-\pi$ and π. Letting R denote the same random number that was used in equation (13), the procedure is

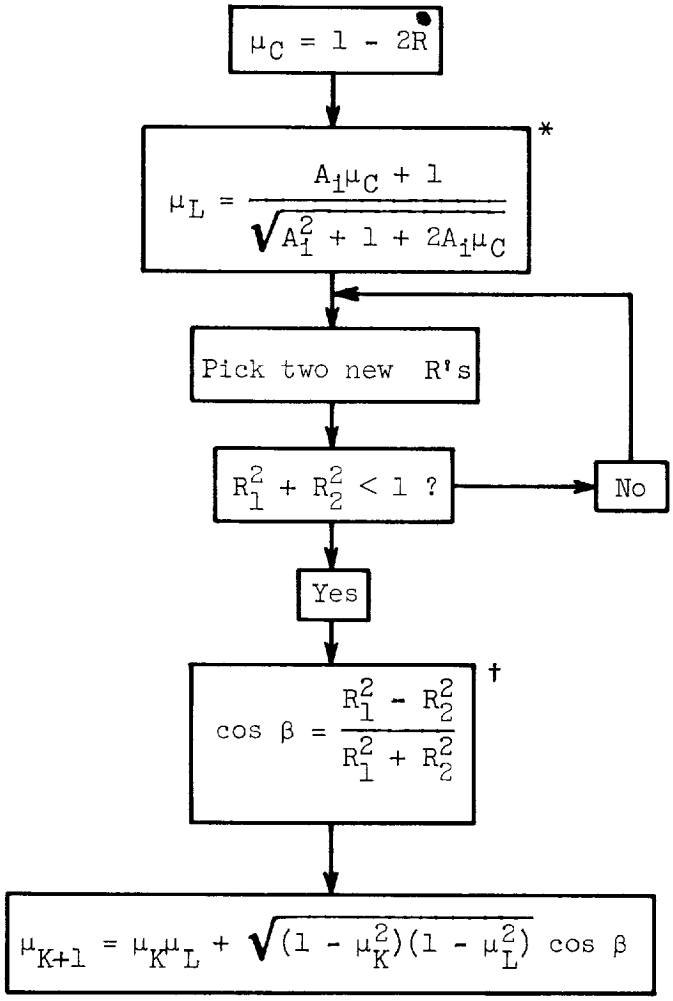

A complete block diagram and IBM 704 Monte Carlo code are given in detail in appendix C.

RESULTS AND DISCUSSION

The IBM 704 machine time required per thousand histories was 15 minutes for the lithium hydride or water moderated cases and 50 minutes for the beryllium oxide cases. (Approximately five times as many collisions

*This is the relation between the cosine of the scattering angle in the laboratory system and the cosine of the angle in the center of mass system.

†From reference 9 for picking from a random cosine distribution.

per history occur in beryllium oxide.) Six thousand histories were run for most of the lithium hydride or water moderated cases and 2000 histories for beryllium oxide.

Figure 1 shows the lowest lying resonances of tungsten (up to 25 ev) and the peak values of the absorption and scattering cross sections. These resonances are responsible for more than 60 percent of the total resonance absorption over the range of tungsten thicknesses considered.

Figure 2 shows $P(E)$ plotted against E for 4 inches of lithium hydride moderator and several thicknesses of tungsten. The location and peak values of the more significant tungsten resonances are indicated by the vertical lines. Each vertical jump corresponds to the peak of a resonance. The absorptions per history between E_1 and $E_2 (E_1 > E_2)$ are given by $P(E_1) - P(E_2)$, from which the absorptions attributable to each resonance are readily obtained. The bulk of the absorptions occur below 25 electron volts, but, as the tungsten thickness increases, there is a progressively larger percentage of absorptions above 25 electron volts. This is seen from tables I to IV which summarize much of the Monte Carlo study for tungsten. These tables give the number of neutrons absorbed in the various specified energy intervals for several thicknesses of water, lithium hydride, or beryllium oxide moderator and a range of tungsten thicknesses. Also presented are the peak absorption and scattering cross sections in the various energy intervals and the fraction of the total dilute resonance absorption integral occupied by each interval.

From the tungsten cross-section data in reference 4, the total dilute resonance absorption integral between 257 electron volts and 1.20 and 0.125 electron volt was evaluated analytically using logarithmic interpolation between successive points at a total of 536 energy values (appendix B). The result to 1.20 and 0.125 electron volt was 315 and 346 barns, respectively, including the $1/v$ contribution.

Figures 3 to 5 show the resonance escape probability from 961 to 1.20 electron volts (called P) as a function of tungsten thickness t_w in mils. The figures are for given thicknesses of water, lithium hydride, and beryllium oxide moderator, respectively.

The value of P decreases with increasing tungsten thickness and with decreasing plate separation. This is to be expected, because neutrons spend progressively more time in the absorber region. The lithium hydride moderators, having moderating properties similar to water, yield nearly equal values of P. The beryllium oxide moderated cases yield much lower values of P for the same tungsten thickness because a neutron makes approximately five times as many collisions to slow down in beryllium oxide as in lithium hydride or water. The cell

interaction effects of 4 inches of moderator were found to be completely negligible. There are good indications that this is still true at 1 inch of lithium hydride or water moderator, which is about 4 mean free paths.

Figure 6 shows how the resonance escape probability correlates as a function of the moderator slowing-down parameter $\bar{\xi}\Sigma_T t_M$ for various absorber thicknesses. In this parameter, $\bar{\xi}$ is the average logarithmic energy decrement and $\Sigma_T t_M$ is the mean free path thickness of the water, lithium hydride, or beryllium oxide moderator. Notice that this parameter involves in the denominator the average number of collisions to slow down from E_{max} to E_{min}, namely, $\Delta u/\bar{\xi}$ where Δu equals $\ln\left(\frac{E_{max}}{E_{min}}\right)$. Thus, for a given tungsten thickness, different moderators having equal $\bar{\xi}\Sigma_T t_M$ values will have roughly equal values of the resonance escape probability. Appendix D indicates how this parameter may be derived.

Figure 7 and table IV show the effect of the temperature of the tungsten or Doppler broadening on the resonance escape probability for 4 inches of water moderator and 8, 80, and 160 mils of tungsten. In general, P is lowered or absorptions increase with higher absorber temperatures, and this progressively lowers the peak cross sections of the resonances but increases the cross sections in the wings. The anomalous behavior at 0.0253 electron volt and 80 mils is evidently statistical. For the cases run, however, the effect of Doppler broadening is seen to be small, on the order of 3 to 5 units in the third digit of P for kT = 0.5 electron volt (20 times room temperature). This effect may become more severe for lower values of P.

Figure 8 shows how the resonance escape probability after H histories deviates from the final value of P arbitrarily taken at 6000 histories. The curves shown are primarily for 1.8 inches of water moderator and a range of tungsten thicknesses. The corresponding values of P after 6000 histories are listed in the figure. As the 6000-history answer is approached, the statistical fluctuations in the accumulating value for P for the last several thousand histories lie within 2 units in the third digit of P.

Comparison of Experimental and Monte Carlo Results

Figure 9 shows the experimental epi-cadmium absorptions (above 0.6 ev) plotted against the tungsten thickness and compared with the Monte Carlo results. The experimental results were obtained from measurements performed with the NASA solution reactor; the preliminary details of these experiments are discussed in reference 5. In these experiments, the relative reactivities of samples of various thicknesses located at

E-1434

the center of the reactor were measured. The experimental absorptions are normalized to the Monte Carlo absorptions at 0.8 mil of tungsten. Agreement over four decades from 1/10 to 160 mils (the largest tungsten foil measured) is seen to be excellent and within the statistical fluctuations of the Monte Carlo method and experimental error.

Figure 10 shows the experimental epi-cadmium absorptions plotted against gold thickness and compared with the Monte Carlo results for the 4-inch water moderated cases. Agreement is again excellent within statistical and experimental error with the possible exception of the 90-mil point, which is 15 percent lower than the experimental value. The gold foils were 1-inch-diameter disks, and at a thickness of 90 mils edge effects may no longer be negligible.

The Monte Carlo model differs from the experimental setup in the following ways:

(1) The calculation assumes a repetitive lattice, whereas the experiment considers a single foil in an effectively infinite medium.

(2) The moderator is nonabsorbing and nonfissile in the calculation, but not in the experiment, where the composition of the moderator is a solution of uranylfluoride and water.

(3) The calculation assumes semi-infinite slabs, finite only in thickness, whereas the experimental foils are rectangular parallelepipeds (5.06 cm^2 in area on the plane perpendicular to the thickness).

The first condition is removed by comparison with the 4-inch water (or lithium hydride) moderated cases for which the cell interaction effects are completely negligible.

The second condition is probably a small effect because the ratio of atoms of U^{235}, U^{238}, and fluorine to atoms of hydrogen and oxygen in water is about 1/500 in the NASA solution reactor.

In all but the thickest tungsten or gold samples, the area of the edges is small in comparison with the area of the plane perpendicular to the thickness. Thus, the last condition may be a second or higher order effect. The Monte Carlo absorption curves of figures 9 and 10 are quite sensitive to the tungsten and gold cross section input data.

Discussion of Tables

Allowing for statistical error, it is seen from tables I to III that, as the tungsten thickness approaches zero, the percentage absorption in a given energy band approaches the percentage of the total dilute resonance absorption integral occupied by that energy band.

The region from 1.20 to 0.125 electron volt is predominantly 1/v absorptive. From the tungsten tables it is seen that the ratio of absorptions in this range to the total absorptions increases from about 5 percent at 0.126 mil to 25 percent at 160 mils. Similarly the percentage absorption in the higher-energy resonances (above 40.3 ev) increases from about 8 percent at 0.126 mil to 25 percent at 160 mils. The larger resonances decrease in importance as the tungsten thickness increases.

Table V presents the absorptions in various energy intervals for 4 inches of water moderator and several slab thicknesses of gold at room temperature. Also presented are the corresponding peak absorption and scattering cross sections. These energy intervals were generally chosen to span the individual more important gold resonances from "valley to valley."

The total dilute resonance absorption integral of gold was calculated to be 1558 barns from 961 to 0.6 electron volt. Approximately 96 percent of this total value occurs in the huge predominantly absorptive resonance at 5 electron volts that occupies the energy band from 10 to 1.4 electron volts in table V. It is seen that this resonance causes 96 percent of the absorptions at a thickness of 0.08 mil and 66 percent of the absorptions at 90 mils. As in tungsten, a progressively larger percentage of the total absorptions occurs in the 1/v energy region and at higher energy resonances with increasing thicknesses of gold.

Examination of the detailed 108-energy-band output (not included herein) for the various thicknesses of tungsten (or gold) shows that absorptions in the peak areas of the resonances saturate out in the first few mils of thickness. As the tungsten or gold thickness increases, the slab becomes progressively grayer to neutrons in the wings and finally black for sufficiently large thicknesses, at which time the levels of the valleys and the 1/v absorptions become predominant. This can also be observed from the tables, where it is interesting to note how the various resonances self-shield.

Figure 11 shows the absorptions in the 4.1- and 18.8-electron-volt resonances as a function of tungsten thickness. The huge scattering absorptive resonance at 18.8 electron volts is strongly self-shielding with increasing tungsten thickness. The energy band from 20.7 to 16 electron volts includes much of the wings of this resonance and causes 36 percent of the total absorptions at 0.126 mil of tungsten and only 10 percent of the total at 160 mils. The corresponding percentages for the predominantly absorptive resonance at 4.1 electron volts (5.7 to 2.3 ev) range from 29 percent at 0.126 mil to 22 percent at 160 mils, which is relatively weak self-shielding.

In addition to causing stronger self-shielding, the scattering portion of the 18.8-electron-volt resonance "albedos" many of the incident neutrons back into the moderator, where they escape resonance capture. The remainder are trapped within the tungsten, where they scatter about for many collisions with the fraction $\frac{\Sigma_a^W(E)}{\Sigma_t^W(E)}$ being absorbed per collision.

Suppression of Scattering

Thick and thin tungsten cases were rerun with the scattering suppressed at all energies; that is, Σ_t was reduced by Σ_s and then Σ_s was set equal to zero. This resulted in 25 percent more absorptions in the 18.8-electron-volt resonance for the 0.8-mil case and 75 percent more absorptions for the 80-mil case. However, P(961 → 0.125 ev) decreased only slightly in all cases tried because the 18.8-electron-volt resonance is not the dominant absorber for thick samples. In the 80-mil tungsten case, P was lowered by 4 units in the third digit. The absorptions in the scattering resonances above 40.3 electron volts were significantly affected by suppression of the scattering, but this did not seriously affect the overall value of P because relatively few absorptions occur in these resonances.

Notice that suppression of the scattering introduces compensating effects. The lowering of Σ_t increases the probability of transmission through the slab. Setting $\Sigma_s = 0$ makes every collision in tungsten an absorption. The net effect is a slightly greater absorption or lower value of P. However, suppression of scattering is a poor approximation for a huge predominantly scattering resonance such as the one at 18.8 electron volts in tungsten and other predominantly scattering resonances (above 40.3 ev).

Analytical Results

Appendix D and table VI demonstrate the analytical prediction of total absorption to 1.20 and 0.125 electron volt for a pure 1/v absorbing region in a repetitive lattice where cell interaction effects are negligible. A thermal absorption cross section of 18.8 barns was assumed in table VI.

Considering the statistical fluctuations of the Monte Carlo results in table VI (4000 histories), agreement is seen to be excellent despite the fact that the analytical results are consistently higher. Perhaps this indicates the existence of small flux depression effects, which are automatically considered in the Monte Carlo calculations, but not in equation (D4). Note that the moderator correlation displayed in figure 6 appears in equation (D5) with a small correction term.

This same model, with the additional approximation of suppression of the scattering, is applied in appendix E to predicting resonance absorption (eq. (E11)). Table VII gives the results of this calculation for a 4-inch-water moderator and several thicknesses of tungsten. Comparison with the Monte Carlo results of table I(d) shows that agreement is generally good except in the 18.8-electron-volt scattering resonance and in some scattering resonances above 40.3 electron volts.

To avoid the suppression of the scattering approximation, equation (E7) may be integrated by performing the identical interpolation on $\kappa(u)$ in the interval $u_Q \rightarrow u_{Q+1}$ as was performed on $\kappa_a(u)$ in this interval (eq. (E9)), and then eliminating u, du, and $\kappa_a(u)$ in terms of $\kappa(u)$, $d\kappa(u)$, $\kappa(u_Q)$, and $\kappa(u_{Q+1})$. The resulting expression can be integrated from $\kappa(u_Q)$ to $\kappa(u_{Q+1})$. Supposing that the true moderator flux is very nearly uniform and $1/E$, this treatment accorded to equation (E7) should yield the correct first-collision absorptions in the absorber region. For a resonance that is also strongly scattering, additional absorptions will result from successive multiple scattering collisions within the absorber region. Thus suppression of the scattering (eq. (E11)) gives the upper bound to the absorption in the interval $u_Q \rightarrow u_{Q+1}$, and this treatment should yield the correct lower bound, providing that the moderator flux is actually that which has been assumed.

Uncorrelating Energy and Angle

Prediction of resonance escape probabilities by analytical methods can be very greatly simplified if the energy and angle correlation of the scattering can be uncoupled. In order to obtain some measure of the error introduced by this approximation, two cases were run with the energy and angle uncoupled and all scattering isotropic in the laboratory system. For a 1-inch water moderator and 8 and 80 mils of tungsten, P changed from 0.961 to 0.965 (2000 histories) and from 0.873 to 0.877 (4000 histories). Thus, an analytical treatment incorporating these simplifying assumptions should be able to predict resonance escape probabilities resonably well, provided that the configuration or model calculated is physically similar.

Lewis Research Center
National Aeronautics and Space Administration
Cleveland, Ohio, November 24, 1961

APPENDIX A

CALCULATION OF NEUTRON DIRECTION AFTER ANISOTROPIC SCATTERING COLLISION

In sketches (c) and (d), $\vec{\Omega}'$ is the unit velocity vector before the collision and $\vec{\Omega}$ is the unit velocity vector after the collision.

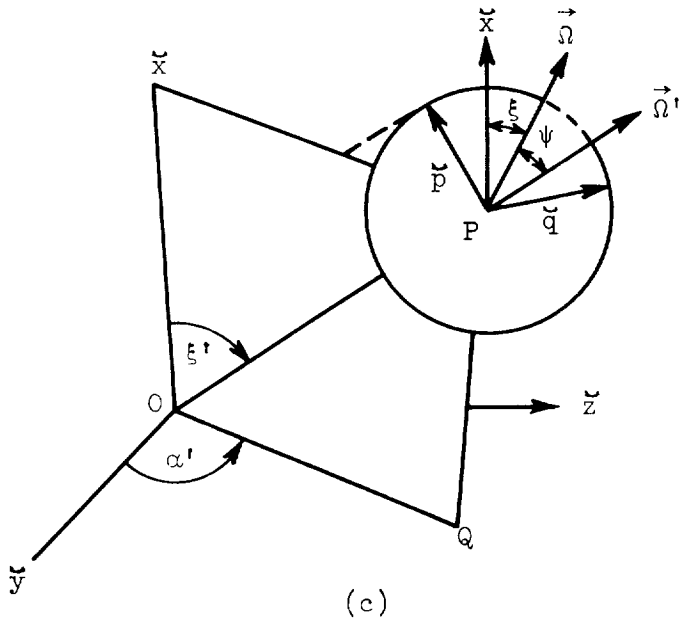

(c)

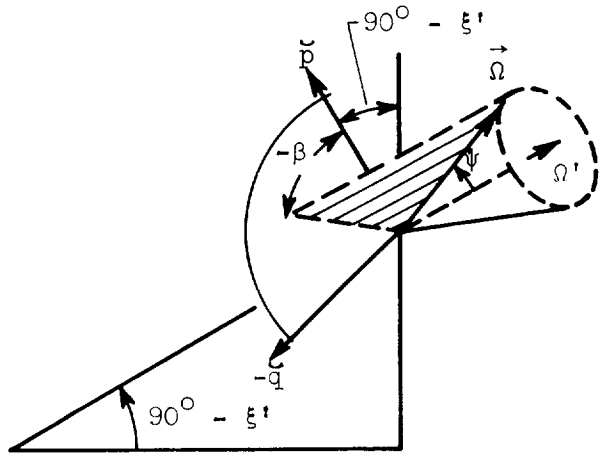

(d)

ψ is the angle between $\vec{\Omega}'$ and $\vec{\Omega}$, and $\vec{\Omega} \cdot \vec{\Omega}' \equiv \mu_L = \cos \psi$. The polar angles that $\vec{\Omega}'$ and $\vec{\Omega}$ make with the x-axis are respectively denoted by ξ' and ξ, whereas the azimuthal angles these vectors make in the y,z-plane are α' and α. The symbols $\breve{p}$ and $\breve{q}$ denote orthogonal unit vectors in a plane perpendicular to $\vec{\Omega}'$; $\breve{p}$ is in the plane formed by OPQ. In sketch (d) β is the azimuthal angle of $\vec{\Omega}$ measured in a plane perpendicular to the OPQ plane. Finally, $\breve{x}$, $\breve{y}$, and $\breve{z}$ represent unit vectors along the x-, y-, and z-axes of the basic reference system. From sketches (c) and (d) it is seen that

$$\vec{\Omega} = \breve{x} \cos \xi + \breve{y} \sin \xi \cos \alpha + \breve{z} \sin \xi \sin \alpha \tag{A1}$$

$$\left.\begin{aligned} \vec{\Omega}' &= \breve{x} \cos \xi' + \breve{y} \sin \xi' \cos \alpha' + \breve{z} \sin \xi' \sin \alpha' \\ \breve{p} &= \breve{x} \sin \xi' - \breve{y} \cos \xi' \cos \alpha' - \breve{z} \cos \xi' \sin \alpha' \\ \breve{q} &= -\breve{y} \sin \alpha' + \breve{z} \cos \alpha' \end{aligned}\right\} \tag{A2}$$

$$\vec{\Omega} = \vec{\Omega}' \cos \psi + \breve{p} \sin \psi \cos \beta + \breve{q} \sin \psi \sin \beta \tag{A3}$$

Equations (A2) substituted into (A3) yield

$$\begin{aligned} \vec{\Omega} = \breve{x}&(\cos \xi' \cos \psi + \sin \xi' \cos \beta \sin \psi) + \breve{y}(\sin \xi' \cos \alpha' \cos \psi \\ &- \cos \xi' \cos \alpha' \cos \beta \sin \psi - \sin \alpha' \sin \beta \sin \psi) \\ &+ \breve{z}(\sin \xi' \sin \alpha' \cos \psi - \cos \xi' \sin \alpha' \cos \beta \sin \psi \\ &+ \cos \alpha' \sin \beta \sin \psi) \end{aligned} \tag{A4}$$

Taking the dot product $\vec{\Omega} \cdot \breve{x}$ in equations (A1) and (A4) gives

$$\cos \xi = \cos \xi' \cos \psi + \sin \xi' \sin \psi \cos \beta$$

which in the notation of the text is

$$\mu_{K+1} = \mu_K \mu_L + \sqrt{(1 - \mu_K^2)(1 - \mu_L^2)} \cos \beta \tag{A5}$$

Taking the dot products $\vec{\Omega} \cdot \breve{y}$ and $\vec{\Omega} \cdot \breve{z}$ in equations (A1) and (A4) yields the relations

$$\begin{aligned} \sin \xi \cos \alpha = &\sin \xi' \cos \alpha' \cos \psi - \cos \xi' \cos \alpha' \cos \beta \sin \psi \\ &- \sin \alpha' \sin \beta \sin \psi \end{aligned} \tag{A6a}$$

$$\sin\xi \sin\alpha = \sin\xi' \sin\alpha' \cos\psi - \cos\xi' \sin\alpha' \cos\beta \sin\psi + \cos\alpha' \sin\beta \sin\psi \qquad \text{(A6b)}$$

Multiplying equation (A6a) by $\sin\alpha'$ and (A6b) by $\cos\alpha'$ and subtracting give

$$\sin(\alpha - \alpha') = \frac{\sin\beta \sin\psi}{\sin\xi}$$

Multiplying equation (A6a) by $\cos\alpha'$ and (A6b) by $\sin\alpha'$ and adding give

$$\cos(\alpha - \alpha') = \frac{\sin\xi' \cos\psi - \cos\xi' \cos\beta \sin\psi}{\sin\xi}$$

In the notation of the text these relations become

$$\left.\begin{aligned} \sin(\alpha_{K+1} - \alpha_K) &= \sqrt{\frac{(1 - \mu_L^2)}{(1 - \mu_{K+1}^2)}} \sin\beta \\ \cos(\alpha_{K+1} - \alpha_K) &= \mu_L \sqrt{\frac{1 - \mu_K^2}{1 - \mu_{K+1}^2}} - \mu_K \sqrt{\frac{1 - \mu_L^2}{1 - \mu_{K+1}^2}} \cos\beta \end{aligned}\right\} \qquad \text{(A7)}$$

Either of equations (A7) may be used to determine the azimuthal angle of the neutron velocity in the x, y, z coordinate system after the K^{th} collision. Clearly, it is unnecessary to determine the azimuthal angle in the Monte Carlo calculations undertaken in this paper.

APPENDIX B

NUMERICAL EVALUATION OF DILUTE RESONANCE ABSORPTION INTEGRAL FOR NATURAL TUNGSTEN

The dilute resonance absorption integral is defined as

$$DRAI = \int_{E_c}^{E_M} \sigma a(E)\,\frac{dE}{E} = \sum_i \int_{E_{i+1}}^{E_i} \sigma_a^i(E)\,\frac{dE}{E} \qquad (B1)$$

where $\sigma_a^i(E)$ is the microscopic absorption cross section of tungsten at energy E. Using logarithmic interpolation between the two given values σ_a^i and σ_a^{i+1},

$$\sigma_a^i(E) = \sigma_a^i \left(\frac{\sigma_a^i}{\sigma_a^{i+1}}\right)^{\frac{E-E_i}{E_i-E_{i+1}}} \qquad (B2)$$

where $E_i > E_{i+1}$. Substituting into equation (B1) gives

$$DRAI = \sum_i \int_{E_{i+1}}^{E_i} \sigma_a^i \left(\frac{\sigma_a^i}{\sigma_a^{i+1}}\right)^{\frac{E-E_i}{E_i-E_{i+1}}} \frac{dE}{E} \qquad (B3)$$

Equation (B3) becomes

$$DRAI = \sum_i \sigma_a^i \left(\frac{\sigma_a^{i+1}}{\sigma_a^i}\right)^{E_i/(E_i-E_{i+1})} \left[J\left(\frac{E_{i+1}}{E_i - E_{i+1}} \ln \frac{\sigma_a^{i+1}}{\sigma_a^i}\right) - J\left(\frac{E_i}{E_i - E_{i+1}} \ln \frac{\sigma_a^{i+1}}{\sigma_a^i}\right) \right] \qquad (B4)$$

$$J(x) = \int_x^\infty \frac{e^{-t}}{t}\,dt$$

The cross-section data for tungsten were taken from reference 4 in evaluating equation (B4). A running sum was maintained in this evaluation so that the dilute resonance absorption integral for the most important resonances could be observed (see tables I to IV). From 257 to 1.2 electron volts, equation (B4) gave a total of 315 barns, and from 257 to 0.125 electron volt a total of 346 barns.

APPENDIX C

IBM 704 MONTE CARLO CODE AND BLOCK DIAGRAM

A code has been written in Fortran for the IBM 704 to compute the resonance escape probability in an infinite slab lattice using the Monte Carlo method. The total absorptions are also directly calculated and may be compared as an internal consistency check with (1 - p). The code will, in addition, compute the percent of absorptions due to any one (specified) element of the three possible in the "fuel" and, as a run time option, the neutron flux at a maximum of 680 energy-space points. If a fissionable element is included in the "fuel," fissions as a function of energy will be listed as part of the output.

Symbols

A	moderator half-thickness, cm
ABSOX2	absorption due to element of constant cross section in "fuel"
$ABSW_i$	absorption due to nonfissionable "fuel" element in energy band i
AM	atomic mass of element neutron has struck
B	total cell (moderator + "fuel") half-thickness, cm
ELOSS	a priori probability that neutron at X_2, E_2, μ_2 in moderator will not suffer its next collision in "fuel"
EP(M)	energies for which values of P(E) will be printed as output (every HTEST number of histories)
E_{max}	maximum energy for which cross sections are read in and at which resonance escape probability P is normalized
E_{min}	lowest energy to which P is computed
E_1, E_2	old and new (current) neutron energy, respectively
FISS	fissions due to fissionable "fuel" element
HTEST	number of histories before each output
IA(1 or 0)	specifies presence (+1) or absence (0) of element number 1, moderator

IB(1 or 0)	specifies presence (+1) or absence (0) of element number 2, moderator
IC(1 or 0)	specifies presence (+1) or absence (0) of element number 1, fuel
ID(1 or 0)	specifies presence (+1) or absence (0) of element number 2, fuel
IE(1 or 0)	specifies presence (+1) or absence (0) of element number 3, fuel
K	number of collisions in given history
N	total number of output energies (1 M N)
RESCP	total resonance escape to E_{min}
R_1, R_2	random numbers
TOTK	total collisions
W_1, W_2	old and new (current) neutron weight, respectively
WLOSS	a priori probability of neutron at x_2 in moderator, with energy E_2 and direction μ_2, being absorbed in "fuel" on next collision
WLOST	a priori probability of neutron at X_2 in moderator, with energy E_2 and direction μ_2, being scattered in "fuel" on next collision
Y	fuel thickness divided by $1 - \Delta$
Z	moderator thickness divided by Δ
α	$[(A - 1)/(A + 1)]^2$, where A is atomic mass
Δ	probability of neutron's being born in moderator
μ_c	cosine of scattering angle in center-of-mass coordinates
μ_L	cosine of scattering angle in laboratory coordinates
μ_1, μ_2	cosines of old and new (or current) cosine of scattering angles, respectively
ξ_n	average logarithmic energy decrement per collision with element n

Σ_a^{II} macroscopic absorption cross section at E_2 in "fuel"

$\Sigma_{a_1}^{II}$ macroscopic absorption cross section at E_2 of element number 1 in fuel

$\Sigma_{a_3}^{II}$ macroscopic absorption cross section at E_2 of element number 3 in fuel

Σ_f^{II} macroscopic fission cross section at E_2 of element number 2 in fuel

Σ_S^{II} macroscopic scattering cross section at E_2 in "fuel"

Σ_T^{I} total (scattering) macroscopic cross section of element neutron has struck in moderator

Σ_T^{II} macroscopic total cross section at E_2 in "fuel"

Subscripts:

KOUNT energies and cross sections in table

M energies used for output (usually every fifth energy in table is an output energy)

Input

The input to the code divides, logically, into three parts, control words, energy independent nuclear and geometric constants, and energy dependent nuclear constants.

Control words. - Five words are necessary to specify the presence (1) or absence (0) of each of the two possible moderator elements and three possible fuel elements. Controls are also necessary to specify: the number of histories per output, the total number of histories per run, the number of space points and energy points at which the fluxes will be calculated, the total number of energies to which p will be calculated, the maximum and minimum energy values which a neutron may see, and the limits over which the absorptions will be summed to indicate total absorptions in certain (usually resonance) energy bands.

One work is necessary determining whether the case being run is a "start" (0) or a "restart" (1). In the latter case it is necessary to include, as part of the input, the binary cards punched as part of the

last run. The number of histories before such dumps occur is also an input word.

Energy independent constants. - The total and scattering microscopic cross sections of the moderator elements and of possibly one of the fuel elements are assumed to be energy independent and are included as part of the input. The average logarithmic energy decrement per collision ξ and $\alpha = (A - 1)^2/(A + 1)^2$ for each element must be included, as must the scattering and total microscopic cross sections above E_{max}. In addition, the atomic masses of each element present must be included.

The geometric constants include the half-width of the entire cell and the half-width of the moderator region.

Energy dependent constants. - A binary card deck containing the microscopic total and scattering cross sections of one "fuel" element and total, scattering, and fission cross sections of another "fuel" element as a function an energy table completes the input. If either element is absent, all the cross sections that pertain to it appear as zeros. The energy table must always be included and may contain no more than 676 values, ranging from E_{max} to E_{min} in descending order.

Code Description

Because of the size limitations of the IBM 704 core, the Monte Carlo code was broken into four logical elements (core loads) utilizing the "ping-pong" feature, whereby a core load is stored on tape in the manner of an open subroutine until needed. These four loads perform roughly the following services:

Core 1: Input and data editing (e.g., multiplying microscopic cross sections by atomic masses to produce macroscopic cross sections, generating internal code words for branching purposes, etc.)

Core 2: All logical operations needed to follow a neutron history as it slows down from E_{max} to E_{min} in a repetitive slab lattice, including keeping a running sum of the number of neutrons absorbed and of the number which escape absorption

Core 3: Data manipulation and output

Core 4: Dummy (Since core 4 is called after core 1 and before core 2, probably its most useful mode of operation is to modify slightly the input data and/or constants and code words to suit some specialized problem.)

The flow of the code through the core loads is as follows:

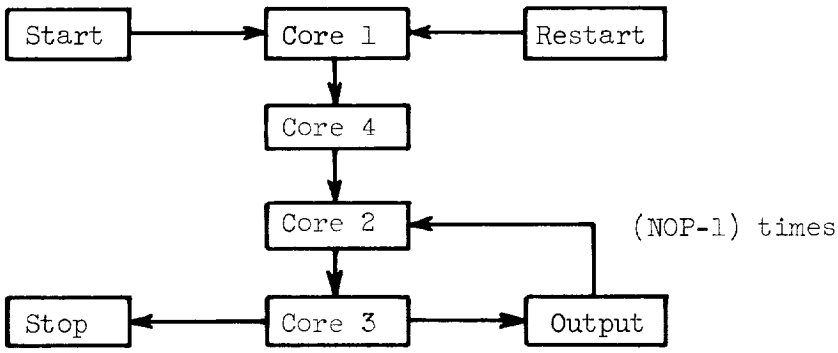

A flow diagram of the logic of core 2 is included along with a list of pertinent symbols. The diagram is self-explanatory with two exceptions. First, the assignation of α and ξ_n is done in the usual way, by comparison of a random number with the probability of striking a given nucleus. Second, the test on the overflow or underflow of a quantity x is achieved in the following manner. The new quantity $x(x - y)$ is formed, where y is involved in the calculation of x and must always, realistically speaking, be larger than x. Both x and y are greater than 0. If the new quantity $x(x - y)$ is zero or positive, an overflow or underflow is considered to have taken place. If it is negative, the value of x is accepted as it is.

Output

Under normal circumstances the output will consist of a list of input constants and parameters and certain code words and the following "machine generated" numbers:

(1) The total number of histories

(2) The maximum number of collisions a neutron has made in any one history

(3) The total collisions made

(4) The total fissions

(5) The resonance escape probability P to E_{min}

(6) Six columns of figures, listing

(a) (Arbitrarily) every fifth input energy

(b) P(E) corresponding to the listed energy value normalized to unity at E_{max}

(c) The total absorptions between each two listed energy values

(d) The absorptions in certain (specified) bands of energy

(e) The fraction of the absorption due to a (specified) "fuel" element between each pair of listed energy values

(f) The fissions as a function of energy

(7) An energy-space matrix of the fluxes

If an "alarm condition" has occurred (i.e., any condition that could send the problem to 99 in the flow chart), the information just listed will be preceded by the words ALARM CONDITION and a list of all words that could possibly have caused such a situation. In the case of an alarm condition the problem will stop with no further computation or output, whether the specified number of histories has been completed or not.

The complete block diagram and Fortran code follow.

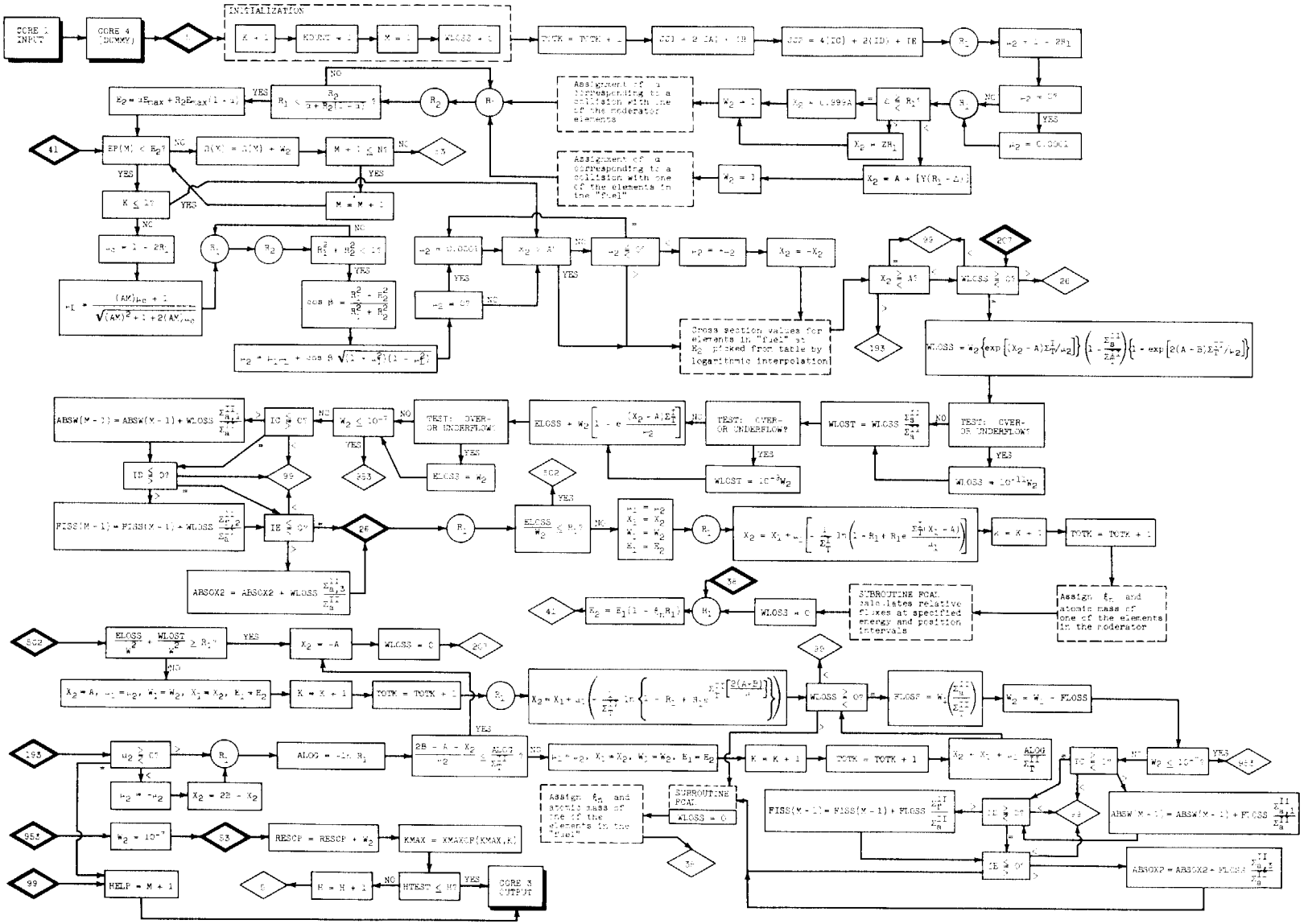
CORE 1 INPUT
CORE 4 (DUMMY)
INITIALIZATION
Assignment of a correspondding to a collision with one of the moderator elements
Assignment of a corresponding to a collision with one of the elements in the "fuel"
Cross section values for elements in "fuel" at E2 picked from table by logarithmic interpolation
SUBROUTINE FCAL calculates relative fluxes at specified energy and position intervals
Assign ξn and atomic mass of one of the elements in the moderator
Assign ξn and atomic mass of one of the elements in the "fuel"
CORE 3 OUTPUT

MONTE CARLO FORTRAN CODE

```
C     MONTE CARLO RESONANCE ESCAPE PROBLEM  CORE 1 INPUT
      DIMENSION EN(676),SIG2UT(676),SG2SUT(676),SG2FUT(676),SIG2WT(676),
     1SG2SWT(676),EP(137),OMEGA(137),ABSW(137),S(7),FISS(137),FLUX(680)
     2,NEXT(50)
      COMMON SIG2UT,SG2SUT,SG2FUT,SIG2WT,SG2SWT,EN,EP,F,FISS,FLUX
     1 ,ABSZ,ABSW,OMEGA,S, SIG1O, SIG1SO, SIG1BE,SG1SBE, SIG2O, SIG2SO,
     2  S2SUEM,S2SWEM, SG2UEM, SG2WEM, EMIN,  EMAX,  X1O, X1U, X1W, X1BE
     3 , A,B, AO,AU,ABE,AW,ALPHO, ALPHU,ALPHBE, ALPHW, DONE, CASE,N,KORA,
     4 , KORB, NUMBER,X1O1, AO1,  ALPHO1,  IA,IB,IC,ID,IE, H, HTEST,
     5 RESCP,E2, KMAX, TOTK, NOP,DELH, BMA, NM1, SIG1, SIG1S, SIG2EM,
     6 SG2SEM,DELTA,Z,Y,THETA,PHI,ETA,TEST,V,T,P,Q,XNO,XNBE,XNU,XNW,XNO1
     7,HELP,R1,R2,AMU2, KOUNT,K,RATIO ,ALPHA,SIG2E1,SG2UE1,SG2WE1,AM,
     8  XN,W1,NFL,NLX ,JFL,JDP,NDP
      COMMON       SG2SE2,SIG2E2,SG2UE2,SG2WE2,W2,NEXT,X1,AMU1,ELOSS,WLO
     1ST,FLOSS,E1,ALOG,JJ1,JJ2,X2
  301 FORMAT (8E9.5/8E9.5/8E9.5/4E9.5,2I5)
  304 FORMAT (8E9.5)
  200 FORMAT(81H1                                   MONTE CARLO RESONANCE ESCAP
     1E PROBABILITY CALCULATION//40H                                CASE NU
     2MBER F5.0)
  201 FORMAT(68H0                                   MODERATOR
     1  CELL WIDTHF8.4,18H  CM       ATOMS/CCF9.6/F103.6//105H
     2                  FUEL AND CLADDING           PER CENT         PER C
     3ENT  (BY VOLUME)  CELL WIDTHF6.3,4H  CM//94H
     4                                                                  AT
     5OMS/CCF9.6/F103.6/F103.6)
   57 READ INPUT TAPE 7,10,IA,IB,IC,ID,IE,NOP,DELH,S(7),NFL,NLX ,NDP
   10 FORMAT (6I5, 2F10.1, 3I5)
      READ INPUT TAPE7,301, SIG1O,SIG1SO,SIG1BE,SG1SBE,SIG2O,SIG2SO,S2SU
     1EM,S2SWEM,SG2UEM,SG2WEM,EMIN,EMAX,X1O,X1U,X1W,X1BE,A,B,AO,AU,ABE,
     2AW,ALPHO,ALPHU,ALPHBE,ALPHW,DONE,CASE,NUMBER,N
      READ INPUT TAPE 7,304,AN1BE,AN1O,AN2O,AN2U,AN2W,X1O1,AO1,ALPHO1
      CALL BCREAD (EN(NUMBER),SIG2UT(1))
      M=1
  403 DO 303 L=1,NUMBER,5
      EP(M)=EN(L)
  303 M=M+1
      IF (S(7)) 59,960,59
   59 CALL BC READ (S(7),S(1))
      CALL BC READ (ABSW(N),ABSZ)
      CALL BC READ (OMEGA(N),OMEGA(1))
      IF (ID) 802,801,802
  802 CALL BC READ (FISS(N), F )
  801 IF (100-NFL) 970,804,804
  804 CALL BC READ (FLUX(NLX), FLUX(1))
  970 CALL SAND (DAM)
      H=S(1)
      TOTK=S(2)
      DAM=S(3)
      RESCP=S(4)
      F=S(5)
      KMAX=S(6)
      HTEST=H+DELH
      H=H+1.
      GO TO 980
  960 CALL SAND (DAM)
      RESCP=0.
      H=1.
      TOTK=0.
      S(3)=DAM
```

```
      HTEST=DELH
  980 BMA=B-A
          NM1 = N-1
      JJ1=2*IA+IB
      JJ2=4*IC+2*ID+IE
      IF (JJ1*(JJ1-4)) 29,34,34
   34 WRITE OUTPUT TAPE 6,10,IA,IB,IC,ID,IE
      GO TO 900
   29 IF (JJ2*(JJ2-8)) 35,34,34
   35 GO TO (39,142,42), JJ1
   39 SIG1BE=0.
      SG1SBE=0.
   44 SIG1O=AN1O*SIG1O
      SIG1SO=AN1O*SIG1SO
      P=SIG1SO/SIG1O
      XNO1= (4.*AO1)/((AO1+1.)**2)
      AN1BE=0.
      GO TO 46
  142 SIG1O=0.
      SIG1SO=0.
      SIG1BE=AN1BE*SIG1BE
      SG1SBE=AN1BE*SG1SBE
      T=SG1SBE/SIG1BE
      XNBE=(4.*ABE)/((ABE+1.)**2)
      AN1O=0.
      GO TO 46
   42 SIG1O=AN1O*SIG1O
      SIG1SO=AN1O*SIG1SO
      SIG1BE=AN1BE*SIG1BE
      SG1SBE=AN1BE*SG1SBE
      P=SIG1SO/SIG1O
      T=SG1SBE/SIG1BE
      V= SIG1BE/(SIG1O+SIG1BE)
      XNO1=(4.*AO1)/((AO1+1.)**2)
      XNBE=(4.*ABE)/((ABE+1.)**2)
      THETA= SG1SBE*XIBE/(SIG1SO*XIO1+SG1SBE*XIBE)
   46 SIG1=SIG1O+SIG1BE
      SIG1S=SIG1SO+SG1SBE
      GO TO (34,38,32,38,32,38,32), JJ2
   32 SIG2O=AN2O*SIG2O
      SIG2SO=AN2O*SIG2SO
      Q=SIG2SO/SIG2O
      XNO=(4.*AO)/((AO+1.)**2)
      GO TO 26
   38 AN2O=0.
      SIG2O=0.
      SIG2SO=0.
   26 GO TO (34,49,49,51,51,49,49), JJ2
   49 SG2UEM=AN2U*SG2UEM
      S2SUEM=AN2U*S2SUEM
      XNU=(4.*AU)/((AU+1.)**2)
      DO 28 J=1,NUMBER
      SG2SUT(J)=AN2U*SG2SUT(J)
      SIG2UT(J)=AN2U*SIG2UT(J)
   28 SG2FUT(J)=AN2U*SG2FUT(J)
      GO TO 21
   51 SG2UEM=0.
      S2SUEM=0.
      AN2U=0.
      SG2UE2=0.
```

```
 21 GO TO (34,24,24,981,981,981,961), JJ2
981 DO100 J=1,NUMBER
    SIG2WT(J)=AN2W*SIG2WT(J)
100 SG2SWT(J)=AN2W*SG2SWT(J)
    S2SWEM=AN2W*S2SWEM
    SG2WEM=AN2W*SG2WEM
    XNW=(4.*AW)/((AW+1.)**2)
    GO TO 91
 24 AN2W=0.
    SG2WEM=0.
    S2SWEM=0.
    SG2WE2=0.
 91 SIG2EM=SG2UEM+SG2WEM+SIG2O
    SG2SEM=S2SUEM+S2SWEM+SIG2SO
    DELTA= (SIG2EM*SIG1S*A)/((SIG2EM*SIG1S*A)+SG2SEM*SIG1*BMA)
    Z=A/DELTA
    Y=BMA/(1.-DELTA)
    PHI=S2SUEM*XIU/((S2SUEM*XIU)+(SIG2SO*XIO)+(S2SWEM*XIW))
    ETA=S2SWEM*XIW/((S2SWEM*XIW)+(SIG2SO*XIO)+(S2SUEM*XIU))
    TEST=ETA+PHI
    WRITE OUTPUT TAPE 6,200, CASE
    WRITE OUTPUT TAPE 6, 201,A,AN1BE,AN1O,BMA,AN2O,AN2U,AN2W
    WRITE OUTPUT TAPE 6,90,SIG1O,SIG1SO,XNO1, P,SIG1,THETA
    WRITE OUTPUT TAPE 6,90,SIG1BE,S G1SBE,XNBE,T,SIG1S,V
    WRITE OUTPUT TAPE 6,90,SIG2O,SIG2SO,XNO,U, SIG2EM,SG2SEM
    WRITE OUTPUT TAPE 6,90,SG2UEM,S2SUEM,XNU,DELTA,Z,Y
    WRITE OUTPUT TAPE 6,90,SG2WEM,S2SWEM, SG2WE2,XNW,PHI,ETA
 90 FORMAT (1P6E20.7)
    IF (NFL-100) 805,989,989
805 READ INPUT TAPE 7,815,NXA,NXB,NXC,NXD,NXE,DXA,DXB,DXC
815 FORMAT (5I5, 3F10.4)
    LL=NXA+2
    MM=75-NXB
    KK=(NXA-1)*(NXB-1)+74
    IF (KK-NLX) 807,808,808
807 IF (NXA+NXB-73) 809,808,808
808 WRITE OUTPUT TAPE 6,10,NXA,NXB,KK,NLX,LL,MM
    GO TO 900
809 FLUX(2)=LL
    READ INPUT TAPE 7,803,(FLUX(M), M=3,LL)
803 FORMAT (8E9.5)
    FLUX(MM)=0.
    NXA=MM+NXC-1
    DO 816 M=MM,NXA
816 FLUX(M+1)= FLUX(M)+DXA
    NXA=NXA+2
    NXB=NXA+NXD-2
    DO 817 M=NXA,NXB
817 FLUX(M)= FLUX(M-1)+DXB
    FLUX(NXB+1)=A
    DO 818 M=NXB,72
818 FLUX(M+2)   =FLUX(M+1)+DXC
    IF (NXC+NXD+NXE-74+MM) 808,819,808
819 FLUX(1)=MM
989 READ INPUT TAPE 7,103,IT
103 FORMAT(I3)
    READ INPUT TAPE 7,104,(NEXT(J),J=1,IT)
104 FORMAT(24I3)
    CALL PONG(4)
900 CONTINUE
* BREAK
```

```
      SUBROUTINE FCAL (XA,XB,XC)
      DIMENSION EN(676),SIG2UT(676),SG2SUT(676),SG2FUT(676),SIG2WT(676),
     1SG2SWT(676),EP(137),OMEGA(137),ABSW(137),S(7),FISS(137),FLUX(680)
     2,NEXT(50)
      COMMON SIG2UT,SG2SUT,SG2FUT,SIG2WT,SG2SWT,EN,EP,F,FISS,FLUX
     1 ,ABSZ,ABSW,OMEGA,S, SIG1O, SIG1SO, SIG1BE,SG1SBE, SIG2O, SIG2SO,
     2  S2SUEM,S2SWEM, SG2UEM, SG2WEM, EMIN,  EMAX,  XIO, XIU, XIW, XIBE
     3 , A,B, AO,AU,ABE,AW,ALPHO, ALPHU,ALPHBE, ALPHW, DONE, CASE,N,KORA
     4 , KORB, NUMBER,XIO1, AO1,  ALPHO1,  IA,IB,IC,ID,IE, H, HTEST,
     5 RESCP,E2, KMAX, TOTK, NOP,DELH, BMA, NM1, SIG1, SIG1S, SIG2EM,
     6 SG2SEM,DELTA,Z,Y,THETA,PHI,ETA,TEST,V,T,P,Q,XNO,XNBE,XNU,XNW,XNO1
     7,HELP,R1,R2,AMU2, KOUNT,K,RATIO ,ALPHA,SIG2E1,SG2UE1,SG2WE1,AM,
     8  XN,W1,NFL,NLX ,JFL,JDP,NDP
      COMMON       SG2SE2,SIG2E2,SG2UE2,SG2WE2,W2,NEXT,X1,AMU1,ELOSS,WLO
     1ST,FLOSS,E1,ALOG,JJ1,JJ2,X2
      ZB = XB
      LL = FLUX(1)
      ZA = ABSF(XA)
      IF (LL) 1,2,1
    2 RETURN
    1 JJ = FLUX(2)
      IF ((ZB-FLUX(3))*(ZB-FLUX(JJ)))3,3,2
    3 KK = 4
    6 IF (ZB-FLUX(KK)) 5,4,4
    5 KK = KK+1
      IF (KK-JJ) 6,6,7
    7 HELP = 22.
      GO TO 2
    4 MM = (KK-4)*(74-LL)+75
      IF (ZA-B) 9,9,8
    8 ZA = 2.*B-ZA
    9 KK = LL+1
   12 IF (ZA-FLUX(KK)) 10,10,11
   11 KK = KK+1
      MM = MM+1
      IF (KK-74) 12,12,7
   10 IF (ZA-A) 13,13,14
   13 FLUX(MM)=FLUX(MM)+XC/  SIG1S
      GO TO 2
   14 FLUX(MM)=FLUX(MM)+XC/SG2SE2
      GO TO 2
```

```
C      MONTE CARLO RESONANCE ESCAPE PROBLEM  CORE 2  MAIN LOOP
       DIMENSION EN(676),SIG2UT(676),SG2SUT(676),SG2FUT(676),SIG2WT(676),
      1SG2SWT(676),EP(137),OMEGA(137),ABSW(137),S(7),FISS(137),FLUX(680)
      2,NEXT(50)
       COMMON SIG2UT,SG2SUT,SG2FUT,SIG2WT,SG2SWT,EN,EP,E,FISS,FLUX
      1 ,ABSZ,ABSW,OMEGA,S, SIG1O, SIG1SO, SIG1BE,SG1SBE, SIG2O, SIG2SO,
      2  S2SUEM,S2SWEM, SG2UEM, SG2WEM, EMIN,  EMAX,  XIO, XIU, XIW, XIBE
      3 , A,B, AO,AU,ABE,AW,ALPHO, ALPHU,ALPHBE, ALPHW, DONE, CASE,N,KORA,
      4 , KORB, NUMBER,XIO1, AO1,  ALPHO1,  IA,IB,IC,ID,IE, H, HTEST,
      5 RESCP,E2, KMAX, TOTK, NOP,DELH, BMA, NM1, SIG1, SIG1S, SIG2EM,
      6 SG2SEM,DELTA,Z,Y,THETA,PHI,ETA,TEST,V,T,P,Q,XNO,XNBE,XNU,XNW,XNO1
      7,HELP,R1,R2,AMU2, KOUNT,K,RATIO ,ALPHA,SIG2E1,SG2UE1,SG2WE1,AM,
      8  XN,W1,NFL,NLX ,JFL,JDP,NDP
       COMMON       SG2SE2,SIG2E2,SG2UE2,SG2WE2,W2,NEXT,X1,AMU1,ELOSS,WLO
      1ST,FLOSS,E1,ALOG,JJ1,JJ2,X2
       CALL SAND (DAM)
       DAM=S(3)
       JJ1=2*IA+IB
       JJ2=4*IC+2*ID+IE
    5  KOUNT=1
       K=1
       TOTK=TOTK+1.
       M=1
       WLOSS = 0.
  472  CALL RAND(R1)
       AMU2=1.-(2.*R1)
       IF(AMU2) 473,474,473
  474  AMU2=.0001
  473  CALL RAND(R1)
    9  IF(DELTA-R1)10, 2,13
    2  X2=A*.999
       GO TO 113
   13  X2=Z*R1
  113  W2=1.
       GO TO (18,17,1), JJ1
    1  CALL RAND(R1)
   16  IF(THETA-R1)18,18,17
   17  ALPHA=ALPHBE
       GO TO 19
   18  ALPHA=ALPHO1
       GO TO 19
   10  X2=A+(Y*(R1-DELTA))
       W2=1.
       CALL RAND(R1)
       GO TO (99,57,15,60,20,25,8), JJ2
    8  IF(PHI-R1)58,58,57
   25  IF (PHI-R1) 60,60,57
   15  IF (PHI-R1) 59,59,57
   20  IF (ETA-R1) 59,59,60
   57  ALPHA=ALPHU
       GO TO 19
   58  IF(TEST-R1)59,59,60
   59  ALPHA=ALPHO
       GO TO 19
   60  ALPHA=ALPHW
   19  CALL RAND(R1)
       CALL RAND(R2)
       IF((R2/(ALPHA+(R2*(1.-ALPHA))))-R1)19,19,21
   21  E2=(ALPHA*EMAX)+(R2*EMAX*(1.-ALPHA))
       GO TO 41
```

```
 22 IF(A-X2)62,23,23
 23 IF (AMU2) 24,52,62
 24 AMU2=-AMU2
    X2=-X2
 62 IF(EN(KOUNT)-E2)92,91,90
 90 KOUNT=KOUNT+1
    GO TO 62
 91 RATIO =0.
    GO TO 93
 92 KOUNT=KOUNT-1
    RATIO=(EN(KOUNT)-E2)/(EN(KOUNT)-EN(KOUNT+1))
 93 GO TO (99,3,3,4,4,6,6), JJ2
  3 SG2UE2=SIG2UT(KOUNT)*((SIG2UT(KOUNT+1)/SIG2UT(KOUNT))**(RATIO))
    S2SUE2 = SG2SUT(KOUNT)*((SG2SUT(KOUNT+1)/SG2SUT(KOUNT))**(RATIO))
    S2FUE2 = SG2FUT(KOUNT)*((SG2FUT(KOUNT+1)/SG2FUT(KOUNT))**(RATIO))
    GO TO 7
  4 SG2WE2=SIG2WT(KOUNT)*((SIG2WT(KOUNT+1)/SIG2WT(KOUNT))**(RATIO))
    S2SWE2 = SG2SWT(KOUNT)*((SG2SWT(KOUNT+1)/SG2SWT(KOUNT))**(RATIO))
    GO TO 7
  6 SG2UE2=SIG2UT(KOUNT)*((SIG2UT(KOUNT+1)/SIG2UT(KOUNT))**(RATIO))
    SG2WE2=SIG2WT(KOUNT)*((SIG2WT(KOUNT+1)/SIG2WT(KOUNT))**(RATIO))
    S2SWE2 = SG2SWT(KOUNT)*((SG2SWT(KOUNT+1)/SG2SWT(KOUNT))**(RATIO))
    S2SUE2 = SG2SUT(KOUNT)*((SG2SUT(KOUNT+1)/SG2SUT(KOUNT))**(RATIO))
    S2FUE2 = SG2FUT(KOUNT)*((SG2FUT(KOUNT+1)/SG2FUT(KOUNT))**(RATIO))
  7 SIG2E2=SIG2O+SG2WE2+SG2UE2
    SG2SE2 = S2SWE2+S2SUE2+SIG2SO
    IF (A-X2) 193,99,207
207 IF (WLOSS) 99,208,26
208 WLOSS=W2*EXPF((X2-A)*SIG1/AMU2)*(1.-SG2SE2/SIG2E2)*(1.-EXPF((A-B)*
   12.*SIG2E2/AMU2))
    IF(WLOSS*(WLOSS-W2)) 301,309,309
309 WLOSS=.1E-10*W2
301 WLOST=WLOSS*(SG2SE2/(SIG2E2-SG2SE2))
    IF(WLOST*(WLOST-W2)) 302,303,303
303 WLOST=.1E-8*W2
302 ELOSS=W2*(1.-EXPF((X2-A)*SIG1/AMU2))
    IF(ELOSS*(ELOSS-W2)) 304,304,305
305 ELOSS=W2
304 W2=W2-WLOSS
    IF(W2-.1E-6)953,953,904
904 IF (IC) 99,211,212
212 ABSW(M-1) = ABSW(M-1)+WLOSS*((SG2WE2-S2SWE2)/(SIG2E2-SG2SE2))
211 IF (ID) 99,214,213
213 FISS(M-1) = FISS(M-1)+WLOSS*(S2FUE2/(SIG2E2-SG2SE2))
214 IF (IE) 99,26,215
215 ABSOX2 = ABSOX2+WLOSS*((SIG2O-SIG2SO)/(SIG2E2-SG2SE2))
 26 CALL RAND(R1)
128 IF((ELOSS/W2)-R1)502,502,29
 29 AMU1=AMU2
    X1=X2
    W1=W2
    E1=E2
500 CALL RAND(R1)
    X2=X1+AMU1*((-1./SIG1)*LOGF(1.-R1+R1*EXPF(SIG1*((X1-A)/AMU1))))
    K=K+1
    TOTK=TOTK+1.
    GO TO (35,34,32), JJ1
 32 CALL RAND(R1)
 33 IF(V-R1)35,35,34
 34 XN=XNBE
```

```
      W2=W1*T
      AM=ABE
      GO TO 37
   35 XN=XNO1
      AM=AO1
      W2=W1*P
   37 CALL F CAL (X2,E2,W2)
      WLOSS=0.
   38 CALL RAND(R1)
   39 E2=E1*(1.-(XN*R1))
   41 IF(EP(M)-E2)46,42,42
   42 OMEGA(M)=OMEGA(M)+W2
      IF (M+1-N) 44,44,53
   44 M=M+1
      GO TO 41
   46 IF(K-1)22,22,146
  146 AMUC=1.-2.*R1
      AMUL=(AM*AMUC+1.)/(SQRTF((AM*AM)+1.+(2.*AM*AMUC)))
   49 CALL RAND(R1)
      CALL RAND(R2)
      SUMSQ=(R1*R1+R2*R2)
   50 IF(1.-SUMSQ)49,49,51
   51 COSBET=((R1*R1)-(R2*R2))/SUMSQ
      AMU2=AMU1*AMUL+((SQRTF((1.-(AMU1**2))*(1.-(AMUL**2))))*COSBET)
      IF(AMU2) 22,52,22
   52 AMU2 = .0001
      GO TO 22
  502 IF(((ELOSS/W2)+(WLOST/W2))-R1)574,503,503
  574 X2=-A
      WLOSS=0.
      GO TO 207
  503 IF(A+X2)99,229,229
  229 X2=A
      AMU1=AMU2
      W1=W2
      X1=X2
      E1=E2
      K=K+1
      TOTK=TOTK+1.
  505 CALL RAND(R1)
      X2=X1+AMU1*((-1./SIG2E2)*LOGF(1.-R1+R1*EXPF(SIG2E2*((2.*(A-B))/AMU
     11))))
      GO TO 506
  193 IF(AMU2) 70,99,72
   70 AMU2=-AMU2
      X2=2.*B-X2
   72 CALL RAND(R1)
      ALOG=-LOGF(R1)
   73 IF(((2.*B-A-X2)/AMU2)-(ALOG/SIG2E2))574,574,75
   75 AMU1=AMU2
      X1=X2
      W1=W2
      E1=E2
      K=K+1
      TOTK=TOTK+1.
      X2=X1+AMU1*ALOG/SIG2E2
  506 IF(WLOSS)99,230,236
  230 FLOSS = W1*((SIG2E2-SG2SE2)/SIG2E2)
      W2 = W1-FLOSS
      IF(W2-.1E-6)953,953,905
```

```
  905 IF (IC) 99,232,231
  231 ABSW(M-1) = ABSW(M-1)+FLOSS*((SG2WE2-S2SWE2)/(SIG2E2-SG2SE2))
  232 IF (ID) 99,234,233
  233 FISS(M-1) = FISS(M-1)+FLOSS*(S2FUE2/(SIG2E2-SG2SE2))
  234 IF(IE) 99,236,235
  235 ABSOX2 = ABSOX2+FLOSS*((SIG2O-SIG2SO)/(SIG2E2-SG2SE2))
  236 CALL F CAL (X2,E2,W2)
      WLOSS=0.
  237 CALL RAND(R1)
      GO TO (99,79,78,87,11,12,14), JJ2
   78 IF(S2SUE2/SG2SE2-R1) 85,85,79
   11 IF(S2SWE2/SG2SE2-R1) 85,85,87
   12 IF(S2SUE2/SG2SE2-R1) 87,87,79
   14 IF(S2SUE2/SG2SE2-R1) 84,84,79
   79 AM=AU
      XN=XNU
      GO TO (99,39,38,237,237,38,38),JJ2
   84 IF(((S2SWE2+S2SUE2)/SG2SE2)-R1) 85,85,87
   85 XN=XNO
      AM=AO
      GO TO 38
   87 XN=XNW
      AM=AW
      GO TO (99,237,237,39,38,38,38),JJ2
  953 W2=.1E-6
   53 RESCP=RESCP+W2
      KMAX=XMAXOF(KMAX,K)
  153 IF(HTEST-H)95,95,94
   94 H=H+1.
      GO TO 5
   99 HELP=M+1
   95 S(3)=DAM
      CALL PONG (3)
* BREAK
```

```
C     MONTE CARLO RESONANCE ESCAPE PROBLEM  CORE 3 OUTPUT
      DIMENSION EN(676),SIG2UT(676),SG2SUT(676),SG2FUT(676),SIG2WT(676),
     1SG2SWT(676),EP(137),OMEGA(137),ABSW(137),S(7),FISS(137),FLUX(680)
     2,BT(10),NEXT(50),XXXD(137)
      COMMON SIG2UT,SG2SUT,SG2FUT,SIG2WT,SG2SWT,EN,EP,F,FISS,FLUX
     1 ,ABSZ,ABSW,OMEGA,S, SIG1O, SIG1SO, SIG1BE,SG1SBE, SIG2O, SIG2SO,
     2  S2SUEM,S2SWEM, SG2UEM, SG2WEM, EMIN,  EMAX,  XIO, XIU, XIW, XIBE
     3 , A,B, AO,AU,ABE,AW,ALPHO, ALPHU,ALPHBE, ALPHW, DONE, CASE,N,KORA
     4 , KORB, NUMBER,XIO1, AO1,  ALPHO1,  IA,IB,IC,ID,IE, H, HTEST,
     5 RESCP,E2, KMAX, TOTK, NOP,DELH, BMA, NM1, SIG1, SIG1S, SIG2EM,
     6 SG2SEM,DELTA,Z,Y,THETA,PHI,ETA,TEST,V,T,P,Q,XNO,XNBE,XNU,XNW,XNO1
     7,HELP,R1,R2,AMU2, KOUNT,K,RATIO ,ALPHA,SIG2E1,SG2UE1,SG2WE1,AM,
     8  XN,W1,NFL,NLX ,JFL,JDP,NDP
      COMMON       SG2SE2,SIG2E2,SG2UE2,SG2WE2,W2,NEXT,X1,AMU1,ELOSS,WLO
     1ST,FLOSS,E1,ALOG,JJ1,JJ2,X2
   90 FORMAT (1P6E20.7)
  202 FORMAT(27H0                          OUTPUT//25H          TOTAL HISTORIES
     1= F7.0 /25H MAX. COLL. IN 1 HISTORY= I6    /25H          TOTAL COLLIS
     2IONS= 1PE14.7 /25H           TOTAL FISSIONS= 0PE12.6 /25H
     3      P THERMAL= 0PE12.6 ////119H      NO.     E                      P(E
     4)              TOTAL ABS            RES ABS        FRACTION W ABS
     5            F(E)     //)
      NLX=NLX
      N=NM1+1
    5    IF(HELP) 4, 3, 4
    4 WRITE OUTPUT TAPE 6,63,N,KORA,KORB,NUMBER,IA,IB,IC,ID,IE,KMAX,NOP,
     1  NM1, KOUNT,K
   63 FORMAT  (19H1  ALARM CONDITION  14I5)
      WRITE OUTPUT TAPE 6,90, H,HTEST,TOTK,DELH,SG2UE2,SG2WE2
      WRITE OUTPUT TAPE 6,90,HELP,R1,R2,AMU2,RATIO,ALPHA
      WRITE OUTPUT TAPE 6,90,WLOSS,X2,SIG2E2,AM,XN,W1
      WRITE OUTPUT TAPE 6,90,X1,W2,AMU1,ELOSS,WLOST,FLOSS
      WRITE OUTPUT TAPE 6,90,SG2SE2,E2,E1,ALOG,JJ1,JJ2
         KORB = NOP
    3 RESOH=RESCP/H
      FISS(N)=F
      DO 815 M=1,NM1
  815 FISS(N)= FISS(N)+FISS(M)
      WRITE OUTPUT TAPE 6,202,H,KMAX,TOTK,FISS(N), RESOH
      ABSW(N)=ABSZ
      MMM=0
  106 XXD=0.
      MMM=MMM+1
      KEV=NEXT(MMM)
      IF(MMM-1)4,100,101
  100 KJS=1
      GO TO 102
  101 KJS=NEXT(MMM-1)+1
  102 DO 69 KAS=KJS,KEV
   69 XXD=XXD+ABSW(KAS)
      XXXD(KEV)=XXD*(10000./H)
      IF(N-KEV)4,105,106
  105 DO 99 M=1,NM1
      ABSW(N)=ABSW(N)+ABSW(M)
      XA=OMEGA(M)/H
      XB=OMEGA(M)-OMEGA(M+1)
         XC = 1.
         IF(XB) 77, 99, 77
   77    XC = ABSW(M)/XB
   99 WRITE OUTPUT TAPE 6,85,M,EP(M),XA,XB,XXXD(M),XC,FISS(M)
```

```
 85 FORMAT (I7,F10.4, 5F19.5)
    XA=OMEGA(N)/H
    XB=H-OMEGA(N)
    XC=ABSW(N)/XB
    WRITE OUTPUT TAPE 6,85,N,EP(N),XA,XB,XXXD(N),XC,FISS(N)
    JFL=JFL+1
    IF (JFL-NFL) 950,817,817
817 JFL=0
    KK=3
824 LL=KK+9
    JM=FLUX(2)-1.
    IF (LL-JM) 816,816,818
818 LL=JM
816 WRITE OUTPUT TAPE 6,819,(FLUX(M),M=KK,LL)
819 FORMAT ( 7H  E HI ,10F11.5)
    WRITE OUTPUT TAPE 6,820,(FLUX(M+1),M=KK,LL)
820 FORMAT ( 7H  E LO ,10F11.5)
    NN=FLUX(1)
    MM=74-NN
    LK=LL-KK+1
    JC=74+MM*(KK-3)
    DO 821 J=1,MM
    JB=NN+J
    JK=JC+J
    XA=(FLUX(JB)-FLUX(JB-1))*H
    DO 822 K=1,LK
    JA=KK+K
    BT(K)=FLUX(JK)/(XA*(FLUX(JA-1)-FLUX(JA)) )
822 JK=JK+MM
821 WRITE OUTPUT TAPE 6,823,J,(BT(K), K=1,LK)
823 FORMAT (I7,1P10E11.3)
    KK=KK+10
    IF (KK-JM) 824,824,950
950 S(1)=H
    S(2)=TOTK
    S(4)=RESCP
    S(5)=F
    S(6)=KMAX
    S(7)=1.
     JDP=JDP+1
    IF (JDP-NDP) 42,46,42
 46 JDP=0
    CALL BC DUMP ( S(7),S(1))
    CALL BC DUMP (ABSW(N),ABSZ)
    CALL BC DUMP ( OMEGA(N),OMEGA(1))
    IF (ID) 802,801,802
802 CALL BC DUMP (FISS(N),F)
801  IF (NFL-100) 805,42,42
805 CALL BC DUMP (FLUX(NLX),FLUX(1))
 42 KORB=KORB+1
    IF (NOP-KORB) 900,900,939
939 IF (SENSE SWITCH 6) 804,97
804 IF (JDP) 46,900,46
 97 HTEST=HTEST+DELH
    H=H+1.
    IF (DONE-H) 900,900,53
 53 CALL PONG (2)
900 MM=FLUX(1)
    WRITE OUTPUT TAPE 6,812
812 FORMAT (11H   X TABLE )
```

```
      LL=1
      DO 810 M=MM,74,8
      KK=M+7
      IF (KK-74) 813,813,814
  814 KK=74
  813 WRITE OUTPUT TAPE 6,811,LL, (FLUX(J),J=M,KK)
  811 FORMAT (I5, 8F12.8)
  810 LL=LL+8
      IF (SENSE SWITCH 6) 951,837
  951 PAUSE 77777
  837 CONTINUE
* BREAK
```

```
C      MONTE CARLO RESONANCE ESCAPE PROBLEM  CORE 4
       DIMENSION EN(676),SIG2UT(676),SG2SUT(676),SG2FUT(676),SIG2WT(676),
      1SG2SWT(676),EP(137),OMEGA(137),ABSW(137),S(7),FISS(137),FLUX(680)
      2,NEXT(50)
       COMMON SIG2UT,SG2SUT,SG2FUT,SIG2WT,SG2SWT,EN,EP,F,FISS,FLUX
      1 ,ABSZ,ABSW,OMEGA,S, SIG1O, SIG1SO, SIG1BE,SG1SBE, SIG2O, SIG2SO,
      2  S2SUEM,S2SWEM, SG2UEM, SG2WEM, EMIN,  EMAX,  XIO, X1U, XIW, XIBE
      3 , A,B, AO,AU,ABE,AW,ALPHO, ALPHU,ALPHBE, ALPHW, DONE, CASE,N,KORA
      4 , KORB, NUMBER,XIO1, AO1,  ALPHO1,  IA,IB,IC,ID,IE, H, HTEST,
      5 RESCP,E2, KMAX, TOTK, NOP,DELH, BMA, NM1, SIG1, SIG1S, SIG2EM,
      6 SG2SEM,DELTA,Z,Y,THETA,PHI,ETA,TEST,V,T,P,U,XNO,XNBE,XNU,XNW,XNO1
      7,HELP,R1,R2,AMU2, KOUNT,K,RATIO ,ALPHA,SIG2E1,SG2UE1,SG2WE1,AM,
      8  XN,W1,NFL,NLX ,JFL,JDP,NDP
       COMMON        SG2SE2,SIG2E2,SG2UE2,SG2WE2,W2,NEXT,X1,AMU1,ELOSS,WLO
      1ST,FLOSS,E1,ALOG,JJ1,JJ2,X2
       CALL PONG(2)
* BREAK
```

DATA

```
   1     1     1                4   500.      1.           101   675     2
38000+01 38000+01 20500+02 20500+02 38000+01 38000+01 18770+02 19440+02
28580+02 20620+02 12500+00 96100+03 11995+00 84840-02 10837-01 10000+01
22860+01 23495+01 16000+02 23500+03 10000+01 18386+03 77855+00 98312+00
00000+00 97848+00 20000+05 76000+02  536  108
66000-01 33000-01 00000+00 00000+00 50560-01 11995+00 16000+02 77855+0
```

E-1434

APPENDIX D

1/v ANALYTIC ABSORPTIONS

The following assumptions are made:

(1) The fuel plates are sufficiently separated that cell interaction effects are negligible.

(2) The moderator is nonabsorbing, and the moderator flux φ_M is nearly isotropic.

(3) $\varphi_M(v)dv \cong \frac{C_0}{v}\,dv$

(4) In the fuel region, $\Sigma_a^F(v) = \gamma/v$ and $\Sigma_s^F = 0$ where γ is a constant.

Referring to sketch (e) and the above assumptions, the number of

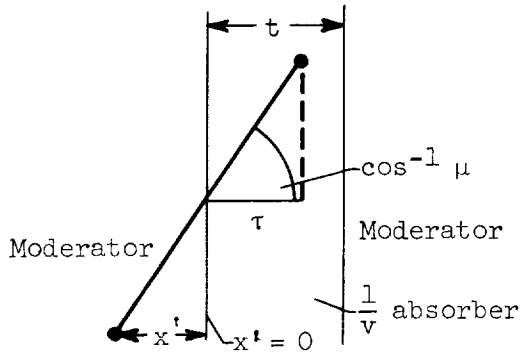

(e)

neutrons $\mathscr{A}$ absorbed per second per unit area in the entire fuel (of thickness t) is

$$\mathscr{A} = 2C_0\gamma \sum_{i=1}^{2} \frac{\Sigma_{s,i}}{1-\alpha_i} \int_{\mu=0}^{1} \frac{d\mu}{\mu} \int_{v=v_{min}}^{\infty} dv \int_{\tau=0}^{t} d\tau\, e^{-\frac{\gamma\tau}{v\mu}} \int_{x'=-\infty}^{0} dx' e^{\frac{\Sigma_s^M x'}{\mu}} \int_{v'=v}^{v/\sqrt{\alpha_i}} \frac{dv'}{v'^3} \qquad (D1)$$

where τ is the fuel penetration distance parallel to the x-axis. Note that the x' integration implies a cosine incident distribution at the surface of the fuel.

Performing the first three integrations, transforming, and letting

$$\kappa = \frac{\gamma t}{v_{min}} = (\Sigma_{a,th} t) \frac{v_{th}}{v_{min}} \tag{D2}$$

where v_{th} is the neutron velocity corresponding to 0.0253 electron volt, yield

$$\frac{\mathscr{A}}{C_0} = \kappa^2 \int_{\kappa}^{\infty} \frac{dy}{y^3} \int_{0}^{y} \frac{dx}{x} (1 - e^{-x}) \tag{D3}$$

Equation (D3) is integrated by parts several times, and the resulting exponential integral is expanded in series form (ref. 8) by

$$\int_{\kappa}^{\infty} \frac{e^{-x}}{x} dx = -0.577216 - \ln \kappa + \sum_{n=1}^{\infty} (-)^{n+1} \frac{\kappa^n}{n!n} \tag{D3a}$$

Equation (D3) finally becomes

$$\frac{\mathscr{A}}{C_0} = \frac{1}{4}\left[1 + e^{-\kappa}(\kappa - 1) + \kappa^2(0.577216 + \ln \kappa) + (2 - \kappa^2) \sum_{n=1}^{\infty} \frac{(-)^{n+1}\kappa^n}{n!n}\right] \tag{D4}$$

For the cases of interest, $\kappa \ll 2$ (eq. (D2)) and the series of equation (D4) converges very rapidly to the results listed in table V.

To achieve correspondence of equation (D4) to the Monte Carlo calculations of repetitive slabs, the constant C_0 was determined from the normalization requirement that 1 neutron per second slow down past E_{max} in the complete cell. Now

$$\varphi(v)dv = \frac{C_0}{v} dv = \frac{C}{E} dE$$

where

$$C = \frac{C_0}{2}$$

The number of neutrons per second slowing down past E_{max} in the entire moderator of thickness t_M is given by

$$q_M(E_{max}) = \sum_{i=1}^{2} \int_{E=\alpha_i E_{max}}^{E_{max}} \int_{E'=E_{max}}^{E/\alpha_i} \frac{dE\, dE'}{E'(1-\alpha_i)} \frac{C}{E'} \int_0^{t_M} \Sigma_{s,i}\, dx'$$

$$= \sum_{i=1}^{2} \frac{t_M C \Sigma_{s,i}}{1-\alpha_i} \left[(1-\alpha_i) - \alpha_i \ln \frac{1}{\alpha_i} \right]$$

But

$$\xi_i \equiv 1 - \frac{\alpha_i}{1-\alpha_i} \ln \frac{1}{\alpha_i}$$

and

$$\overline{\xi}_M \Sigma_s^M \equiv \sum_{i=1}^{2} \xi_i^M \Sigma_{s,i}^M$$

where ξ_i^M is the average logarithmic energy decrement of the i^{th} type of nucleus in the moderator. Therefore,

$$q_M(E_{max}) = C \overline{\xi}_M \Sigma_s^M t_M$$

Similarly,

$$q_F(E_{max}) = C \overline{\xi}_F \Sigma_s^F t_F$$

where Σ_s^F is some average scattering cross section of the "fuel" above but in the near vicinity of E_{max}. The normalization condition $q_M + q_F = 1$ gives

$$C = \frac{C_0}{2} = \frac{1}{\overline{\xi}^M \Sigma_s^M t_M + \overline{\xi}^F \Sigma_s^F t_F} \qquad (t_F \equiv t) \qquad \text{(D5)}$$

Equation (D5) contains the moderator correlation of figure 6 with a small correction term.

APPENDIX E

ANALYTIC CALCULATION OF RESONANCE ABSORPTION

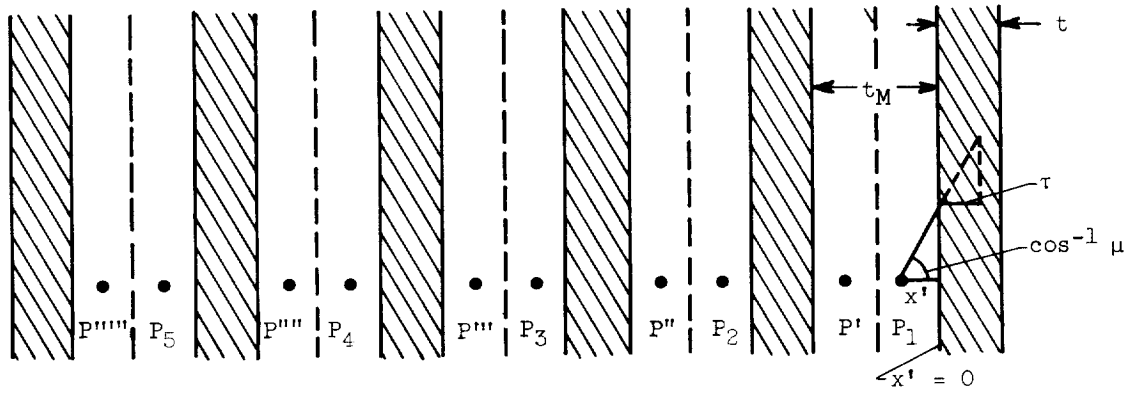

(f)

Consider sketch (f), which shows the repetitive slab lattice studied. The positive x- and μ-directions are taken toward the right. Let $\varphi^M(x',E')dE'$ be the total moderator flux per unit energy at x' and E' in dE'. It will be supposed that φ^M is known or can be obtained approximately. A reasonable choice appears to be, for example, a uniform $1/E$ moderator flux providing the plates are not too closely spaced.

Let $\Sigma_{s,i}$ be the macroscopic scattering cross section of the i^{th} type of moderator nucleus and Σ_s^M the total moderator scattering cross section. Let $\Sigma_a(E)$ and $\Sigma(E)$ be the "fuel" macroscopic absorption and total cross sections at energy E. Let τ be the fuel penetration distance in the x-direction, μ be the neutron direction cosine, and $\alpha_i = \dfrac{(A_i - 1)^2}{(A_i + 1)^2}$, where A_i is the target mass of the i^{th} moderator nucleus.

By the time neutrons have entered the resonance region, their directions are nearly randomized. Thus, after a scattering collision, their directions are still randomized or isotropic in the laboratory system. From symmetry considerations, the flux $\varphi^M(x',E')$ is identical at points P_1,P',P_2,P'', and so forth. The contribution to the absorptions per second in the fuel plate at $x' = 0$ from all such points to

the left of $x' = 0$ in the phase element $d\mu\ dE\ d\tau\ dx'\ dE'$ is

$$A_i^L\, d\mu\, dE\, d\tau\, dx'\, dE' = \varphi^M(x',E')dE'\left\{e^{-\frac{\Sigma_s^M x'}{\mu}}\left[1 + e^{-\frac{\Sigma_s^M}{\mu}t_M - \frac{\Sigma(E)t}{\mu}} + e^{-\frac{\Sigma_s^M}{\mu}2t_M - \frac{2\Sigma(E)t}{\mu}} + \cdots\right] + e^{-\frac{\Sigma_s^M}{\mu}(t_M+x')}\left[1 + e^{-\frac{\Sigma_s^M t_M}{\mu} - \frac{\Sigma(E)t}{\mu}} + e^{-\frac{\Sigma_s^M}{\mu}2t_M - \frac{2\Sigma(E)t}{\mu}} + \cdots\right]\right\}\left(\Sigma_{s,i}^M dx'\right)\left[\frac{dE}{E'(1-\alpha_i)}\right]\left(\frac{1}{2}\,d\mu\right)$$

$$\times\left[e^{-\frac{\Sigma(E)\tau}{\mu}}\right]\left[\Sigma a(E)\,\frac{d\tau}{\mu}\right] \qquad \text{(E1)}$$

The term $\varphi^M(x',E')dE'\Sigma_{s,i}^M dx'$ gives the number of neutrons scattered per second in $dx'\ dE'$ from the i^{th} type of moderator nucleus. The bracket containing dE is the probability that after collision the neutron will emerge with energy E in dE. The quantity $1/2\ d\mu$ is the probability that the neutron will emerge with a direction cosine μ in $d\mu$. The terms in the bracket multiplying $e^{-\frac{\Sigma_s^M x'}{\mu}}$ give the probability that neutrons scattered, respectively, from points P_1, P_2, and so forth of sketch (f) will reach the surface of the plate at $x' = 0$ without an intervening collision. Similarly, the terms in the bracket multiplying $e^{-\frac{\Sigma_s(t_M+x')}{\mu}}$ are the respective contributions from the points P', P'', and so forth. Finally, the last two terms of equation (E1) give the fraction of those neutrons incident on the plate at $x' = 0$ with direction μ and energy E that penetrate the plate and are absorbed at τ in $d\tau$. It is assumed in equation (E1) that the contributions to the plate at $x' = 0$ from neutrons scattered within the other plates are negligible. This is probably a very good approximation. An approximation is necessary because otherwise the fuel flux $\varphi^F(x,E)$ would have to be known. Because of the geometric progression in equation (E1), there follows

$$A_i^L \, d\mu \, dE \, d\tau \, dx' \, dE' = \varphi^M(x',E')dE' \left\{ \frac{e^{\frac{\Sigma_s^M}{\mu} x'} + e^{-\frac{\Sigma_s^M}{\mu}(t_M+x')}}{1 - e^{-\frac{1}{\mu}\left[\Sigma_s^M t_M + \Sigma(E)t\right]}} \right\}$$

$$\times \left(\Sigma_{s,i}^M \, dx'\right) \left[\frac{dE}{E'(1-\alpha_i)}\right] \left(\frac{1}{2} \, d\mu\right) \left[e^{-\frac{\Sigma(E)\tau}{\mu}}\right] \left[\frac{\Sigma_a(E)d\tau}{\mu}\right]$$

E-1434

The total absorption in dE per second in the plate at $x' = 0$, including the identical contribution from the region $t \leq x' < \infty$, is

$$A \, dE = \sum_i \frac{\Sigma_{s,i}^M}{1-\alpha_i} \Sigma_a(E)dE \int_0^1 \frac{d\mu}{\mu} \int_{x'} dx'$$

$$\times \left\{ \frac{e^{\frac{\Sigma_s^M}{\mu} x'} + e^{-\frac{\Sigma_s^M}{\mu}(t_M+x')}}{1 - e^{-\frac{1}{\mu}\left[\Sigma_s^M t_M + \Sigma(E)t\right]}} \right\} \int_E^{E/\alpha_i} \frac{dE'}{E'} \varphi^M(x',E') \int_0^t e^{-\frac{\Sigma(E)\tau}{\mu}} \, d\tau \quad \text{(E2)}$$

Here it is assumed that the moderator flux can be reasonably approximated by $\varphi^M(x',E') \cong \frac{C}{E'}$, where C is a constant. Equation (E2) becomes

$$A \, dE = C\Sigma_s^M \frac{\Sigma_a(E)}{\Sigma(E)} \frac{dE}{E} \int_0^1 d\mu \left(1 - e^{-\frac{\Sigma(E)t}{\mu}}\right) \int_{x'} dx' \left\{ \frac{e^{\frac{\Sigma_s^M x'}{\mu}} + e^{-\frac{\Sigma_s^M}{\mu}(t_M+x')}}{1 - e^{-\frac{1}{\mu}\left[\Sigma_s^M t_M + \Sigma(E)t\right]}} \right\} \quad \text{(E3)}$$

where

$$\int_{x'} dx' = \int_{-t_M/2}^{0} dx' + \int_{-\frac{3}{2}t_M - t}^{-t_M - t} dx' + \int_{-\frac{5}{2}t_M - 2t}^{-2t_M - 2t} dx' + \cdots$$

If the plates are separated by at least several moderator mean free paths, $\int_{x'} dx' \cong \int_{-t_M/2}^{0} dx'$ is an excellent approximation. Thus letting

$$\left.\begin{aligned} \mu &\equiv \frac{1}{y} & \kappa(E) &\equiv \Sigma(E)t \\ \kappa_M &\equiv \Sigma_s^M t_M & \kappa_a(E) &= \Sigma_a(E)t \end{aligned}\right\} \tag{E4}$$

equation (E3) becomes

$$\left.\begin{aligned} A(E)dE &= C\,\frac{dE}{E}\,\frac{\kappa_a(E)}{\kappa(E)} \int_1^\infty \frac{\left(1 - e^{-\kappa_M y}\right)\left[1 - e^{-\kappa(E)y}\right]}{\left\{1 - e^{-\left[\kappa_M + \kappa(E)\right]y}\right\}}\,\frac{dy}{y^3} \\ \text{where} \qquad C &= \frac{1}{\xi^M \Sigma_s^M t_M + \xi^F \Sigma_s^F t^F} \end{aligned}\right\} \tag{E5}$$

where ξ is the average logarithmic energy decrement $t^F \equiv t$, and Σ_s^F is the scattering cross section of the fuel at some value above but near E_{max}. (See appendix D for a discussion of this expression for C.)

Equations (E5) give the absorptions per second in dE in each of the plates in the repetitive lattice. The contribution to the absorption by neutrons that suffer successive multiple collisions inside the "fuel" region (tungsten) has been neglected. For a predominantly scattering resonance which is also strongly absorptive, such as the 18.8-electron-volt resonance in tungsten, one would expect equation (E5) to underestimate the absorptions because of this neglect of successive multiple scattering collisions within the fuel. However, equations (E5) may considerably exaggerate the absorptions in a resonance such as the 18.8-electron-volt resonance because of the neglect of moderator flux depression effects. Thus, instead of assuming a uniform spatial dependence for $\varphi^M(x', E')$, a more realistic assumption might be some appropriately attenuated moderator flux in the vicinity of the fuel plate merging into a uniform spatial dependence several moderator mean free paths from the fuel region.

In equation (E5), $\kappa(E)$ is the fuel thickness in total mean free paths for a neutron of energy E. At a resonant energy where the bulk of the absorptions occur, $\kappa(E)$ is quite large. Since κ_M has been

assumed to be at least several moderator mean free paths, the denominator of equation (E5) can be set equal to 1. Converting to lethargy, equation (E5) gives

$$A(u)du = -C\,du\,\frac{\kappa_a(u)}{\kappa(u)}\int_1^\infty \left(1 - e^{-\kappa_M y}\right)\left[1 - e^{-\kappa(u)y}\right]\frac{dy}{y^3}$$

$$= -C\,du\,\frac{\kappa_a(u)}{\kappa(u)}\left\{\frac{1}{2} - I\left[\kappa(u)\right] - I(\kappa_M) + I\left[\kappa_M + \kappa(u)\right]\right\} \qquad \text{(E6)}$$

$$I(\kappa) \equiv \int_1^\infty \frac{e^{-\kappa y}}{y^3}\,dy = \frac{1}{2}(1 - \kappa)e^{-\kappa} + \frac{\kappa^2}{2}\int_\kappa^\infty \frac{e^{-y}}{y}\,dy$$

A considerable simplification of equations (E6) occurs if $\kappa_M \to \infty$. For the 4-inch-water-moderated cases $\kappa_M \cong 15$. Thus $I(\kappa_M) = I(\kappa_M + \kappa(u)) \cong 0$. Hence,

$$A(u)du = -\frac{C}{2}\,du\,\frac{\kappa_a(u)}{\kappa(u)}\left\{1 - \left[1 - \kappa(u)\right]e^{-\kappa(u)} - \kappa^2(u)\int_{\kappa(u)}^\infty \frac{e^{-y}}{y}\,dy\right\} \qquad \text{(E7)}$$

As mentioned in the section RESULTS AND DISCUSSION, a good approximation to the overall resonance escape probability and to the absorptions in most tungsten resonances occurs if the scattering is suppressed; that is, if the total cross section at energy E is set equal to the absorption cross section at E, and then the scattering cross section is set equal to zero. In equation (E6) this means $\frac{\kappa_a(u)}{\kappa(u)} \to 1$ and $\kappa(u) \to \kappa_a(u)$. This is exact for a pure absorptive resonance, but overestimates the absorptions in a scattering-absorptive resonance.

Equation (E7) becomes

$$A(u)du \cong -\frac{C}{2}\,du\left\{1 - \left[1 - \kappa_a(u)\right]e^{-\kappa_a(u)} - \kappa_a^2(u)\int_{\kappa_a(u)}^\infty \frac{e^{-y}}{y}\,dy\right\} \qquad \text{(E8)}$$

$\kappa_a(u)$ is given by equation (E4) and is generally a rapidly varying function of lethargy in the resonance region.

As in the Monte Carlo calculation, the region from 961 to 0.125 electron volt is divided into 536 distinct lethargy (or energy) groups u_Q (where $Q = 1, 2, \ldots, 536$) properly spaced so that all the resonances are accurately described by knowledge of the cross section at those values. Thus, in the Q^{th} lethargy interval $u_Q \rightarrow u_{Q+1}$, a linear interpolation on the cross section may be used:

$$\left.\begin{aligned} \kappa_a(u) &= \kappa_a(u_{Q+1}) + \frac{u_{Q+1} - u}{u_{Q+1} - u_Q}\left[\kappa_a(u_Q) - \kappa_a(u_{Q+1})\right] && u_Q \le u \le u_{Q+1} \\ d\kappa_a(u) &= \frac{u_{Q+1} - u_Q}{\kappa_a(u_Q) - \kappa_a(u_{Q+1})} = -du && u_{Q+1} > u_Q \end{aligned}\right\} \quad \text{(E9)}$$

Substituted into equation (E8), the absorptions per second in the interval $u_Q \rightarrow u_{Q+1}$ in the entire plate are

$$A_{Q\rightarrow Q+1} = \frac{C}{2}\frac{(u_{Q+1} - u_Q)}{(\kappa_{a,Q} - \kappa_{a,Q+1})}\int_{\kappa_{a,Q+1}}^{\kappa_{a,Q}}\left(1 - e^{-F} + Fe^{-F} - F^2\int_F^\infty \frac{e^{-y}}{y}\,dy\right)dF \quad \text{(E10)}$$

$$\kappa_{a,Q} \equiv \kappa_a(u_Q)$$

Performing the integrations and converting back to energy give the final result for equation (E10)

$$\begin{aligned} A_{Q\rightarrow Q+1} = \frac{C}{6}\frac{\ln(E_Q/E_{Q+1})}{(\kappa_{a,Q} - \kappa_{a,Q+1})}\Bigg[& e^{-\kappa_{a,Q+1}}\left(\kappa_{a,Q+1} - \kappa_{a,Q+1}^2 - 2\right) \\ & - e^{-\kappa_{a,Q}}\left(\kappa_{a,Q} - \kappa_{a,Q}^2 - 2\right) + 3\left(\kappa_{a,Q} - \kappa_{a,Q+1}\right) \\ & + \kappa_{a,Q+1}^3\int_{\kappa_{a,Q+1}}^\infty \frac{e^{-y}}{y}\,dy - \kappa_{a,Q}^3\int_{\kappa_{a,Q}}^\infty \frac{e^{-y}}{y}\,dy\Bigg] \quad Q = 1,2,\ldots,536 \end{aligned} \quad \text{(E11)}$$

The constant C in equation (E11) is given by equation (E5) and $\kappa_{a,Q} \equiv \kappa_a(u_Q)$. Values of $Q = 1,2, \ldots, 536$ are the same as the tungsten cross sections used in the Monte Carlo calculations. The last

integral in equation (E11) is the well known exponential integral that is evaluated by equation (D3a) of appendix D for $\kappa_{a,Q} \leq 1$ and by the following continued fraction for $\kappa_{a,Q} > 1$:

$$\int_{\kappa}^{\infty} \frac{e^{-y}}{y}\,dy = \cfrac{e^{-\kappa}}{1 + \kappa - \cfrac{1}{3 + \kappa - \cfrac{4}{5 + \kappa - \cfrac{9}{7 + \kappa \cdots}}}} \qquad \text{(E12)}$$

The 536 energy intervals (eq. (E11)) were grouped into the larger intervals of the first column of table I(a). Table VII gives the absorptions in these same energy intervals as calculated for the 4-inch-water-moderated tungsten cases using equation (E11). The results in table VII compare favorably with the Monte Carlo results of table I(d).

It should be remembered that the Monte Carlo results in table I(d) are subject to appreciable statistical deviations. However, the excessive absorption predicted by equation (E11) for the 18.8-electron-volt scattering resonance (20.7 → 16 ev) is clearly not statistical.

REFERENCES

1. Sampson, J. B., and Chernick, J.: Resonance Escape Probability in Thermal Reactors. Progress in Nuclear Energy. Ser. I. Physics and Mathematics. Pergamon Press, 1958.

2. Richtmeyer, R. D.: Proceedings of the Brookhaven Conference on Resonance Absorption of Neutrons in Nuclear Reactors. BNL 433, AEC, Sept. 25, 1956.

3. Eastwood, T. A., and Werner, R. D.: Neutron Self-Shielding in Cobalt Wires and Foils. Trans. Am. Nuclear Soc., vol. 4, no. 1, June 1961, pp. 61-63.

4. Devaney, J. J., Devaney, M. A., and Coward, David: Tungsten Cross Sections and Their Temperature Dependence. LA-2289, Los Alamos Sci. Lab., Univ. Calif., May 22, 1958.

5. Bogart, D., and Shook, D.: Self-Shielding in Tungsten Resonances Dominated by the 18.8 ev Strongly Scattering Absorptive Resonance. Trans. Am. Nuclear Soc., vol. 3, no. 2, Dec. 1960, pp. 461-462.

6. Hughes, D. J., Magurno, B. A., and Brussel, M. K.: Neutron Cross Sections. BNL 325, Second ed. Supp. 1, Jan. 1, 1960.

7. Dresner, L.: Effective Resonance Integrals of U-238 and TH-232. Nuclear Sci. & Eng., vol. I, no. 1, Mar. 1956, pp. 68-79.

8. Schneider, Harold: A Numerical Method for Obtaining Monoenergetic Neutron Flux Distributions and Transmissions in Multiple-Region Slabs. NASA MEMO 2-23-59E, 1959.

9. Meyer, Herbert A., ed.: Symposium on Monte Carlo Methods. John Wiley & Sons, Inc., c. 1956.

TABLE I. - ABSORPTIONS IN VARIOUS ENERGY INTERVALS FOR VARIOUS THICKNESSES OF TUNGSTEN WITH WATER MODERATOR

[kT = 0.0253 ev.]

(a) 0.291-inch-water moderator

E_1 to E_2, ev	$\sigma_{a,max}$, barns	$\sigma_{s,max}$, barns	DRAI($E_1 \rightarrow E_2$) / Total DRAI × 100, percent	Tungsten thickness, t_W, mils		
				0.818	8	40
				Monte Carlo absorptions[a] per history ×10^4 from E_1 to E_2		
961 → 40.3	(b)	(b)	5.54	22.1(8.58)	155.5(13.89)	508.3(22.63)
40.3 → 28.5	4	33	.12	.5(0.19)	4.9(0.44)	23.7(0.98)
28.5 → 26	865	1,163	3.25	11.1(4.31)	55.0(4.91)	117.8(4.86)
26 → 20.7	3764	3,175	15.86	36.6(14.21)	132.0(11.78)	244.1(10.06)
20.7 → 16	4200	25,660	40.38	88.3(34.29)	292.1(26.06)	445.9(18.38)
16 → 9.5	19	74	.99	3.8(1.48)	37.1(3.31)	163.4(6.74)
9.5 → 8.9	3	7	.06	.2(0.08)	1.9(0.17)	9.9(0.41)
8.9 → 6.2	691	50	5.21	15.7(6.10)	103.7(9.25)	229.3(9.45)
6.2 → 5.7	3	6.1	.08	.3(0.12)	2.1(0.19)	11.8(0.49)
5.7 → 2.3	2712	93	27.90	76.5(29.71)	312(27.89)	578.0(23.82)
2.3 → 1.2	3	5	.61	2.4(0.93)	24.1(2.15)	94.3(3.89)
961 → 1.2	(c)	(c)	100	257.5(100)	1121.0(100)	2426.5(100)
961 → 0.125	(c)	(c)	------	272.6	1244.9	2920.1

[a]Percent of total absorption given in parentheses.

[b]Fifteen resonances in this energy region.

[c]Twenty-one resonances in this energy region.

TABLE I. - Continued. ABSORPTIONS IN VARIOUS ENERGY INTERVALS FOR VARIOUS THICKNESSES OF TUNGSTEN WITH WATER MODERATOR

[kT = 0.0253 ev.]

(b) 1-inch-water moderator

E_1 to E_2, ev	$\sigma_{a,max}$, barns	$\sigma_{s,max}$, barns	$\frac{DRAI(E_1 \rightarrow E_2)}{\text{Total DRAI}} \times 100$, percent	Tungsten thickness, t_W, mils			
				0.818	8	40	80
				Monte Carlo absorptions[a] per history $\times 10^4$ from E_1 to E_2			
961 → 40.3	(b)	(b)	5.54	6.7(7.90)	49.3(13.20)	158.1(18.79)	272.5(21.84)
40.3 → 28.5	4	33	.12	.15(0.17)	1.59(0.424)	7.54(0.90)	15.5(1.24)
28.5 → 26	865	1,163	3.25	3.60(4.25)	19.71(5.28)	44.37(5.27)	49.7(3.98)
26 → 20.7	3764	3,175	15.86	14.64(17.27)	37.74(10.10)	86.91(10.33)	126.8(10.16)
20.7 → 16	4200	25,660	40.38	27.62(32.58)	105.98(28.38)	152.55(18.13)	180.3(14.45)
16 → 9.5	19	74	.99	1.00(1.18)	11.63(3.11)	51.51(6.12)	101.9(8.17)
9.5 → 8.9	3	7	.06	.05(0.06)	.52(0.14)	2.70(0.32)	4.6(0.37)
8.9 → 6.2	691	50	5.21	5.27(6.21)	33.05(8.85)	88.28(10.49)	113.9(9.13)
6.2 → 5.7	3	6.1	.08	.09(0.11)	.83(0.22)	3.59(0.43)	6.8(0.55)
5.7 → 2.3	2712	93	27.90	24.99(29.47)	105.11(28.14)	215.48(25.61)	319.1(25.58)
2.3 → 1.2	3	5	.61	.69(0.81)	6.79(1.82)	30.31(3.60)	56.4(4.52)
961 → 1.2	(c)	(c)	100	84.79(100)	373.47(100)	841.32(100)	1247.5(100)
961 → 0.125	(c)	(c)	------	88.9	411.4	1014.2	1562.4

[a]Percent of total absorption given in parentheses.

[b]Fifteen resonances in this energy region.

[c]Twenty-one resonances in this energy region.

TABLE I. - Continued. ABSORPTIONS IN VARIOUS ENERGY INTERVALS FOR VARIOUS THICKNESSES OF TUNGSTEN WITH WATER MODERATOR

[kT = 0.0253 ev.]

(c) 1.8-inch-water moderator

E_1 to E_2, ev	$\sigma_{a,max}$, barns	$\sigma_{s,max}$, barns	$\frac{DRAI(E_1 \rightarrow E_2)}{\text{Total DRAI}} \times 100$, percent	Tungsten thickness, t_W, mils				
				0.1248	0.819	8	40	80
				Monte Carlo absorptions[a] per history $\times 10^4$ from E_1 to E_2				
961 → 40.3	(b)	(b)	5.54	0.8(9.03)	3.8(8.48)	28.1(13.93)	83.0(17.61)	133.3(20.20)
40.3 → 28.5	4	33	.12	.02(0.19)	.07(0.16)	.72(0.36)	4.19(0.89)	7.1(1.08)
28.5 → 26	865	1,163	3.25	.21(2.34)	1.36(3.04)	8.42(4.17)	27.97(5.93)	29.9(4.53)
26 → 20.7	3764	3,175	15.86	1.73(19.54)	8.88(19.81)	24.67(12.33)	50.51(10.72)	70.3(10.65)
20.7 → 16	4200	25,660	40.38	3.18(35.89)	13.66(30.48)	50.16(24.87)	79.01(16.76)	87.6(13.28)
16 → 9.5	19	74	.99	.10(1.14)	.65(1.46)	5.99(2.97)	31.14(6.60)	59.8(9.06)
9.5 → 8.9	3	7	.06	.01(0.07)	.04(0.09)	.36(0.18)	1.81(0.38)	3.8(0.58)
8.9 → 6.2	691	50	5.21	.42(4.72)	2.57(5.73)	18.61(9.22)	45.85(9.73)	59.9(9.08)
6.2 → 5.7	3	6.1	.08	.01(0.09)	.05(0.10)	.44(0.22)	3.07(0.65)	3.6(0.55)
5.7 → 2.3	2712	93	27.90	2.32(26.15)	13.31(29.70)	60.95(30.21)	127.50(27.05)	172.7(26.17)
2.3 → 1.2	3	5	.61	.06(0.66)	.38(0.84)	3.29(1.63)	17.41(3.69)	31.8(4.82)
961 → 1.2	(c)	(c)	100	8.86(100)	44.82(100)	201.73(100)	471.41(100)	659.8(100)
961 → 0.125	(c)	(c)	------	9.20	47.20	223.6	568.5	842.1

[a]Percent of total absorption given in parentheses.

[b]Fifteen resonances in this energy region.

[c]Twenty-one resonances in this energy region.

TABLE I. - Concluded. ABSORPTIONS IN VARIOUS ENERGY INTERVALS FOR VARIOUS THICKNESSES OF TUNGSTEN WITH WATER MODERATOR

[kT = 0.0253 ev.]

(d) 4-inch-water moderator

E_1 to E_2, ev	$\sigma_{a,max}$, barns	$\sigma_{s,max}$, barns	$\frac{DRAI(E_1 \rightarrow E_2)}{\text{Total DRAI}} \times 100$, percent	Tungsten thickness, t_W, mils						
				0.126	0.252	0.818	8	40	80	160
				Monte Carlo absorptions[a] per history $\times 10^4$ from E_1 to E_2						
961 → 40.3	(b)	(b)	5.54	0.4(9.76)	0.7(8.64)	1.87(8.21)	11.28(11.46)	41.83(18.25)	71.19(20.68)	120.6(25.00)
40.3 → 28.5	4	33	.12	.1(2.44)	.1(1.23)	.034(0.15)	.255(0.26)	1.34(0.58)	3.10(0.90)	5.7(1.2)
28.5 → 26	865	1,163	3.25	.1(2.44)	.1(1.23)	.538(2.37)	5.52(5.61)	12.26(5.35)	16.30(4.74)	12.7(2.6)
26 → 20.7	3764	3,175	15.86	.9(21.95)	2.2(27.16)	6.31(27.84)	19.33(19.64)	27.28(11.90)	36.27(10.53)	52.1(10.8)
20.7 → 16	4200	25,660	40.38	1.1(26.83)	2.4(29.63)	6.83(30.13)	24.22(24.61)	40.83(17.81)	47.79(13.88)	49.7(10.3)
16 → 9.5	19	74	.99	0(0)	.1(1.23)	.258(1.14)	2.63(2.67)	11.79(5.14)	25.32(7.35)	57.1(11.84)
9.5 → 8.9	3	7	.06	0(0)	0(0)	.033(0.14)	.23(0.23)	.84(0.37)	1.90(0.55)	2.7(0.56)
8.9 → 6.2	691	50	5.21	.3(7.32)	.5(6.17)	1.29(5.68)	8.85(8.99)	23.25(10.14)	33.52(9.74)	50.2(10.4)
6.2 → 5.7	3	6.1	.08	0(0)	0(0)	.02(0.09)	.20(0.20)	.72(0.31)	2.68(0.78)	3.1(0.64)
5.7 → 2.3	2712	93	27.90	1.2(29.27)	1.9(23.45)	5.32(23.48)	24.23(24.62)	61.40(27.79)	91.74(26.65)	106.1(22.0)
2.3 → 1.2	3	5	.61	0(0)	.1(1.23)	.17(0.77)	1.68(1.71)	7.69(3.35)	14.46(4.2)	22.3(1.18)
961 → 1.2	(c)	(c)	100	4.1(100)	8.1(100)	22.67(100)	98.43(100)	229.23(100)	344.27(100)	482.3(100)
961 → 0.125	(c)	(c)	------	4.3	8.4	23.7	108.4	273.5	431.5	631.1

[a]Percent of total absorption given in parentheses.

[b]Fifteen resonances in this energy region.

[c]Twenty-one resonances in this energy region.

TABLE II. - ABSORPTIONS IN VARIOUS ENERGY INTERVALS FOR VARIOUS THICKNESSES OF TUNGSTEN WITH LITHIUM HYDRIDE MODERATOR

[kT = 0.0253 ev.]

(a) 0.0320-inch-lithium-hydride moderator

E_1 to E_2, ev	$\sigma_{a,max}$, barns	$\sigma_{s,max}$, barns	$\frac{DRAI(E_1 \rightarrow E_2)}{\text{Total DRAI}} \times 100$, percent	Tungsten thickness, t_W, mils		
				0.818	8	40
				Monte Carlo absorptions[a] per history $\times 10^4$ from E_1 to E_2		
961 → 40.3	(b)	(b)	5.54	20.3(7.38)	161.1(14.22)	488.8(19.93)
40.3 → 28.5	4	33	.12	.5(0.18)	4.6(0.41)	21.9(0.89)
28.5 → 26	865	1,163	3.25	13.5(4.91)	63.2(5.58)	11.0(4.53)
26 → 20.7	3764	3,175	15.86	35.0(12.72)	130.3(11.50)	247.5(10.09)
20.7 → 16	4200	25,660	40.38	95.0(34.52)	297.2(26.23)	483.5(19.71)
16 → 9.5	19	74	.99	3.9(1.42)	38.1(3.36)	155.1(6.32)
9.5 → 8.9	3	7	.06	.3(0.11)	1.8(0.16)	7.8(0.32)
8.9 → 6.2	691	50	5.21	17.4(6.32)	110.4(9.74)	238.1(9.71)
6.2 → 5.7	3	6.1	.08	.4(0.15)	2.6(0.23)	10.7(0.44)
5.7 → 2.3	2712	93	27.90	86.4(31.40)	303.6(26.80)	596.5(24.32)
2.3 → 1.2	3	5	.61	2.5(0.91)	20.4(1.80)	92.6(3.77)
961 → 1.2	(c)	(c)	100	275.2(100)	1133.3(100)	2453.5(100)
961 → 0.125	(c)	(c)	------	289.9	1258.4	2933.2

[a]Percent of total absorption given in parentheses.

[b]Fifteen resonances in this energy region.

[c]Twenty-one resonances in this energy region.

TABLE II. - Continued. ABSORPTIONS IN VARIOUS ENERGY INTERVALS FOR VARIOUS THICKNESSES OF TUNGSTEN WITH LITHIUM HYDRIDE MODERATOR

[kT = 0.0253 ev.]

(b) 1-inch-lithium-hydride moderator

E_1 to E_2, ev	$\sigma_{a,max}$, barns	$\sigma_{s,max}$, barns	$\frac{DRAI(E_1 \rightarrow E_2)}{\text{Total DRAI}} \times 100$, percent	Tungsten thickness, t_W, mils			
				0.818	8	40	80
				Monte Carlo absorptions[a] per history $\times 10^4$ from E_1 to E_2			
961 → 40.3	(b)	(b)	5.54	7.6(9.22)	50.9(12.40)	174.8(17.75)	298.5(21.98)
40.3 → 28.5	4	33	.12	.2(0.24)	1.7(0.41)	9.1(0.92)	14.9(1.10)
28.5 → 26	865	1,163	3.25	2.9(3.52)	16.4(4.00)	53.7(5.45)	62(4.57)
26 → 20.7	3764	3,175	15.86	12.0(14.56)	50.1(12.21)	104.2(10.58)	123.3(9.08)
20.7 → 16	4200	25,660	40.38	28.9(35.07)	124.9(30.43)	198.0(20.10)	204.7(15.07)
16 → 9.5	19	74	.99	1.2(1.46)	10.6(2.58)	57.4(5.83)	106.8(7.86)
9.5 → 8.9	3	7	.06	.1(0.12)	.7(0.17)	2.2(0.22)	8.0(0.59)
8.9 → 6.2	691	50	5.21	5.2(6.31)	35.6(8.67)	103.4(10.50)	139.0(10.24)
6.2 → 5.7	3	6.1	.08	.1(0.12)	1.0(0.24)	4.4(0.45)	7.4(0.54)
5.7 → 2.3	2712	93	27.90	23.4(28.40)	111.8(27.24)	243.8(24.75)	325.6(23.98)
2.3 → 1.2	3	5	.61	.8(0.97)	6.7(1.63)	33.0(3.35)	67.7(4.99)
961 → 1.2	(c)	(c)	100	82.4(100)	410.4(100)	985.0(100)	1357.9(100)
961 → 0.125	(c)	(c)	------	87.0	454.1	1168.6	1694.0

[a]Percent of total absorption given in parentheses.

[b]Fifteen resonances in this energy region.

[c]Twenty-one resonances in this energy region.

TABLE II. - Continued. ABSORPTIONS IN VARIOUS ENERGY INTERVALS FOR VARIOUS THICKNESSES OF TUNGSTEN WITH LITHIUM HYDRIDE MODERATOR

[kT = 0.0253 ev.]

(c) 2-inch-lithium-hydride moderator

E_1 to E_2, ev	$\sigma_{a,max}$, barns	$\sigma_{s,max}$, barns	$\frac{DRAI(E_1 \rightarrow E_2)}{\text{Total DRAI}} \times 100$, percent	Tungsten thickness, t_W, mils			
				0.818	8	40	80
				Monte Carlo absorptions[a] per history $\times 10^4$ from E_1 to E_2			
961 → 40.3	(b)	(b)	5.54	3.7(8.64)	24.7(11.93)	83.2(17.26)	139.3(19.90)
40.3 → 28.5	4	33	.12	.1(0.23)	.8(0.39)	3.9(0.81)	6.7(0.96)
28.5 → 26	865	1,163	3.25	2.3(5.37)	12.9(6.23)	22.6(4.69)	29.2(4.17)
26 → 20.7	3764	3,175	15.86	5.7(13.32)	15.7(7.58)	37.8(7.84)	61.7(8.81)
20.7 → 16	4200	25,660	40.38	11.6(27.10)	55.2(26.65)	89.9(18.65)	101.5(14.50)
16 → 9.5	19	74	.99	.6(1.40)	6.7(3.23)	31.7(6.58)	59.6(8.51)
9.5 → 8.9	3	7	.06	.1(0.23)	.2(0.10)	1.7(0.35)	3.1(0.44)
8.9 → 6.2	691	50	5.21	2.8(6.54)	19.2(9.27)	56.2(11.66)	65.1(9.30)
6.2 → 5.7	3	6.1	.08	0.0(0)	.4(0.19)	2.1(0.44)	4.5(0.64)
5.7 → 2.3	2712	93	27.90	15.5(36.21)	67.5(32.59)	134.6(27.92)	194.4(27.77)
2.3 → 1.2	3	5	.61	.4(0.93)	3.8(1.83)	18.4(3.82)	33.8(4.83)
961 → 1.2	(c)	(c)	100	42.8(100)	207.1(100)	482.1(100)	699.9(100)
961 → 0.125	(c)	(c)	------	45.1	228.9	584.7	887.4

[a]Percent of total absorption given in parentheses.

[b]Fifteen resonances in this energy region.

[c]Twenty-one resonances in this energy region.

TABLE II. - Continued. ABSORPTIONS IN VARIOUS ENERGY INTERVALS FOR VARIOUS THICKNESSES OF TUNGSTEN WITH LITHIUM HYDRIDE MODERATOR

[kT = 0.0253 ev.]

(d) 3-inch-lithium-hydride moderator

E_1 to E_2, ev	$\sigma_{a,max}$, barns	$\sigma_{s,max}$, barns	$\frac{DRAI(E_1 \rightarrow E_2)}{\text{Total DRAI}} \times 100$, percent	Tungsten thickness, t_W, mils			
				0.818	8	40	80
				Monte Carlo absorptions[a] per history $\times 10^4$ from E_1 to E_2			
961 → 40.3	(b)	(b)	5.54	2.5(8.28)	15.5(11.83)	51.6(16.30)	107.5(22.47)
40.3 → 28.5	4	33	.12	.1(0.33)	.7(0.53)	2.3(0.73)	5.4(1.13)
28.5 → 26	865	1,163	3.25	.8(2.65)	5.8(4.43)	17.1(5.40)	18.5(3.87)
26 → 20.7	3764	3,175	15.86	4.4(14.57)	15.6(11.91)	30.5(9.63)	42.7(8.92)
20.7 → 16	4200	25,660	40.38	9.1(30.13)	37.1(28.32)	61.1(19.30)	71.3(14.90)
16 → 9.5	19	74	.99	.3(0.99)	3.0(2.29)	17.1(5.40)	36.0(7.52)
9.5 → 8.9	3	7	.06	0.0(0)	.2(0.15)	1.0(0.32)	1.9(0.40)
8.9 → 6.2	691	50	5.21	2.4(7.95)	14.3(10.92)	39.5(12.48)	47.1(9.84)
6.2 → 5.7	3	6.1	.08	.1(0.33)	.3(0.23)	1.0(0.32)	2.5(0.52)
5.7 → 2.3	2712	93	27.90	10.2(33.77)	36.0(27.48)	83.5(26.37)	124.5(26.02)
2.3 → 1.2	3	5	.61	.3(0.99)	2.5(1.91)	11.9(3.76)	21.1(4.41)
961 → 1.2	(c)	(c)	100	30.2(100)	131.0(100)	316.6(100)	478.5(100)
961 → 0.125	(c)	(c)	------	31.6	145.3	385.1	615.4

[a]Percent of total absorption given in parentheses.

[b]Fifteen resonances in this energy region.

[c]Twenty-one resonances in this energy region.

TABLE II. - Concluded. ABSORPTIONS IN VARIOUS ENERGY INTERVALS FOR VARIOUS THICKNESSES OF TUNGSTEN WITH LITHIUM HYDRIDE MODERATOR

[kT = 0.0253 ev.]

(e) 4-inch-lithium-hydride moderator

E_1 to E_2, ev	$\sigma_{a,max}$, barns	$\sigma_{s,max}$, barns	$\frac{DRAI(E_1 \rightarrow E_2)}{\text{Total DRAI}} \times 100$, percent	Tungsten thickness, t_W, mils			
				0.818	8	40	80
				Monte Carlo absorptions[a] per history $\times 10^4$ from E_1 to E_2			
961 → 40.3	(b)	(b)	5.54	2.8(12.84)	12.0(12.24)	42.0(18.42)	70.3(20.82)
40.3 → 28.5	4	33	.12	0.0(0)	.4(0.41)	1.6(0.70)	4.1(1.21)
28.5 → 26	865	1,163	3.25	.5(2.29)	3.8(3.88)	11.3(4.96)	11.5(3.41)
26 → 20.7	3764	3,175	15.86	4.6(21.10)	16.2(16.53)	22.2(9.74)	28.0(8.29)
20.7 → 16	4200	25,660	40.38	5.7(26.15)	24.4(24.90)	34.6(15.18)	40.9(12.11)
16 → 9.5	19	74	.99	.3(1.38)	2.7(2.76)	12.1(5.31)	32.8(9.71)
9.5 → 8.9	3	7	.06	0.0(0)	.2(0.20)	2.4(1.05)	2.5(0.74)
8.9 → 6.2	691	50	5.21	1.8(8.26)	8.8(8.98)	29.6(12.98)	35.4(10.48)
6.2 → 5.7	3	6.1	.08	0.0(0)	.3(0.31)	1.0(0.44)	3.7(1.10)
5.7 → 2.3	2712	93	27.90	5.9(27.06)	27.4(27.96)	60.6(26.58)	89.5(26.50)
2.3 → 1.2	3	5	.61	.2(0.92)	1.8(1.84)	10.7(4.69)	19.0(5.63)
961 → 1.2	(c)	(c)	100	21.8(100)	98.0(100)	228.1(100)	337.7(100)
961 → 0.125	(c)	(c)	------	23.0	109.7	282.1	450.8

[a]Percent of total absorption given in parentheses.

[b]Fifteen resonances in this energy region.

[c]Twenty-one resonances in this energy region.

TABLE III. - ABSORPTIONS IN VARIOUS ENERGY INTERVALS FOR VARIOUS THICKNESSES OF TUNGSTEN WITH BERYLLIUM OXIDE MODERATOR

[kT = 0.0253 ev.]

(a) 4-inch-beryllium-oxide moderator

E_1 to E_2, ev	$\sigma_{a,max}$, barns	$\sigma_{s,max}$, barns	$\frac{DRAI(E_1 \rightarrow E_2)}{\text{Total DRAI}} \times 100$, percent	Tungsten thickness, t_W, mils				
				0.818	8	40	80	160
				Monte Carlo absorptions[a] per history $\times 10^4$ from E_1 to E_2				
961 → 40.3	(b)	(b)	5.54	18.2(7.41)	117.4(12.39)	443.4(20.67)	677.0(24.39)	1041.7(27.88)
40.3 → 28.5	4	33	.12	.5(0.20)	4.1(0.43)	16.2(0.76)	36.5(1.31)	69.3(1.86)
28.5 → 26	865	1,163	3.25	10.7(4.36)	51.1(5.39)	102.7(4.79)	133.3(4.80)	173.1(4.63)
26 → 20.7	3764	3,175	15.86	46.8(19.06)	95.7(10.10)	198.4(9.26)	293.2(10.56)	375.1(10.04)
20.7 → 16	4200	25,660	40.38	83.0(33.81)	261.2(27.56)	434.5(20.28)	337.0(12.14)	373.7(10.01)
16 → 9.5	19	74	.99	3.2(1.30)	30.3(3.20)	103.3(4.82)	201.5(7.26)	316.7(8.48)
9.5 → 8.9	3	7	.06	.1(0.04)	1.5(0.16)	6.9(0.32)	13.1(0.47)	25.3(0.68)
8.9 → 6.2	691	50	5.21	16.1(6.56)	112.1(11.83)	243.2(11.35)	295.6(10.65)	319.6(8.56)
6.2 → 5.7	3	6.1	.08	.3(0.12)	4.2(0.44)	8.7(0.41)	17.3(0.62)	21.9(0.59)
5.7 → 2.3	2712	93	27.90	64.8(26.40)	252.6(26.65)	515.6(24.06)	643.4(23.18)	822.5(22.03)
2.3 → 1.2	3	5	.61	1.8(0.73)	17.6(1.86)	70.2(3.28)	128.3(4.62)	195.4(5.23)
961 → 1.2	(c)	(c)	100	245.5(100)	947.8(100)	2143.1(100)	2776.2(100)	3734.3(100)
961 → 0.125	(c)	(c)	------	256.5	1049.5	2550.9	3461.6	4723.4

[a]Percent of total absorption given in parentheses.

[b]Fifteen resonances in this energy region.

[c]Twenty-one resonances in this energy region.

TABLE III. - Concluded. ABSORPTIONS IN VARIOUS ENERGY INTERVALS FOR VARIOUS THICKNESSES OF TUNGSTEN WITH BERYLLIUM OXIDE MODERATOR

[kT = 0.0253 ev.]

(b) 8-inch-beryllium-oxide moderator

E_1 to E_2, ev	$\sigma_{a,max}$, barns	$\sigma_{s,max}$, barns	$\frac{DRAI(E_1 \rightarrow E_2)}{\text{Total DRAI}} \times 100$, percent	Tungsten thickness, t_W, mils				
				0.630	8.16	40.3	80	160
				Monte Carlo absorptions[a] per history $\times 10^4$ from E_1 to E_2				
961 → 40.3	(b)	(b)	5.54	6.9(6.82)	63.3(13.90)	205.9(19.42)	364.9(24.66)	544.0(27.19)
40.3 → 28.5	4	33	.12	.1(0.10)	2.2(0.48)	10.6(1.00)	18.0(1.22)	35.8(1.79)
28.5 → 26	865	1,163	3.25	4.7(4.64)	25.3(5.55)	66.0(6.23)	49.8(3.36)	89.6(4.48)
26 → 20.7	3764	3,175	15.86	14.6(14.43)	58.2(12.78)	115.8(10.92)	160.3(10.81)	179.9(9.00)
20.7 → 16	4200	25,660	40.38	43.2(42.69)	117.2(25.73)	238.7(22.52)	202.3(13.67)	193.9(9.70)
16 → 9.5	19	74	.99	1.2(1.19)	12.4(2.72)	63.3(5.97)	116.6(7.88)	170.4(8.50)
9.5 → 8.9	3	7	.06	0(0)	.9(0.20)	3.9(0.37)	5.2(0.35)	12.3(0.615)
8.9 → 6.2	691	50	5.21	4.2(4.15)	42.7(9.37)	92.4(8.72)	147.3(9.93)	203.3(10.17)
6.2 → 5.7	3	6.1	.08	.1(0.10)	1.2(0.26)	6.3(0.59)	7.5(0.51)	13.5(0.68)
5.7 → 2.3	2712	93	27.90	25.4(25.10)	124.6(27.35)	213.9(20.18)	341.0(23.04)	438.7(21.94)
2.3 → 1.2	3	5	.61	.8(0.79)	7.5(1.65)	42.8(4.04)	67.5(4.56)	120.2(6.01)
961 → 1.2	(c)	(c)	100	101.2(100)	455.5(100)	1059.6(100)	1480.4(100)	2001.6(100)
961 → 0.125	(c)	(c)	------	105.8	509.7	1284.2	1855.8	2555.8

[a]Percent of total absorption given in parentheses.

[b]Fifteen resonances in this energy region.

[c]Twenty-one resonances in this energy region.

TABLE IV. - DOPPLER BROADENED ABSORPTIONS IN VARIOUS ENERGY INTERVALS WITH 4-INCH-WATER MODERATOR

(a) 8 mils of tungsten

E_1 to E_2, ev	Energy, kT, ev					
	0	0.0253	0.05	0.1	0.2	0.5
	Monte Carlo absorptions[a] per history $\times 10^4$ from E_1 to E_2					
961 → 40.3	9.6(10.8)	11.28(11.46)	11.7(11.24)	13.5(12.06)	14.1(11.24)	12.3(8.68)
40.3 → 28.5 40.3 → 27.75(0 ev)	.9(1.03)	.255(0.26)	.3(0.29)	.3(0.27)	.2(0.16)	.3(0.21)
28.5 → 26 27.75 → 26.1(0 ev)	2.8(3.19)	5.52(5.61)	5.9(5.67)	7.8(6.97)	8.6(6.85)	7.6(5.36)
26.1 → 20.7 26.1 → 20.31(0 ev)	12.6(14.35)	19.33(19.64)	20.2(19.40)	21.0(18.77)	24.5(19.52)	31.6(22.30)
20.3 → 15.8(0 ev) 20.7 → 16 20.7 → 15(0.5 ev)	25.7(29.27)	24.22(24.61)	24.2(23.25)	24.4(21.81)	28.1(22.39)	33.4(23.57)
15.8 → 9.50(0 ev) 16 → 9.5 15 → 9.3(0.5 ev)	2.6(2.96)	2.63(2.67)	2.6(2.50)	2.6(2.32)	2.5(1.99)	2.7(1.91)
9.5 → 8.9 9.3 → 8.7(0.5 ev)	.1(0.11)	.23(0.23)	.2(0.19)	.2(0.18)	.3(0.24)	.2(0.14)
8.9 → 6.2 8.7 → 6.2(0.5 ev)	6.3(7.18)	8.85(8.89)	10.2(9.80)	10.9(9.74)	11.7(9.52)	11.3(7.97)
6.2 → 5.7	.1(0.11)	.20(0.20)	.2(0.19)	.2(0.18)	.2(0.16)	.1(0.07)
5.7 → 2.3	25.3(28.82)	24.23(24.62)	26.9(25.84)	29.3(26.18)	33.6(26.77)	40.5(28.58)
2.3 → 1.2	1.8(2.05)	1.68(1.71)	1.7(1.63)	1.7(1.52)	1.7(1.35)	1.7(1.20)
961 → 1.2 961 → 0.125 961 → 0.0252(0 ev)	87.8(100) 116.2	98.43(100) 108.4	104.1(100) 113.9	111.9(100) 122.0	125.5(100) 134.7	141.7(100) 150.8

[a]Percent of total absorption given in parentheses.

TABLE IV. - Continued. DOPPLER BROADENED ABSORPTIONS IN VARIOUS ENERGY INTERVALS WITH 4-INCH-WATER MODERATOR

(b) 80 mils of tungsten

E_1 to E_2, ev	Energy, kT, ev					
	0	0.0253	0.05	0.1	0.2	0.5
	Monte Carlo absorptions[a] per history $\times 10^4$ from E_1 to E_2					
961 → 40.3	46.9(15.09)	71.19(20.68)	72.0(22.24)	71.8(21.95)	76.6(22.60)	85.2(22.67)
40.3 → 28.5 40.3 → 27.7(0 ev)	7.8(2.51)	3.10(0.90)	2.9(0.90)	2.8(0.86)	2.8(0.83)	3.2(0.85)
28.5 → 26 27.7 → 26(0 ev)	16.1(5.18)	16.30(4.74)	11.2(3.46)	12.4(3.67)	13.6(4.01)	17.7(4.71)
26 → 20.7 26 → 20.3(0 ev)	37.0(11.90)	36.27(10.53)	31.0(9.58)	33.4(10.21)	35.5(10.47)	35.8(9.52)
20.3 → 15.8(0 ev) 20.7 → 16 20.7 → 15(0.5 ev)	48.4(15.56)	47.79(13.88)	42.6(13.16)	42.2(12.87)	41.2(12.15)	49.3(13.12)
15.8 → 9.5(0 ev) 16 → 9.5 15 → 9.3(0.5 ev)	27.9(8.97)	25.32(7.35)	25.2(7.78)	23.9(7.31)	23.3(6.87)	17.6(4.68)
9.5 → 8.9 9.3 → 8.7(0.5 ev)	1.1(0.35)	1.90(0.55)	1.3(0.40)	1.3(0.40)	1.3(0.38)	1.3(0.35)
8.9 → 6.2 8.7 → 6.2(0.5 ev)	25.0(8.04)	33.52(9.74)	31.0(9.58)	34.8(10.64)	36.4(10.74)	44.1(11.73)
6.2 → 5.7	2.8(0.90)	2.68(0.78)	1.7(0.53)	1.8(0.55)	1.7(0.50)	1.7(0.45)
5.7 → 2.3	79.6(25.59)	91.74(26.65)	90.9(28.08)	88.8(27.15)	93.0(27.43)	105.5(28.07)
2.3 → 1.2	18.2(5.85)	14.46(4.2)	13.9(4.29)	13.9(4.25)	13.6(4.01)	14.5(3.86)
961 → 1.2	310.8(100)	344.27(100)	323.7(100)	327.1(100)	339.0(100)	375.9(100)
961 → 0.125 961 → 0.0252(0 ev)	543.2	431.5	413.7	416.7	424.7	463.7

[a]Percent of total absorption given in parentheses.

TABLE IV. - Concluded. DOPPLER BROADENED ABSORPTIONS IN VARIOUS ENERGY INTERVALS WITH 4-INCH-WATER MODERATOR

(c) 160 mils of tungsten

E_1 to E_2, ev	Energy, kT, ev					
	0	0.0253	0.05	0.1	0.2	0.5
	Monte Carlo absorptions[a] per history $\times 10^4$ from E_1 to E_2					
961 → 40.3	75.3(17.63)	120.6(25.00)	125.2(25.68)	133.8(27.23)	140.3(27.84)	146.0(27.78)
40.3 → 28.5 40.3 → 27.7(0 ev)	8.4(1.97)	5.7(1.2)	5.3(1.09)	5.3(1.08)	4.7(0.93)	4.9(0.93)
28.5 → 26 27.7 → 26(0 ev)	16.2(3.79)	12.7(2.6)	13.4(2.75)	12.2(2.48)	18.8(3.73)	23.1(4.40)
26 → 20.7 26 → 20.3(0 ev)	36.2(8.48)	52.1(10.8)	55.6(11.41)	53.8(10.95)	44.6(8.85)	46.7(8.89)
20.3 → 15.8(0 ev) 20.7 → 16 20.7 → 15(0.5 ev)	40.1(9.39)	49.7(10.3)	50.4(10.34)	52.3(10.65)	47.3(9.38)	61.0(11.61)
15.8 → 9.5(0 ev) 16 → 9.5 15 → 9.3(0.5 ev)	45.0(10.54)	57.1(11.84)	55.4(11.36)	54.5(11.09)	55.4(10.99)	41.4(7.88)
9.5 → 8.9 9.3 → 8.7(0.5 ev)	2.0(0.47)	2.7(0.56)	2.7(0.55)	2.7(0.55)	3.9(0.77)	4.3(0.82)
8.9 → 6.2 8.7 → 6.2(0.5 ev)	44.8(10.49)	50.2(10.4)	47.1(9.66)	44.9(9.14)	51.4(10.20)	55.1(10.49)
6.2 → 5.7	4.3(1.01)	3.1(0.64)	3.0(0.62)	3.0(0.61)	3.0(0.60)	2.8(0.53)
5.816 → 2.278(0 ev) 5.7 → 2.3	125.9(29.48)	106.1(22.0)	107(21.95)	106.4(21.66)	113.1(22.44)	119.7(22.78)
2.278 → 1.219(0 ev) 2.3 → 1.2	28.9(6.77)	22.3(1.18)	22.4(4.59)	22.4(4.56)	21.5(4.27)	20.5(3.90)
961 → 1.2191(0 ev) 961 → 1.2	427.1(100)	482.3(100)	487.5(100)	491(100)	504.0(100)	525.5(100)
961 → 0.025(0 ev) 961 → 0.125	813.3	631.1	634.9	637.0	649.5	668.3

[a]Percent of total absorption given in parentheses.

TABLE V. - ABSORPTIONS IN VARIOUS ENERGY INTERVALS WITH 4-INCH-WATER MODERATOR AND VARIOUS THICKNESSES OF GOLD

[kT = 0.0253 ev.]

E_1 to E_2, ev	Gold thickness, mils					
	0.08	0.316	1.0236	10	50	90
	Monte Carlo absorptions[a] per history $\times 10^4$ from E_1 to E_2					
961 → 193.5	0(0)	0.1(0.31)	0.1(0.16)	0.4(0.20)	1.4(0.31)	2.8(0.48)
193.5 → 109.5	.1(0.76)	.2(0.63)	.6(0.93)	4.2(2.07)	15.0(3.27)	25.6(4.41)
109.5 → 94	0(0)	0(0)	.1(0.16)	.6(0.30)	2.2(0.48)	1.9(0.33)
94 → 72.1	0(0)	.1(0.31)	.3(0.47)	2.6(1.28)	5.2(1.14)	6.2(1.07)
72.1 → 50.8	.2(1.53)	.6(1.88)	1.7(2.64)	12.7(6.26)	23.5(5.13)	32.4(5.59)
50.8 → 10.16	0(0)	.1(0.31)	.2(0.31)	1.6(0.79)	7.8(1.70)	1.2(2.10)
10.16 → 1.37	12.6(96.18)	30.2(94.67)	59.3(92.22)	164.6(81.12)	332.7(72.64)	386.7(66.67)
1.37 → 1.06	.1(0.76)	.1(0.31)	.5(0.78)	4.0(1.97)	22.8(4.98)	34.0(5.86)
1.06 → 0.6	.1(0.76)	.5(1.57)	1.5(2.33)	12.2(6.01)	47.4(10.35)	78.2(13.48)
0.6 → 0.1633	.4	1.4	4.6	40.6	152.6	215.9
961 → 0.6	13.1(100)	31.9(100)	64.3(100)	202.9(100)	458(100)	580(100)
961 → 0.1633	13.5	33.3	68.9	243.5	610.6	795.9

[a]Percent of total absorption given in parentheses.

TABLE VI. - COMPARISON OF MONTE CARLO AND ANALYTICAL 1/v ABSORPTIONS

Tungsten thickness, t_W, mils	E_{min} = 1.20 ev				E_{min} = 0.125 ev			
	$\kappa = (\Sigma_{a,th} t_W) \frac{v_{th}}{v_{min}}$	Monte Carlo absorptions to 1.20 ev $\times 10^5$	$\frac{A}{C_0}$	Analytic A $\times 10^5$	$\kappa = (\Sigma_{a,th} t_W) \frac{v_{th}}{v_{min}}$	Monte Carlo absorptions to 0.125 ev $\times 10^5$	$\frac{A}{C_0}$	Analytic A $\times 10^5$
4-inch-water moderator (C_0 = 0.14256)								
0.818	0.00034830	5	0.00034803	5	0.0010798	15	0.0010774	15.4
8	.0034830	47	.0034615	49.3	.010798	143	.010624	151
40	.017415	226	.017000	242	.053990	685	.050817	724
80	.034830	449	.033378	476	.10798	1,297	.097276	1,387
160	.069660	874	.064683	922	.21596	2,413	.18095	2,580
1.8-inch-water moderator (C_0 = 0.316676)								
80	0.034830	988	0.033378	1057	0.10798	3,010	0.097276	3,080
4-inch-beryllium-oxide moderator (C_0 = 1.6000)								
80	0.034830	5276	0.033378	5340	0.10798	14,250	0.097276	15,564
8-inch-beryllium-oxide moderator (C_0 = 0.80064)								
80	0.034830	2550	0.033378	2672	0.10798	6,838	0.097276	7,788

TABLE VII. - ANALYTICAL RESULTS (EQ. (E11)) FOR COMPARISON WITH MONTE CARLO RESULTS OF TABLE I(d)

[4-in.-water moderator.]

E_1 to E_2, ev	Tungsten thickness, t_W, mils			
	0.818	8	40	80
	Absorptions[a] per history $\times 10^4$ from E_1 to E_2			
961 → 40.3	10.25(31.5)	23.9(20.39)	58.95(22.46)	86.75(23.7)
40.3 → 28.5	0(0)	.35(0.30)	1.7(0.647)	3.35(0.92)
28.5 → 26	.9(2.77)	5.55(4.74)	12.15(4.63)	15.7(4.29)
26 → 20.7	3.4(10.46)	12.35(10.54)	23.7(9.03)	30.95(8.45)
20.7 → 16	8.55(26.31)	32.65(27.86)	60.1(22.89)	71.7(19.58)
16 → 9.5	.3(0.92)	2.85(2.43)	12.95(4.93)	23.75(6.49)
9.5 → 8.9	0(0)	.15(0.12)	.8(0.30)	1.55(0.42)
8.9 → 6.2	1.45(4.46)	9.25(7.89)	22.5(8.57)	31.05(8.48)
6.2 → 5.7	.1(0.31)	.2(0.17)	1.1(0.42)	2.05(0.56)
5.7 → 2.3	6.65(20.46)	28.25(24.10)	60.2(22.93)	83.3(22.75)
2.3 → 1.2	.8(2.46)	1.7(1.45)	8.35(3.18)	15.4(4.21)
961 → 1.2	32.5(100)	117.2(100)	262.5(100)	366.1(100)
961 → 0.125	33.5	127.25	309.7	454.2

[a]Percent of total absorption given in parentheses.

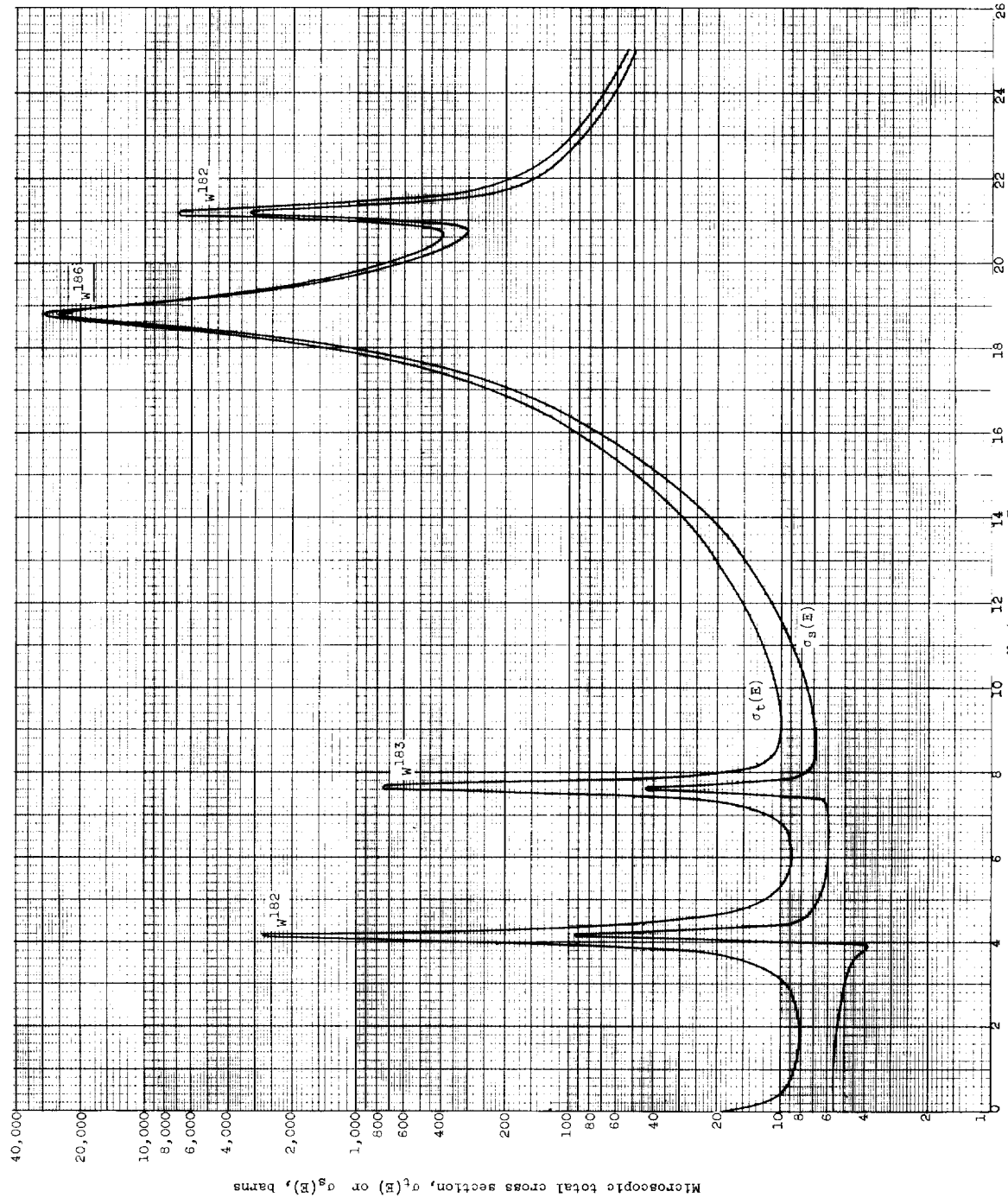

Figure 1. - Total and scattering cross sections of lowest four tungsten resonances as function of energy. kT = 0.0253 ev.

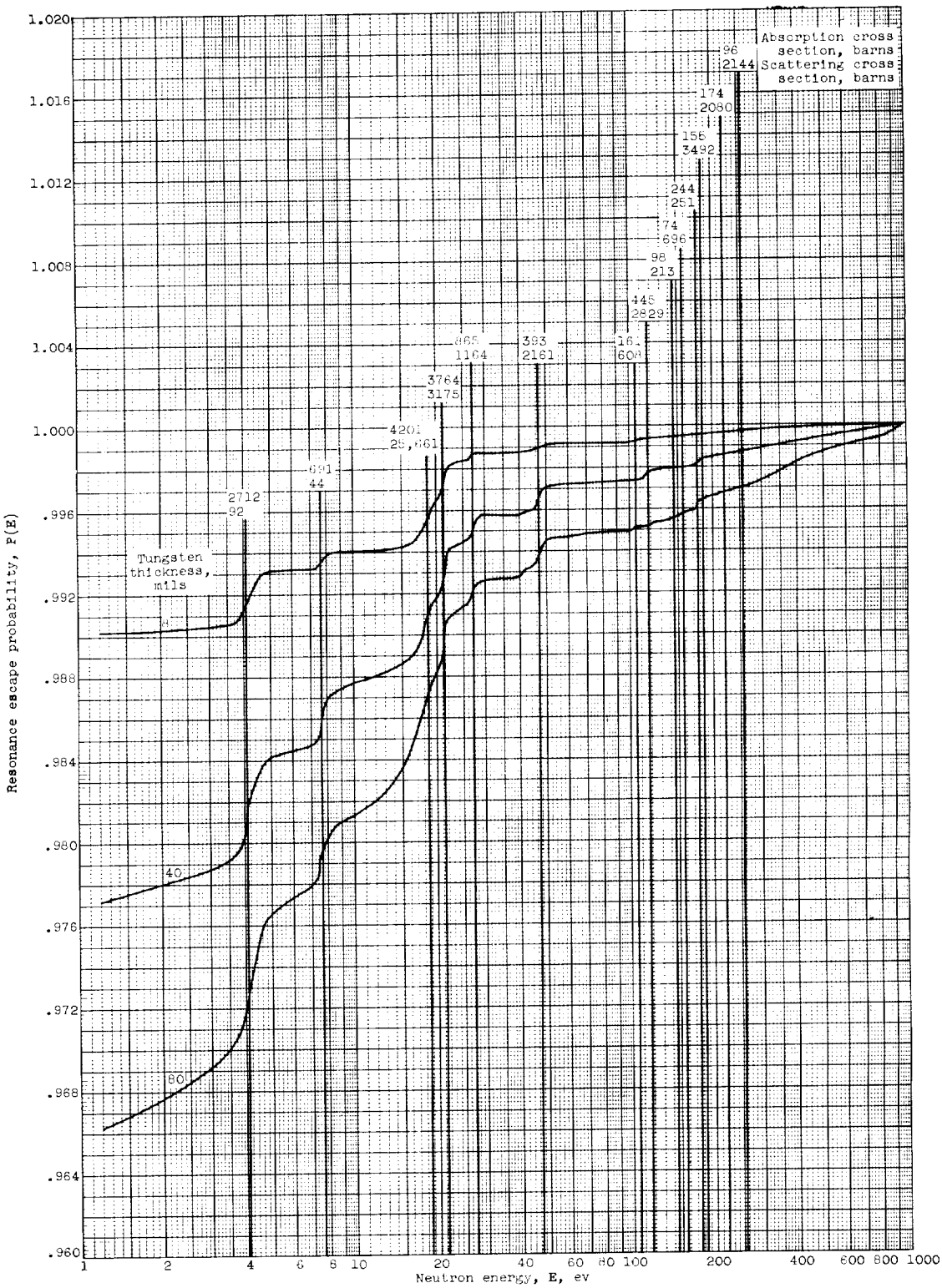

Figure 2. - Resonance escape probability as function of energy for several thicknesses of tungsten and lithium^{7} hydride moderator. Location and peak values of more important tungsten resonances are indicated by vertical lines; kT = 0.0253 electron volt.

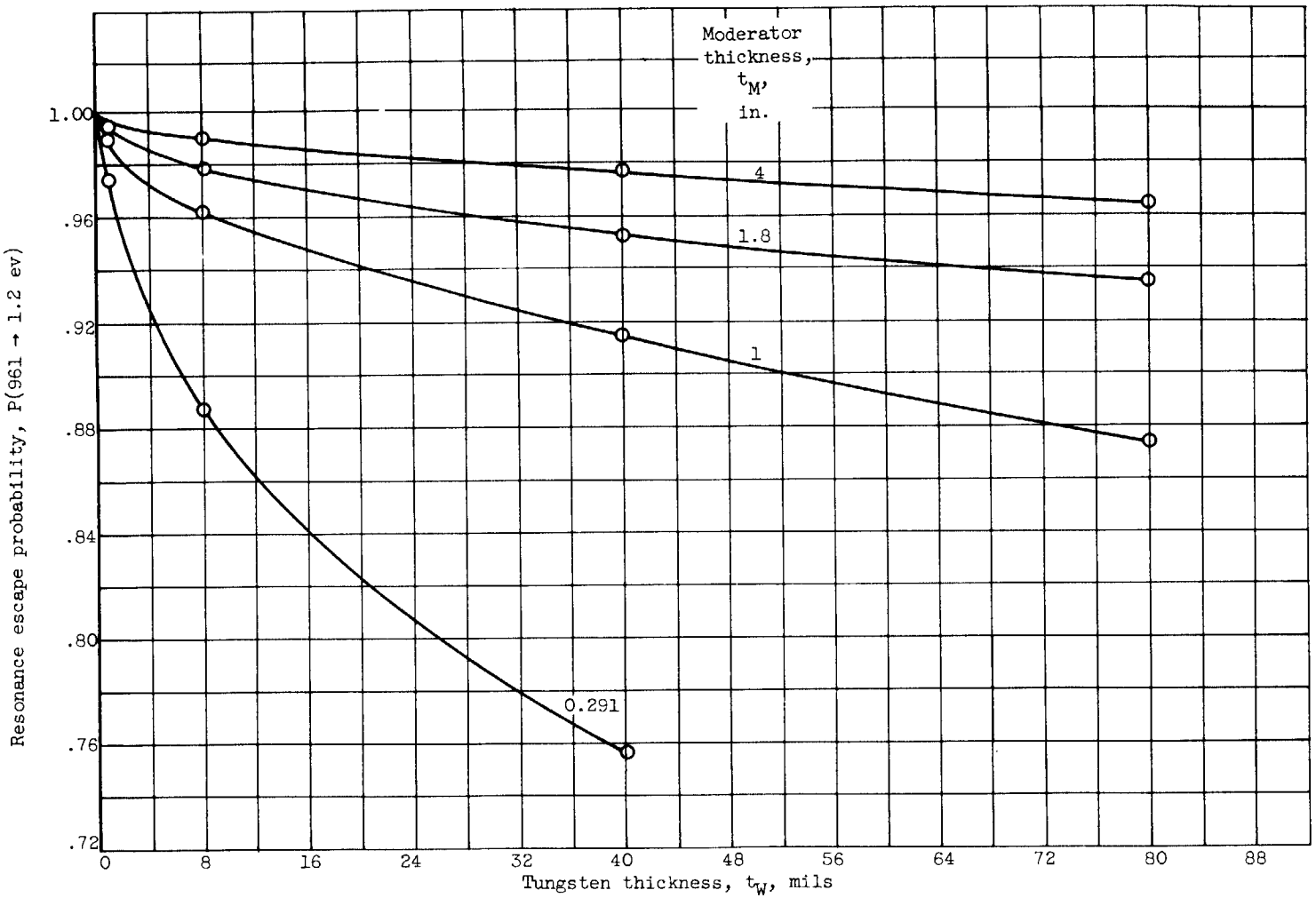

Figure 3. - Resonance escape probability as function of tungsten thickness for water moderator. kT = 0.0253 electron volt; number of atoms per cubic centimeter: hydrogen, 0.066×10^{24}; oxygen, 0.033×10^{24}; tungsten, 0.0632×10^{24}.

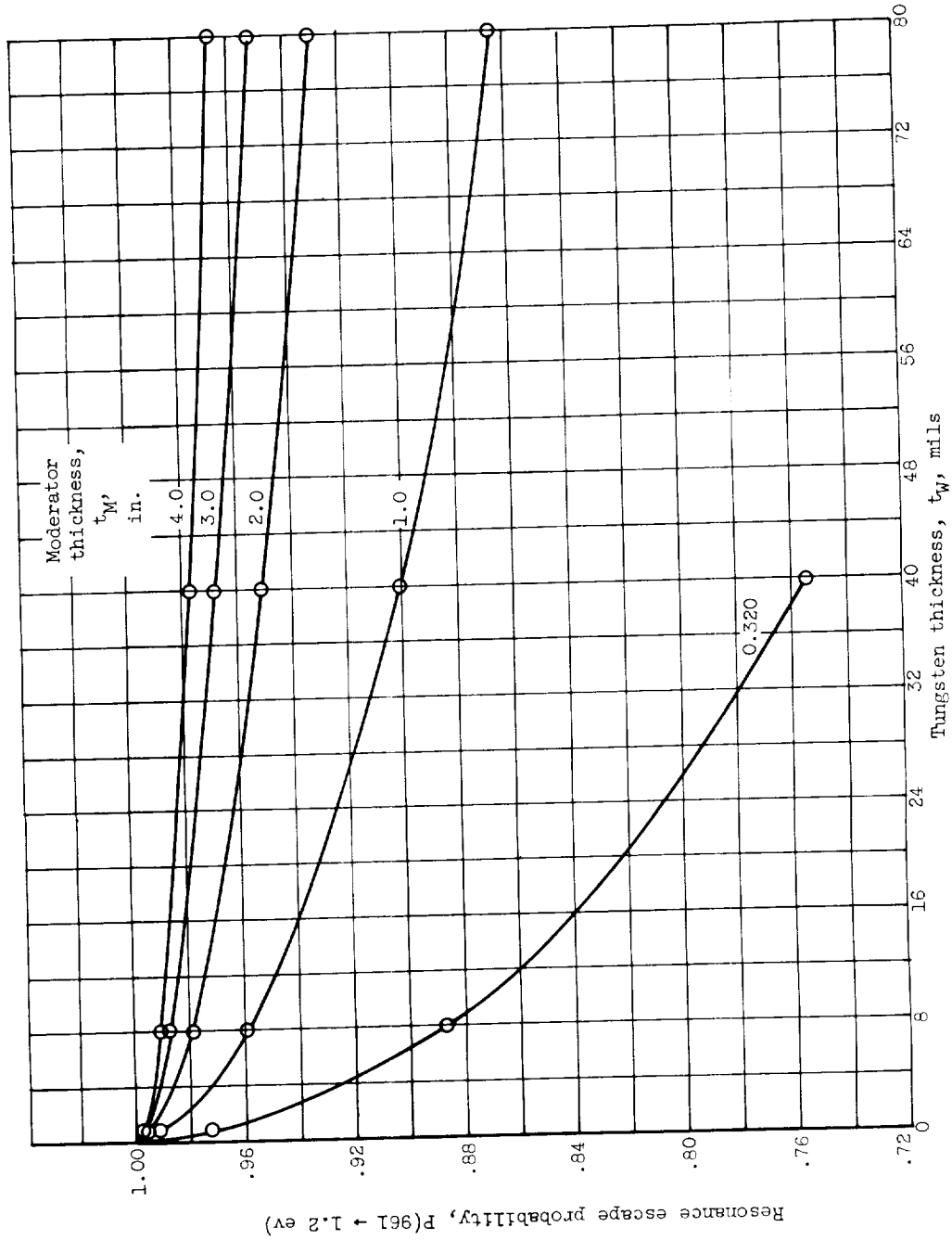

Figure 4. - Resonance escape probability as function of tungsten thickness for lithium^7 hydride moderator. kT = 0.0253 electron volt; number of atoms per cubic centimeter: hydrogen, 0.06×10^{24}; lithium, 0.06×10^{24}; tungsten, 0.0632×10^{24}.

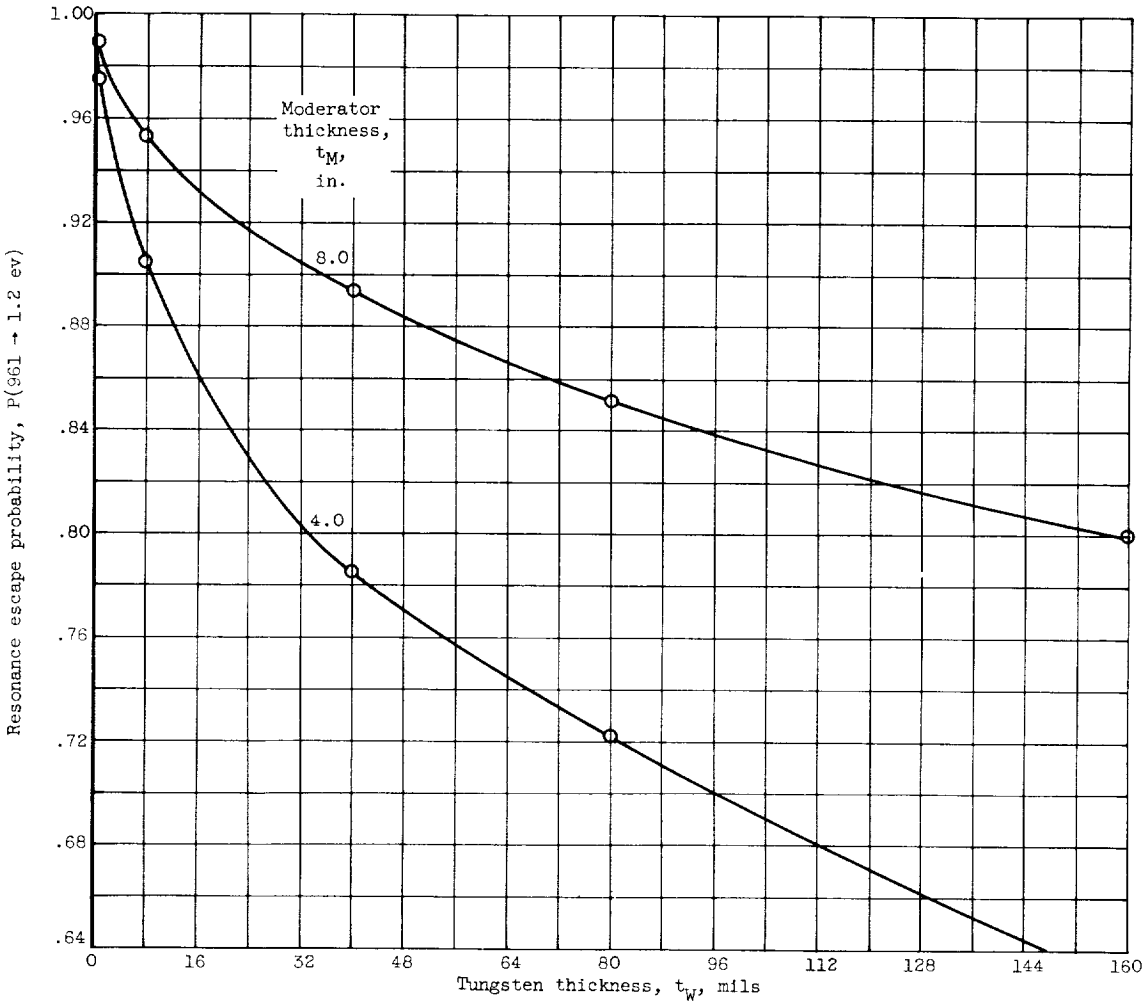

Figure 5. - Resonance escape probability as function of tungsten thickness for beryllium oxide moderator. kT = 0.0253 electron volt; number of atoms per cubic centimeter: beryllium, 0.0725×10^{24}; oxygen, 0.0725×10^{24}; tungsten, 0.0632×10^{24}.

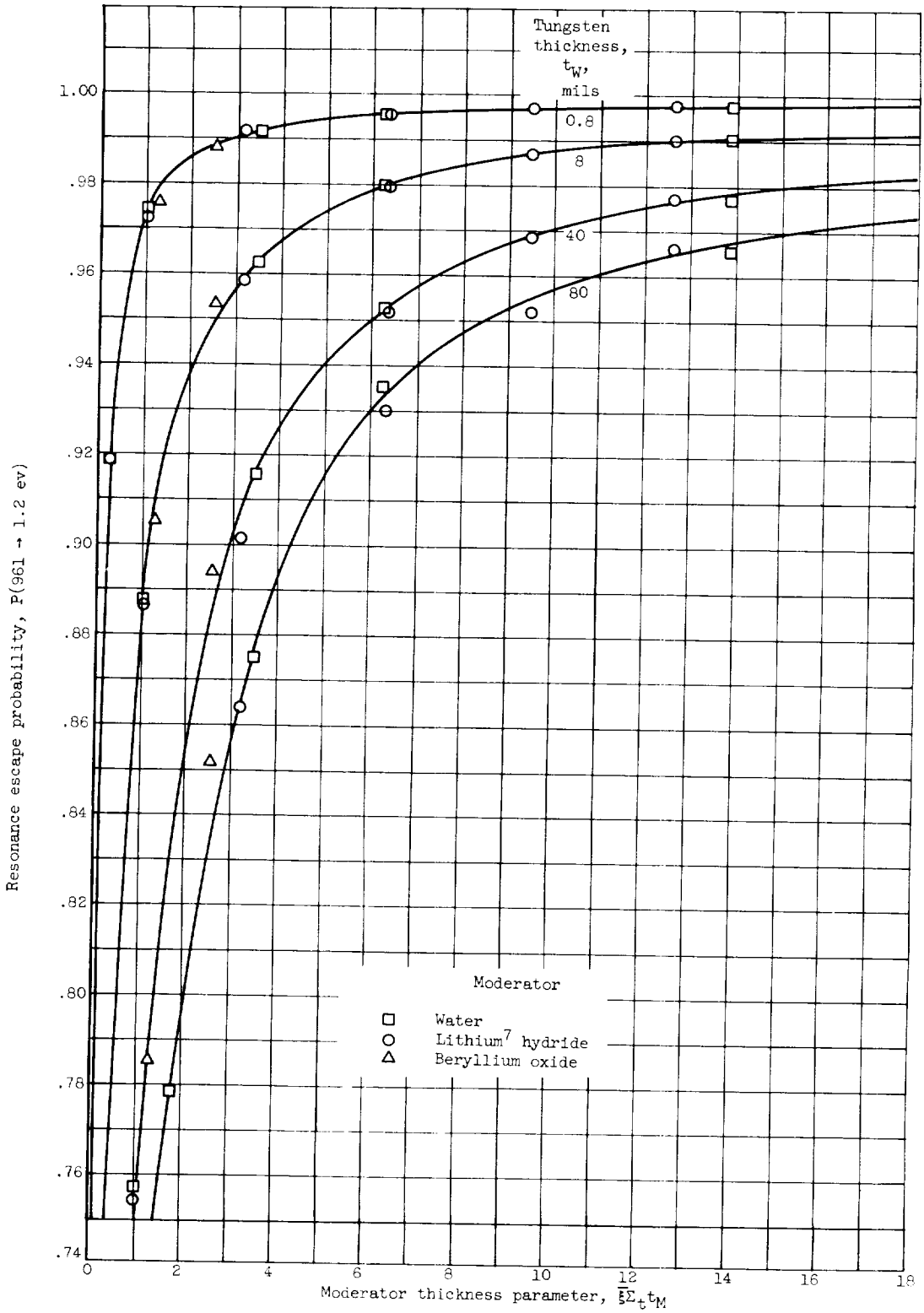

Figure 6. - Resonance escape probability as function of moderator thickness parameter.

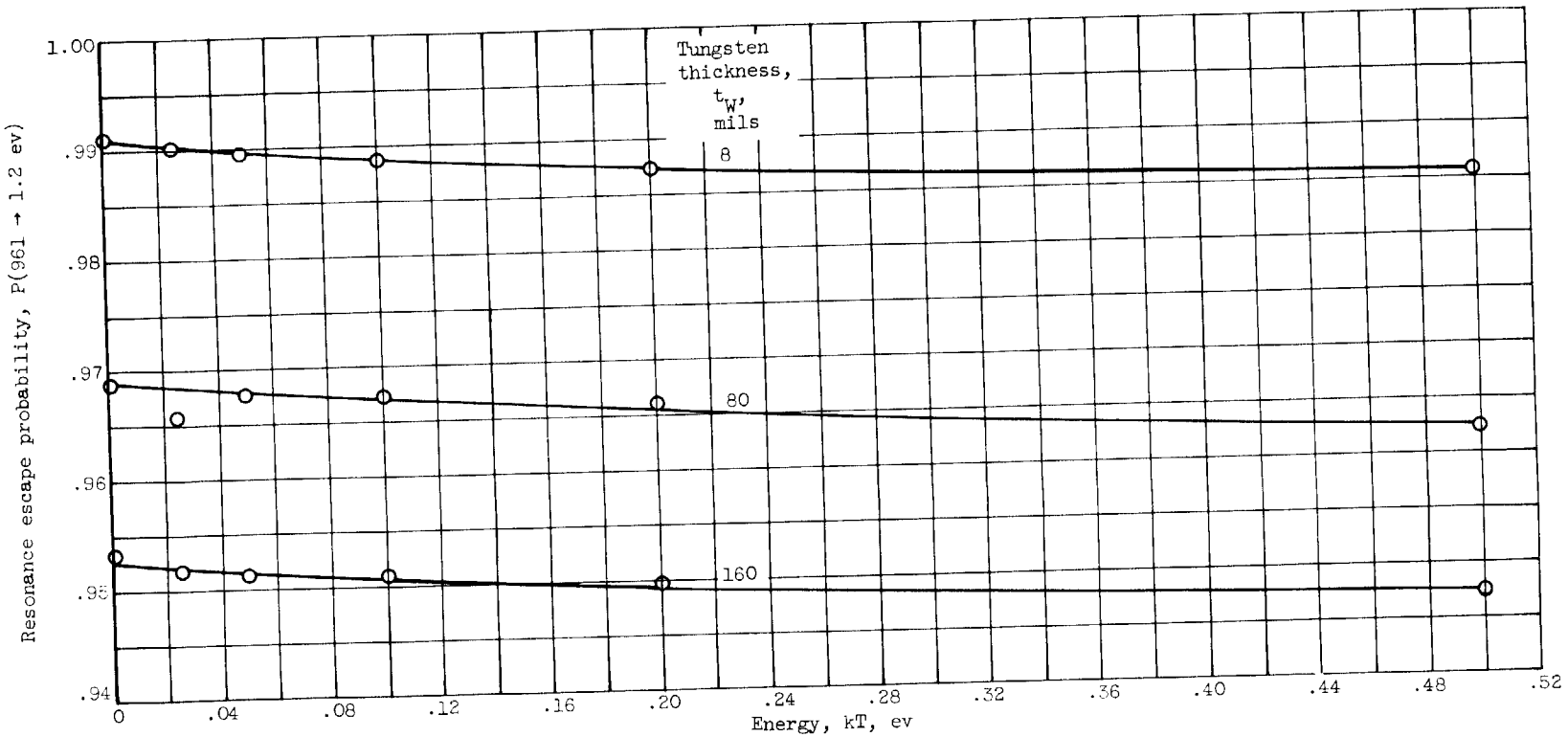

Figure 7. - Resonance escape probability as function of tungsten temperature for 4-inch-water moderator.

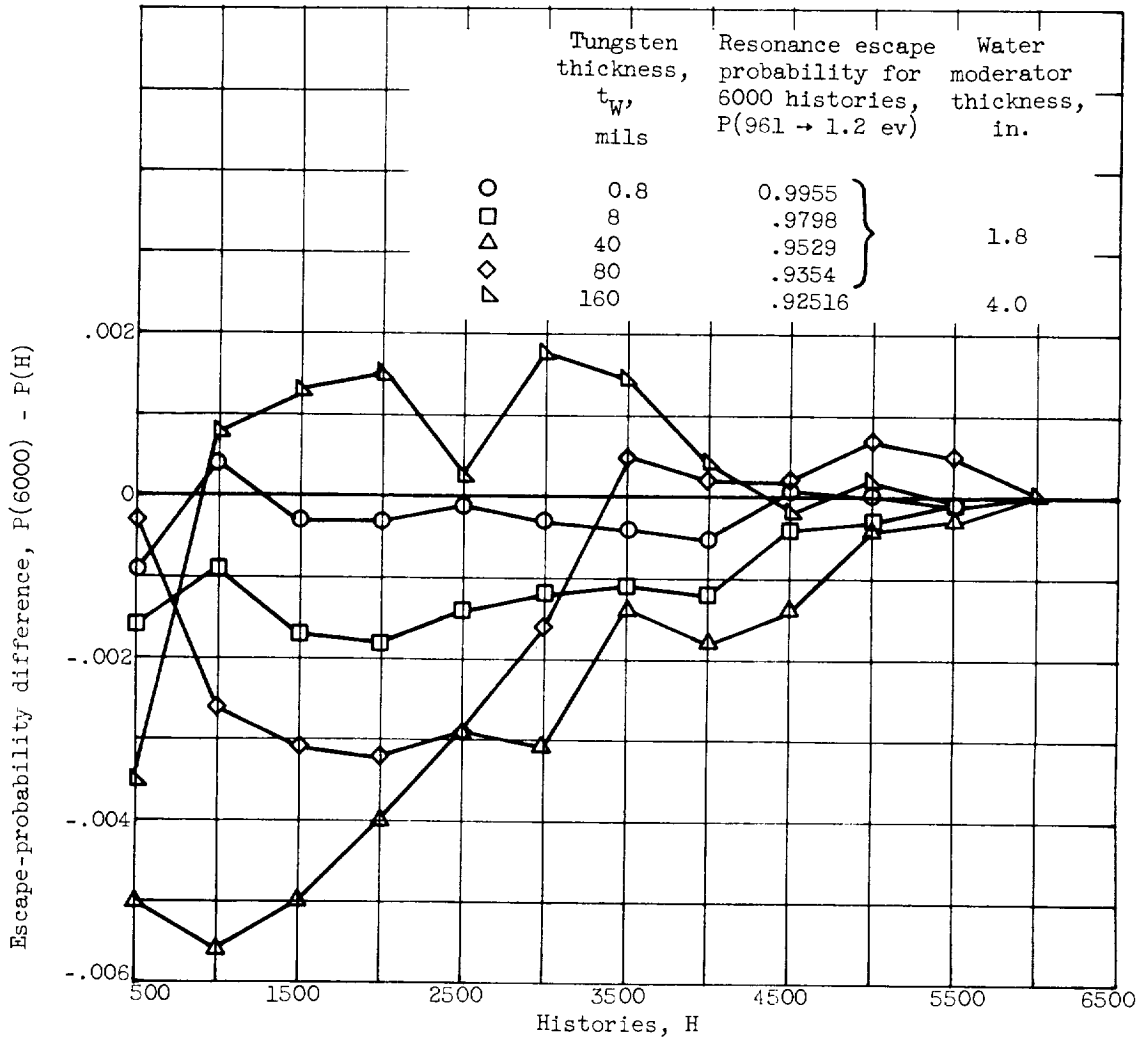

Figure 8. - Deviation of resonance escape probability after H histories from 6000-history answer.

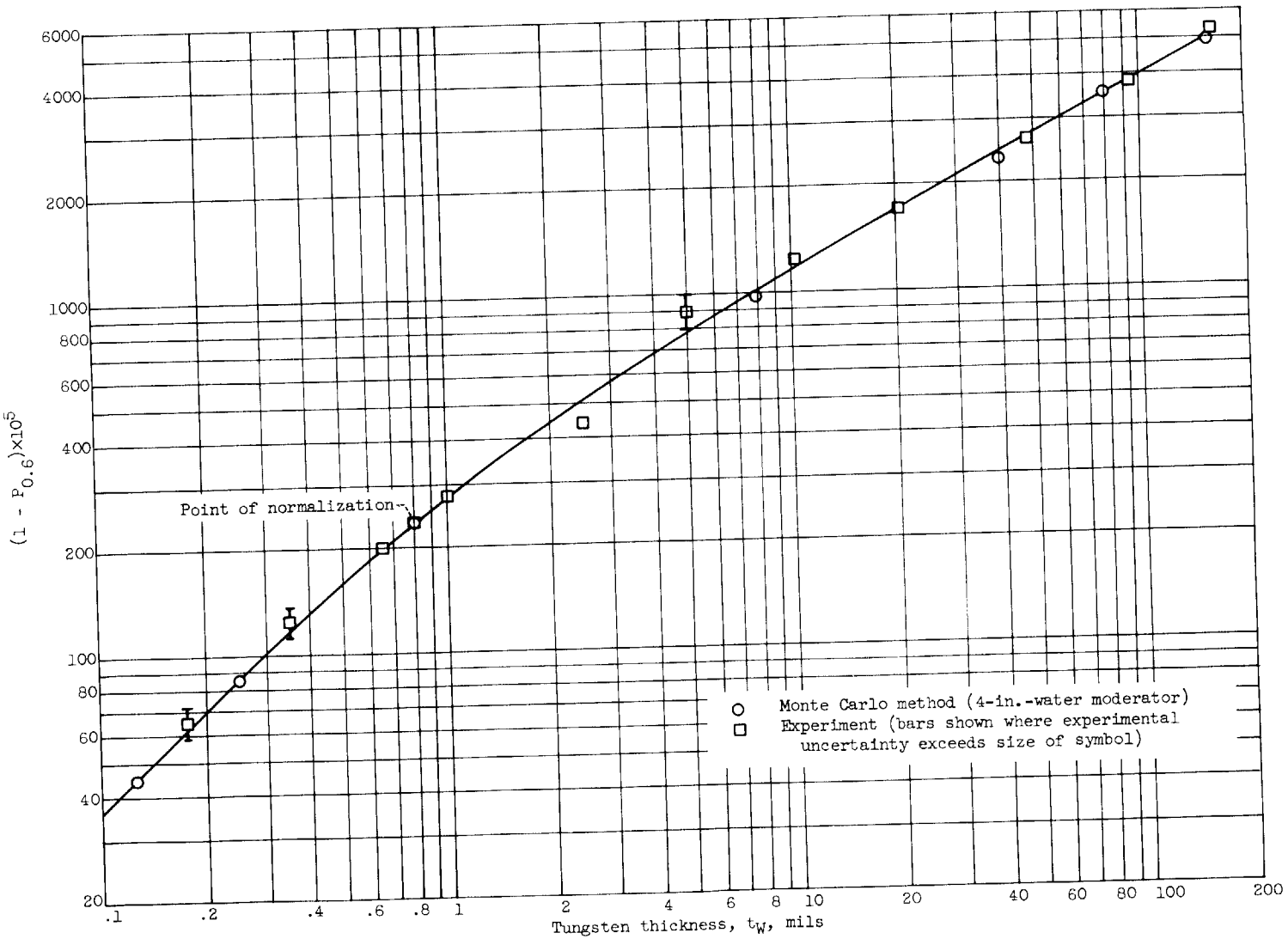

Figure 9. - Comparison of Monte Carlo and experimental solution reactor absorptions for natural tungsten samples.

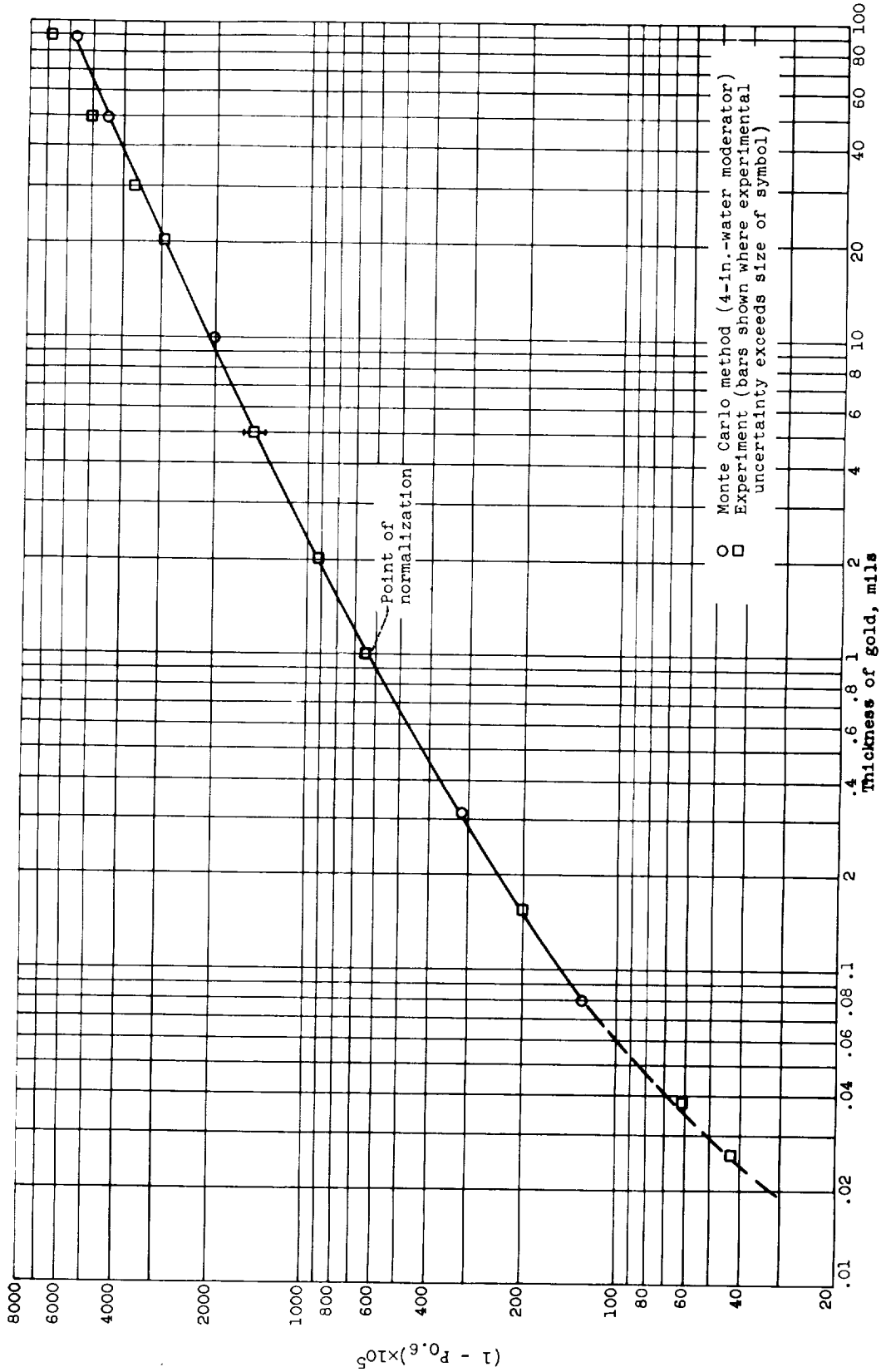

Figure 10. - Comparison of Monte Carlo and experimental solution reactor absorptions for gold foils.

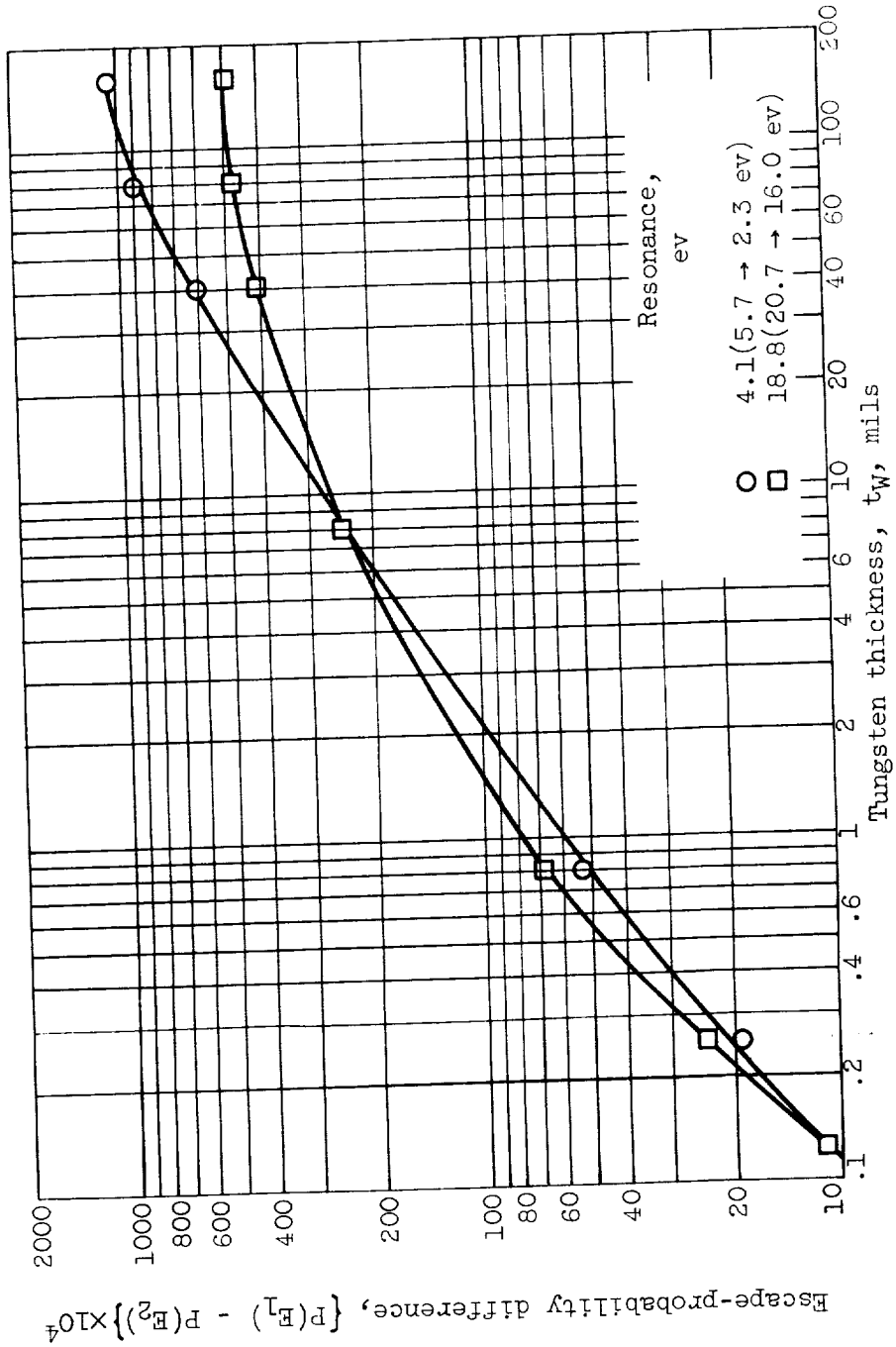

Figure 11. - Absorption in 4.1- and 18.8-electron-volt resonances as function of tungsten thickness.